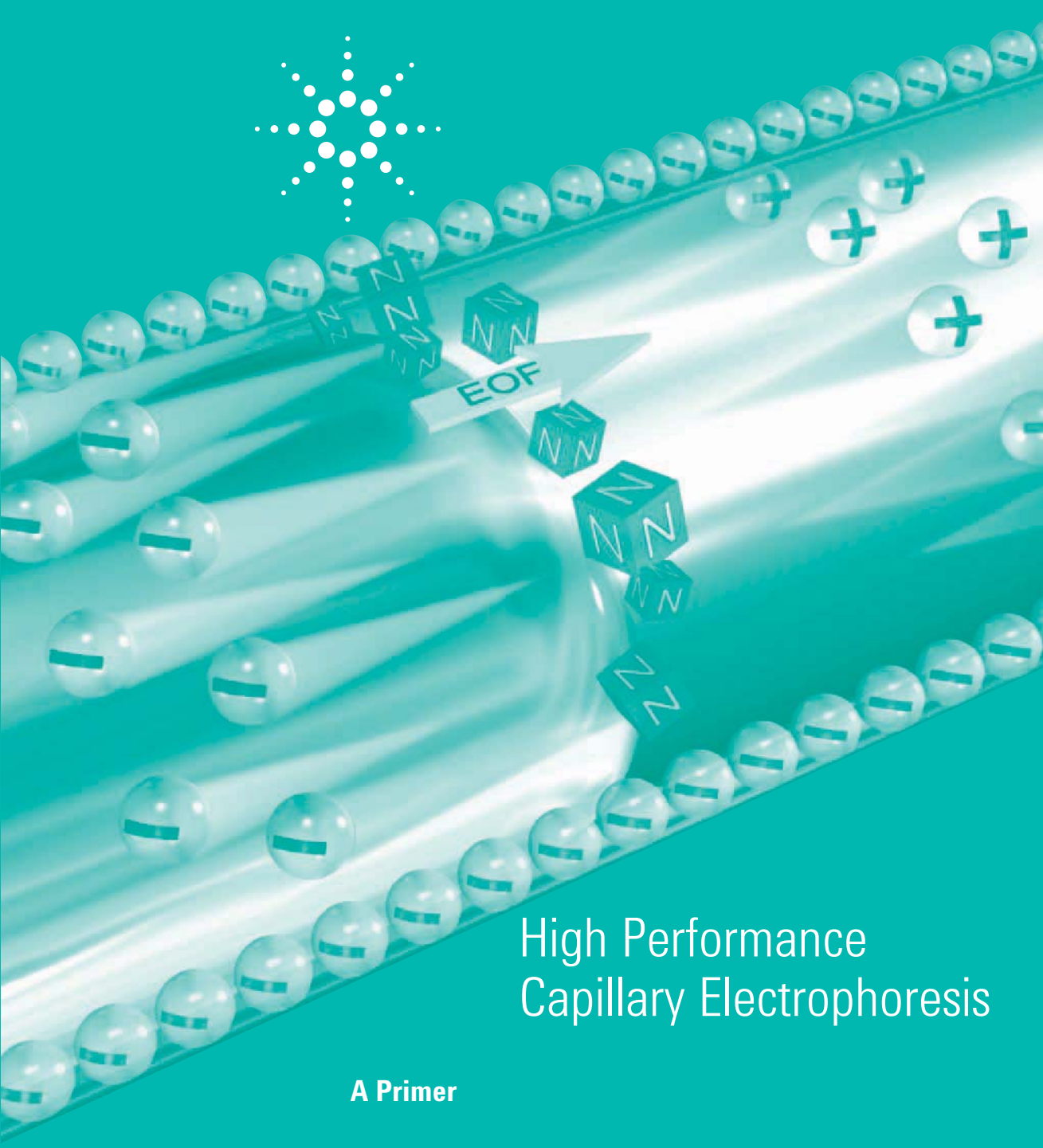

High Performance Capillary Electrophoresis

A Primer

Agilent Technologies

A Primer

High Performance Capillary Electrophoresis

Second completely revised edition by **Henk H. Lauer and Gerard P. Rozing**

Foreword

Electrophoresis was born at the beginning of nineteenth century, even earlier than chromatography. It has taken a long development path, which in the early days was framed by names like Kohlrausch, Tiselius and later Everaerts. At the beginning of eighties in the last century, Jorgenson cause a paradigm shift by executing electrophoresis in a very thin capillary with inner diameter less then 100 µm leading to capillary electrophoresis. Since then, capillary electrophoresis has been constantly improved and has become a routine technique. Instrument manufacturers like Agilent Technologies have developed instrumentation for capillary electrophoresis serving many analytical laboratories reliably for many years. After a decline at the beginning of this decade, the capillary electrophoresis market is recovering strongly. Especially, hyphenation with mass spectrometers has been very fruitful and brought a remarkable ability to unravel complex structures of biomolecules with invincible speed and sensitivity. And there are several modes of capillary electrophoresis, which make it useful for separation of really wide class of compounds, such as small ions, peptides, proteins, DNA fragments both sequencing and restriction ones, and even complete cells or uncharged molecules.

When compared with liquid chromatography capillary electrophoresis has one big advantage: the separation process takes place in a rather simple environment – in homogeneous solutions or in a polymeric sieving network and in a separation space with simple geometry, like a cylindrical channel. The equations describing completely movement of matter in space and time can be than easily formulated and solved by advanced mathematical methods. Here several researchers have done a great job. The deep understanding of basic principles of the separation process allows fast development of instrumentation, sophisticated simulation and prediction of separation, and easier development of new electrophoretic separation methods.

This primer is an excellent entry for novices in the field. I am sure capillary electrophoresis will live long in the new instrumentation and will serve well for separation scientists. And will excite them with its elegancy and efficiency.

Bohuslav Gaš
Professor
Faculty of Science, Charles University in Prague

From the early days of electrophoresis as separation technique, introduced by Tiselius, capillary electrophoresis has been applied for the separation of substances from many different origins. After the pioneering work of Hjertén, Everaerts and Jorgenson, the 1990s showed a real explosion of applications using capillary electrophoresis (CE). Both creative solutions to separation problems as well as validated methods from industry appeared in literature.

After the dust of the application explosion settled at the start of this century, it became apparent that the CE techniques are an important part in the toolbox of analytical scientists. Some of the applications are easy to observe, such as general chapters in Pharmacopoeia, CE methods in pharmacopoeial monographs and new drug applications from pharmaceutical companies and CE methods replacing slab gel methods in the biotech industry. Many pharmaceutical companies use CE for chiral separations and small ions. There are many application kits available through several suppliers. But there are also "hidden" applications. Several instruments for specific applications such as DNA/RNA analyzers and protein analyzers use CE as the separation mechanism. Through further miniaturization, CE contributes to the development of lab-on-a-chip.

Today's challenges to strengthen the implementation of CE techniques in the pharmaceutical industry, are further improved equipment and training. After the big steps made towards good instrumentation in the late 1980s and 1990s lots of lessons have been learned from the use of CE in both R&D and quality control laboratories which should be translated in new generation instruments. For future instrumental improvements it is important to work from the fundamental concepts of electrophoresis. As for training, there is a strong need for skilled people. CE method development is very much a conceptual approach, that is thinking in mechanisms. Additionally it is important to train on "Good CE Practice", since CE in its handling is neither liquid chromatography nor slab gel electrophoresis.

The first primer from HP/Agilent was an important tool in acquainting and training people in the CE techniques. Hopefully this renewed primer will prove an as good, or even better, instrument for that.

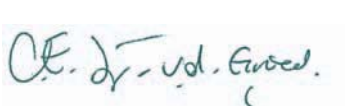

Dr. Cari Sänger – van de Griend **Pim Muijselaar**
Senior Analytical Scientists, Solvay Pharmaceuticals BV
New Chemical Entities Development NCED, Weesp, The Netherlands

Table of Content

Chapter 1

Principles of Capillary Electrophoresis

Principles of capillary electrophoresis

1.1. Historical background, current status and applications of CE

Electrophoresis has been defined as the differential movement of charged species (ions) by attraction or repulsion in an electric field. Electrophoresis as a separation technique was introduced by Tiselius in 1937. Placing protein mixtures between buffer solutions in a tube and applying an electric field, he found that sample components migrated in a direction and at a rate determined by their charge and mobility. For his work in separation science Tiselius was awarded a Nobel Prize.

Separation efficiency in free solution, as performed by Tiselius, was limited by thermal diffusion and convection. For this reason, electrophoresis traditionally has been performed in anti-convective media, such as polyacrylamide or agarose gels. Gels in the slab or tube format have been used primarily for the size-dependent separation of biological macromolecules, such as nucleic acids and proteins.

Although it is one of the most widely used separation techniques, slab gel electrophoresis generally suffers from long analysis times, low efficiencies, and difficulties in detection and automation.
An alternative to the slab-format is to perform the electrophoretic separation in narrow-bore open tubes or capillaries. The dimensional differences of both techniques are depicted in figure 1.1.

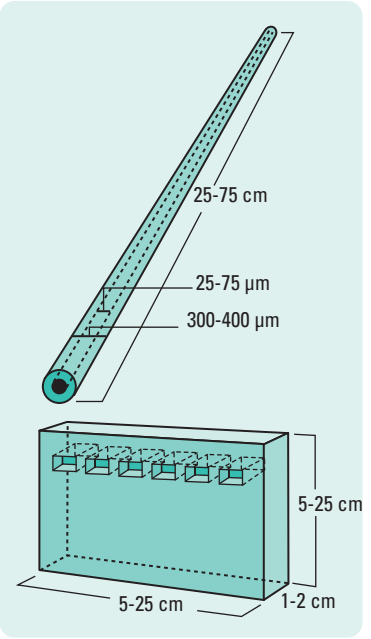

Figure 1.1
Comparison of gel used for slab gel electrophoresis and capillary for CE.

Since narrow capillaries have a low conductance, they generate only small amounts of heat and are in principle anti-convective. The use of gel media in capillaries is therefore not essential for electrophoresis in an open tube. This allows the application of free-solution (or capillary) electrophoresis, as well as the use of traditional gel media in the capillary.

Initial work in open tube electrophoresis was described by Hjertén in 1967. At that time, since only millimeter-bore capillaries were available, Hjertén rotated them along their longitudinal axis to minimize the effects of convection. Later Virtanen and then Mikkers and Everaerts performed electrophoresis in approximately 200-µm internal diameter (id) capillaries made from glass and PTFE, respectively. In the early 1980s Jorgenson and Lukacs advanced the technique by using 75-µm id fused silica capillaries. Jorgenson also clarified the theory, described the relationships between operational parameters and separation quality, and demonstrated the potential of capillary electrophoresis (CE) as an analytical technique.

In the last decades CE evolved from the reseach lab into practical applications in many fields such as, (bio)pharmaceutical-, forensics-, clinical-, foodstuff-, environmental-, chemical- and biochemical analysis. The trends in CE are coupling of CE with mass spectrometry (CE-MS) and further miniaturization (microfluidic systems on chips) are, however, strongly dependent on the current and future advances in analytical methodologies and instrumentation. During this episode numerous reviews and books have been written describing various aspects of CE.

To date, CE is still mainly performed in the capillary format, typically 25- to 150 µm inner diameter (id), which are usually filled only with buffer. Use of the capillary has numerous advantages, particularly with respect to the detrimental effects of Joule heating (heat generated when a electric current flows through a conductor such as a buffer filled capillary, see section 1.3.4.2.). The high electrical resistance of the capillary enables the application of very high electrical fields (100 to 500 V/cm) with only minimal heat generation. Moreover, the large surface area-to-volume ratio of the capillary efficiently dissipates the heat that is generated. The use of the high electrical fields results in short analysis times and high efficiency and resolution. Peak efficiency, often in excess of 10^5 theoretical plates, is due in part to the plug flow velocity profile of the electroosmotic flow, an electrophoretic phenomenon that generates the bulk flow of solution within the capillary. This flow also enables the simultaneous analysis of all solutes, regardless of charge. In addition the numerous separation modes offer different separation mechanisms and selectivities, minimal sample volume requirements (1 to 50 nL), on-capillary detection, and the potential for quantitative analysis and automation.

One of the greatest advantages of CE is its diverse application range. Originally considered primarily for the analysis of biological macromolecules, CE has proved useful for separations of compounds such as amino acids, chiral drugs, vitamins, pesticides, inorganic ions, organic acids, dyes, surfactants, peptides and proteins, carbohydrates, oligonucleotides and DNA restriction fragments, and even whole cells and virus particles.

The mechanisms responsible for separation in CE are different from those in chromatography, and thus can offer orthogonal, complementary analyses. In addition, CE may offer simpler method development, minimal

sample volume requirements, and lack of organic waste. Significant advances have already been achieved by increasing performance and standardizing the use of CE. These include improvements in migration time and peak area reproducibility as well as quantitative analysis, methods for on-capillary sample preconcentration to improve sensitivity, development of capillary coatings to both control electroosmotic flow and limit solute-wall interactions, low viscosity replaceable sieving polymers, stationary phases for open tubular, monolithic and particle packed columns.

In this primer the basic concepts, theory and mechanisms of the diverse electrophoretic modes applied to the capillary format are discussed together with additional progress made in detection, applications, method development and an associated technique such as on-chip electrophoresis.

1.2. Basic components

One key feature of CE is the overall simplicity of the instrumentation. A schematic diagram of a generic capillary electrophoresis system is shown in figure 1.2. Briefly, the ends of a narrow-bore, fused silica capillary are placed in buffer reservoirs. The content of the reservoirs is identical to that within the capillary. The reservoirs also contain the electrodes used to make electrical contact between high voltage power supply and capillary.

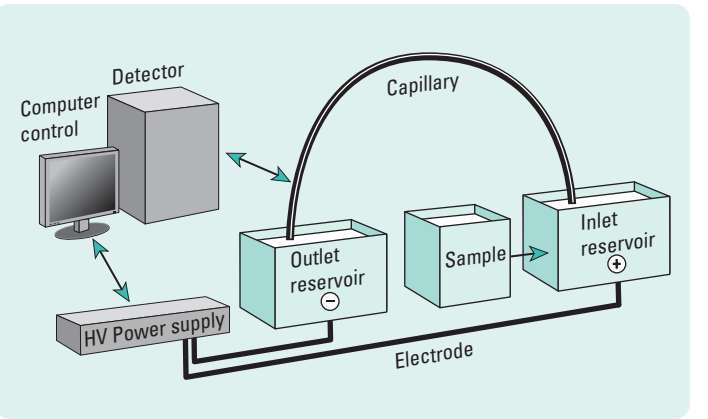

Figure 1.2
Basic components of CE instrumentation.

Sample is loaded onto the capillary by replacing one of the reservoirs (usually at the anode) with a sample reservoir and applying either an electric field or an external pressure. After replacing the buffer reservoir, the electric field is applied and the separation performed. Optical detection can be made at the opposite end, directly through the capillary wall. The theoretical and practical details regarding injection, separation, detection, quantitative analysis, equipment, automation and so on, are discussed in this primer.

1.3. Theory

1.3.1. Electrophoresis[1, 2, 3, 4]

Separation by electrophoresis is based on differences in solute velocity in an electric field. The velocity of an ion can be given by equation 1.1:

1.1 $$v = \mu_e E$$

where v = ion velocity
μ_e = electrophoretic mobility
E = applied electric field

The electric field is simply the quotient of the applied voltage and capillary length (in volts/cm). The mobility, for a given ion and medium, is a constant which is characteristic of that ion. The mobility is determined by the electric force that the ionized species (molecule or particle) experiences, balanced by its frictional drag through the medium.

The electric force can be given by:

1.2 $$F_E = q E$$

and the frictional force (for a spherical ion) by Stoke's law

1.3 $$F_F = -6 \pi \eta r v$$

where q = ion charge
η = solution viscosity
r = ion radius
v = ion velocity

During a short transient period when the electric force is first applied a steady state, defined by the balance of these forces, is attained. At this point the forces are equal but opposite and

$$q E = 6 \pi \eta r v \quad (1.4)$$

Solving for velocity and substituting equation 1.4 into equation 1.1 yields an equation that describes the mobility in terms of physical parameters

$$\mu_e = \frac{q}{6 \pi \eta r} \quad (1.5)$$

From this equation it is evident that small, highly charged species have high mobilities whereas large, minimally charged species have low mobilities. The electrophoretic mobility (μ_e), usually found in standard tables, is a physical constant, determined at the point of full solute charge ($\alpha_i = 1$) and extrapolated to infinite dilution. In practice this differs from the mobility determined experimentally. The latter is called the effective mobility:

$$\mu_{eff} = \alpha_i \cdot \mu_e \quad (1.6)$$

where α_i = degree of ionization (or dissociation) of a molecule. (Not to be confused with the selectivity, $\alpha = k'_2 / k'_1$, as used in chromatography.)

and is highly dependent on pH (that is, solute pK_a) and composition of the running buffer. The differences between the absolute and effective mobilities are demonstrated in figure 1.3.

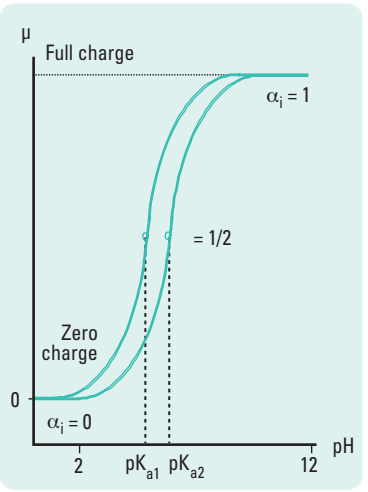

Figure 1.3
Mobility of two weak acids as a function of pH.

Here, two hypothetical solutes are shown to possess the same electrophoretic mobility at full charge. From a mobility table, these solutes would appear to be inseparable since there would be no differential migration. However, these species have different pK_a values and therefore different mobilities depending on their pH-controlled charge. (In the following sections the effective mobility is simply expressed by μ_e).

1.3.2. Electroosmotic flow (EOF) and control of EOF

A fundamental constituent of CE operation is electroosmotic, or electroendosmotic flow (EOF). EOF is the bulkflow of liquid in the capillary and is a consequence of the surface charge on the interior capillary wall. The EOF results from the effect of the applied electric field on the solution double-layer at the wall (figure 1.4). The EOF controls the amount of time solutes remain in the capillary by superposition of flow on to solute mobility. This can have the effect of altering the required capillary length, but does not affect selectivity.

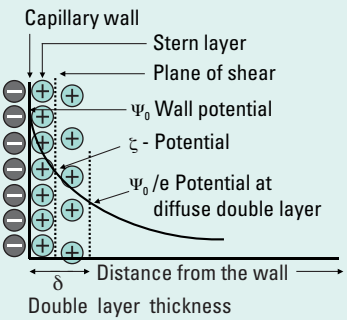

Figure 1.4
Illustration of the electrical double layer at the capillary wall.[2]

Under aqueous conditions most solid surfaces possess an excess charge. This can result from ionization of the surface and/or from adsorption of ionic species at the surface. For fused silica both processes probably occur, although the EOF is most strongly controlled by the numerous silanol groups (SiOH) that can exist in anionic form (SiO^-) (figure 1.5A). Although

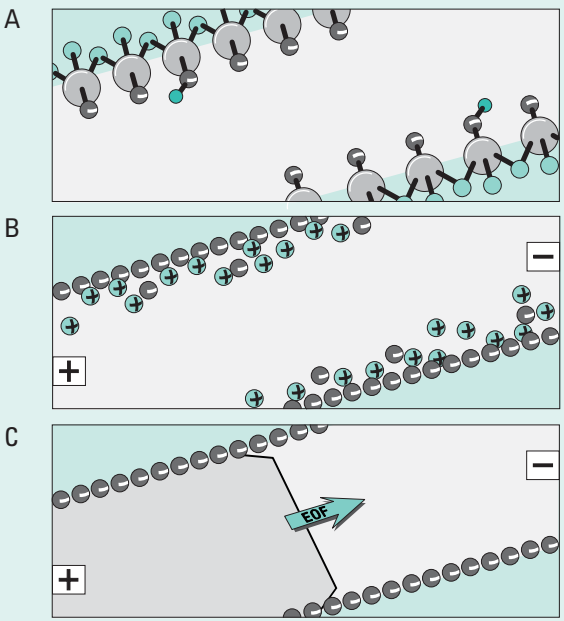

Figure 1.5
Development of the electroosmotic flow: A) negatively charged fused silica surface (Si-O^-), B) hydrated cations accumulating near surface, C) bulk flow towards the cathode upon application of electric field.

the pK_a of the surface silanol groups is difficult to determine and mostly not known, in general EOF becomes significant above pH 4. Non-ionic materials such as PTFE also exhibit EOF, presumably resulting from adsorption of anions.

Counterions (cations, in most cases), which build up near the surface to maintain charge balance, form a diffuse double-layer and create a potential difference very close to the wall (figure 1.5B). This is known as the zeta potential. When the voltage is applied across the capillary the cations forming the diffuse double-layer are attracted toward the cathode. Because they are solvated their movement drags the bulk solution in the capillary toward the cathode. This process is shown in schematic form in figure 1.5C. The magnitude of the EOF can be expressed in terms of velocity or mobility by

1.7

$$v_{EOF} = (\varepsilon \zeta / \eta) E$$

or

$$\mu_{EOF} = (\varepsilon \zeta / \eta)$$

where:

v_{EOF} = velocity
μ_{EOF} = EOF "mobility"
ζ = zeta potential
ε = solution dielectric constant

(note the independence of mobility on applied electric field)

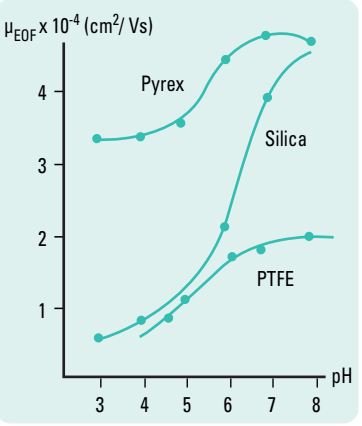

Figure 1.6
Effect of pH on electroosmotic flow mobility in various capillary materials.[5]

The zeta potential is essentially determined by the surface charge on the capillary wall ($\zeta \approx \Psi_0$). Since this charge is strongly pH dependent, the magnitude of the EOF varies with pH. At high pH, where the silanol groups are predominantly deprotonated, the EOF is significantly greater than at low pH where they become protonated. Depending on the specific conditions, the EOF can vary by more than an order of magnitude between pH 2 and 12. Figure 1.6 illustrates this effect for fused silica and other materials. The zeta potential is also dependent on the ionic strength of the buffer, as described by double-layer theory. Increased ionic strength results in double-layer compression, decreased zeta potential, and reduced EOF (see figure 1.9).

A unique feature of EOF in the capillary is the flat flow velocity profile, as depicted in figures 1.5C and 1.7A. Since the electro-driven force of the flow is uniformly distributed along the capillary (that is, at the walls) there is no pressure drop within the capillary, and the velocity is nearly uniform throughout. The flat flow velocity profile is beneficial since it does not contribute to the broadening (dispersion) of solute zones. This is in contrast to the flow velocity profile generated by pressure, which yields a laminar flow with a parabolic flow velocity profile due to the shear forces at the wall and at the sliding liquid layers (laminae) constituting the bulk solution (figure 1.7B).

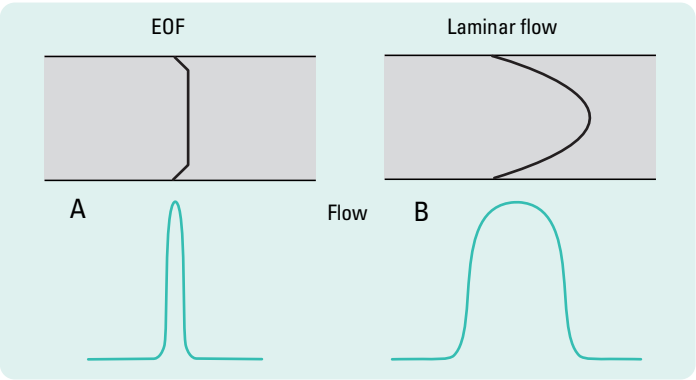

Figure 1.7 A, B
Flow velocity profiles and corresponding solute zones in electro- and pressure-driven flow.

Figure 1.7A shows that the flow rate drops off rapidly at the wall. This quiescent solution layer is caused by friction against flow at the surface. Since this layer extends a short way into the solution, it is relatively unimportant to the overall separation process (that is, other dispersive processes dominate). Further, the EOF and its velocity profile are generally independent of capillary diameter. The profile will be disrupted, however, if the capillary internal diameter is too wide (≥ 200 to 300 µm). In this case, surface tension becomes insufficient to uniformly drag the center portion of the liquid at the velocity generated at the walls. Details of the effect of the EOF velocity profile on peak shape and other zone broadening factors are given in section 1.3.4. Zone broadening and efficiency.

Another benefit of the EOF is that it causes movement of nearly all species, regardless of charge, in the same direction. Under normal conditions (that is, negatively charged capillary surface), the flow is from the anode (positive electrode) to the cathode (negative electrode). Anions will be flushed towards the cathode since the magnitude of the EOF can be more than an order of magnitude greater than their effective electrophoretic mobilities. Thus cations, neutrals, and anions can be electrophoresed in a single run since they all "migrate" in the same direction. This process is depicted in figure 1.8. Here, cations migrate fastest since the electrophoretic attraction towards the cathode and the EOF are in the same direction, neutrals are all carried at the velocity of the EOF but are not separated from each other, and anions migrate slowest since they are attracted to the anode but are still carried by the EOF toward the cathode.

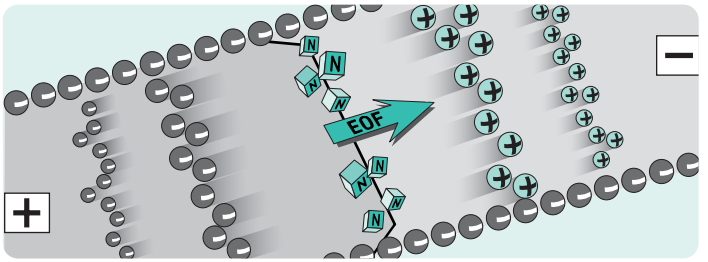

Figure 1.8
Differential solute migration superimposed on electroosmotic flow in capillary zone electrophoresis.

Modification of capillary wall charge (by pH or additives) can decrease or even reverse EOF while leaving solute mobility unaffected. Under these circumstances, anions and cations can migrate in opposite directions.

While the EOF is usually beneficial, it needs to be controlled. At high pH, for example, the EOF may be too rapid, resulting in elution of solutes before separation has occurred. Conversely, at low or moderate pH, the low negative charge of the inner capillary surface can cause adsorption of cationic solutes through coulombic interactions. This latter phenomenon has been especially problematic for basic protein separations. In addition, electrophoretic separation modes such as isoelectric focusing, isotachophoresis, and capillary gel electrophoresis require reduction or absence of EOF.

Fundamentally, control of EOF requires alteration of the capillary surface charge or buffer viscosity. There are several methods to accomplish this, as discussed in detail in the following paragraphs. Note that conditions that affect the surface charge of the wall often also affect the solute (such as buffer pH). Successful separations are usually obtained when the conditions optimize both EOF and solute mobility properties.

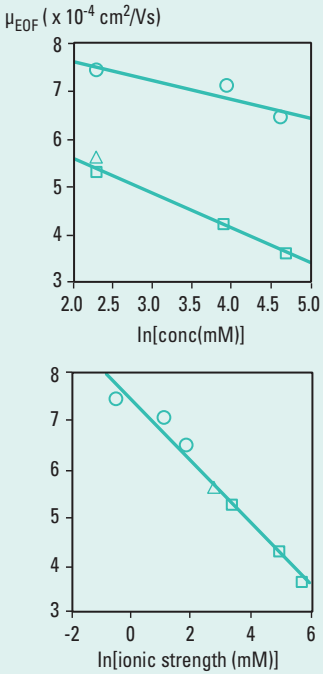

Figure 1.9
Electroosmotic flow mobility as a function of buffer concentration and ionic strength.[6]
Circles = borate buffer
Squares = phosphate buffer
Triangles = carbonate buffer, all pH 8.

The rate of EOF can most easily be decreased by lowering the electric field, as described by equation 1.7. This action, however, has numerous disadvantages with regard to analysis time, efficiency, and resolution. From a practical point of view, the most dramatic changes in EOF can be made simply by altering the pH of the buffer, as described above (figure 1.6). Adjusting the pH, however, can also affect the solute charge and therefore its mobility. Low pH buffers will protonate both the capillary surface and an acidic solute, while high pH buffers deprotonate both. Knowledge of a solute's pK_a or pI (for zwitterionic substances) is therefore mandatory in selecting the appropriate pH range of the running buffer.

EOF can also be affected by adjusting the concentration and/or the ionic strength of the buffer. The magnitude of this effect is illustrated in figure 1.9. High buffer concentrations are also useful in limiting coulombic interactions of solute with the walls by decreasing the effective charge at the wall. Heating within the capillary, however, constrains the use of high concentration buffers (the effects of heating are described in 1.3.4.2 Joule heating). Typical buffer concentrations range from 10 to 50 mM, although 100 to 500 mM and higher have also been used. With common buffer concentrations (10-50 mM), instrumentally controlled temperature change appears to be an easy and useful manner to control EOF due to the inherent viscosity changes of the buffer (see equation 1.7).

Lastly, EOF can be controlled by modification of the capillary wall by means of dynamic coatings (that is, buffer additives) or covalent coatings. These coatings can increase, decrease, or reverse the surface charge and thus the EOF. Details regarding the nature of coatings are given in section 4.1.

All methods and variables that control EOF are summarized in table 1.1.

Variable	Result	Comment (see subsequent sections)
Electric field	EOF changes proportionally with electrical field.	High field generates more heat in the capillary. Eventually short-circuits and sparking.
Buffer pH	EOF decreases at low pH and increases at high pH.	May change solute charge (figure 1.6).
Ionic strength or buffer concentration	EOF increases at low ion strength.	High ionic strength generates high current causing Joule heating. Lower buffer capacity at low ion strength; possible sample adsorption; limits sample stacking (see chapter 3). Peak shape distort ion if conductivity of the electrolyte differs from sample conductivity.
Temperature	EOF changes due to viscosity change (2 - 3%/°C).	Capillary temperature must be controlled.
Organic modifier to the electrolyte	Changes zeta potential and electrolyte viscosity.	Complex changes of EOF; effect most easily determined experimentally. May alter selectivity of separation.
Additives to the electrolyte (e.g. surfactants)	Change magnitude and direction of EOFs. Anionic surfactants can increase EOF; Cationic surfactants can decrease EOF.	Dynamical adsorption to capillary wall via hydrophobic and or ionic interaction.
Neutral hydrophilic polymer	Decreases but controls EOF by shielding surface charge and increasing viscosity.	Adsorbs to capillary wall via hydrophilic interactions. Suppresses solute/wall interactions.
Covalent bonded surface coating	EOF changes depending on the charge and polarity of the coating.	Many modifications possible (hydrophilicity or charge). Stability can be problematic. Changes surface properties and therefore solute/surface interactions possible.

Table 1.1
Methods to control the EOF.

1.3.3. Mobility and migration time

The time required for a solute to migrate to the point of detection is called the "migration time", and is given by the quotient of migration distance and velocity. The migration time and other experimental parameters can be used to calculate the apparent solute mobility (μ_a) using

1.8 $$\mu_a = \frac{l}{t_a E} = \frac{lL}{t_a V}$$

where:

$\mu_a = \mu_e + \mu_{EOF}$

V = applied voltage

l = effective capillary length (to the detector)

L = total capillary length

t_a = migration time (analyte ion)

E = electric field

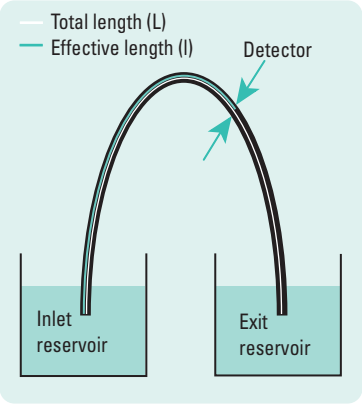

Figure 1.10
Definition of effective and total capillary lengths.

The two different capillary lengths, effective (l) and total (L), are described schematically in figure 1.10. The effective length is that from the point of injection to the point of detection. For on-capillary spectroscopic detection, this length is typically 5 to 10 cm shorter than the total length. For off-column detection (mass spectrometry, for example), the two lengths are equivalent. Knowledge of both lengths is important since the migration time of an analyte ion, t_a, and its apparent mobility, μ_a, are defined by the effective length, whereas the electric field is defined by the total length (E = V/L).

A sample calculation of the different mobilities, using a vitamin separation, is illustrated in figure 1.11.

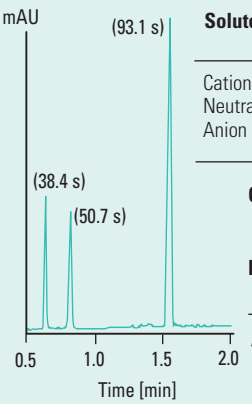

Solute	Migration time (s)	μ_a(cm²/Vs)	μ_e(cm²/Vs)
Cation	38.4	3.05×10^{-3}	7.40×10^{-4}
Neutral	50.7	2.31×10^{-3}	2.31×10^{-3}
Anion	93.1	1.26×10^{-3}	-1.05×10^{-3}

Cation: $\mu_a = \frac{lL}{Vt} = \frac{(50)(58.5)}{(25{,}000)(38.4)} = 3.05 \times 10^{-3}$

Neutral: $\mu_{EOF} = \frac{(50)(58.5)}{(25{,}000)(50.7)} = 2.31 \times 10^{-3}$

$\mu_e = \mu_a - \mu_{EOF} = (3.05 \times 10^{-3}) - (2.31 \times 10^{-3}) = 7.40 \times 10^{-4}$

(note: μ_e will be negative for the anion)

Figure 1.11
Calculation of electroosmotic flow mobility and effective solute mobility.

1.3.4. Zone broadening and efficiency

Separation in electrophoresis is based on differences in solute mobility. The difference necessary to resolve two zones is dependent on the width of the zones and their difference in migration time. Zone width is strongly dependent on the zone broadening (or dispersive) processes that act on it. Dispersion should be controlled to avoid an increase zone width and the mobility difference necessary to achieve separation.

1.3.4.1. Longitudinal diffusion

Spreading of the solute zone, results from differences in solute velocity within that zone, and can be defined as the baseline peak width, w_b. For a Gaussian peak,

1.9 $$w_b = 4\sigma$$

where σ = standard deviation of the peak (in time, length, or volume)

The efficiency, expressed in number of theoretical plates, N, can be obtained by

1.10 $$N = \left(\frac{l}{\sigma}\right)^2$$

where l = capillary effective length and can be related to the HETP (the dispersion per unit length or height equivalent to a theoretical plate), H, by

$$H = \left(\frac{l}{N}\right)$$

Under ideal conditions (that is, small injection plug length, no solute-wall interactions, and so on) the sole contribution to solute-zone broadening in CE can be considered to be longitudinal or axial diffusion (along the capillary). Radial diffusion (across the capillary) is unimportant due to the plug flow velocity profile. Similarly, convective broadening is unimportant due to

the anti-convective properties of the capillary. Thus, the efficiency can be related to the molecular diffusion term as in chromatography. That is:

1.11

$$\sigma^2 = 2Dt = \frac{2DIL}{\mu_a V} = \frac{2DI}{\mu_a E}$$

where D = diffusion coefficient of the solute
L = capillary total length

Substituting equation (1.11) into equation (1.10) yields a fundamental electrophoretic expression for plate number

1.12

$$N = \frac{\mu_a V I}{2DL} = \frac{\mu_a E I}{2D}$$

From equation (1.12), the reason for the application of high electric fields is evident. This follows simply because the solute spends less time in the capillary at high field and has less time to diffuse. In addition, this equation shows that large molecules such as proteins and DNA, which have low diffusion coefficients, will exhibit less zone broadening than small molecules. The wide range of possible diffusion coefficients is illustrated in table 1.2.

	D (x 10^{-5} cm^2/s)
HCl	3.05
NaCl	1.48
Glycine	1.06
Citrate	0.66
Cytochrome C	0.11
Hemoglobin (human)	0.069
Tobacco mosaic virus	0.0046

Table 1.2
Diffusion coefficients of selected molecules (in water, 25 °C).

The theoretical plate number can be determined directly from an electropherogram, using, for example,

1.13

$$N = 5.54 \left(\frac{t}{w_{1/2}}\right)^2$$

where: t = migration time
$w_{1/2}$ = temporal peak width at half height

Note *that equation (1.13) should only be used for Gaussian peaks. Any asymmetry should be taken into account, for example, by use of variance (σ^2) calculation from the second central peak moment*[7] *($\mu_2 = \sigma^2$).*

In practice, the measured efficiency (equation 1.13), is usually lower than the calculated efficiency (equation 1.12). This is because the theoretical calculation accounts only for zone broadening due to longitudinal diffusion. As described in the next section, other dispersive processes are often present.

Zone broadening in CE can have a number of contributors in addition to longitudinal diffusion. Among the most important are temperature gradients induced by Joule heating, injection plug length, and solute interactions with the capillary walls. Fortunately, these phenomena are usually controllable, as discussed below. These and other zone broadening mechanisms are described in table 1.3.

Source	Comment
Longitudinal diffusion	Defines the fundamental limit of efficiency. Solutes with lower diffusion coefficients form narrower zones (section 1.3.4.1.).
Joule heating	Leads to radial temperature gradients and parabolic flow velocity profiles (1.3.4.2.).
Length of injection zone	Injection lengths should be less than the diffusion-controlled zone length. Detection limit difficulties often necessitate longer than ideal injection lengths (1.3.4.3.).
Sample adsorption	Interaction of solute with the capillary walls usually causes severe peak tailing (1.3.4.4.).
Mismatched conductivities of sample and buffer (electrodispersion)	Solutes with higher conductivities than the running buffer result in fronted peaks. Solutes with lower conductivities than the running buffer result in tailed peaks (1.3.4.5.)
Unleveled buffer reservoirs	Generates laminar flow (1.3.4.6.).
Detector cell size	Should be small relative to peak width (1.3.4.7.).

Table 1.3
Sources of zone broadening.

Zone broadening, as described by equation (1.13), was derived with the assumption that the only contributor was molecular diffusion. The variance is better described by the total variance of the system, σ^2_T , which is given by the sum of the contributing variances

$$\sigma^2_T = \sigma^2_{DIF} + \sigma^2_{INJ} + \sigma^2_{TEMP} + \sigma^2_{ADS} + \sigma^2_{DET} + \sigma^2_{Electrodispersion} + \ldots \quad (1.14)$$

where the subscripts refer to diffusion, injection, temperature gradients, adsorption, detection, and electrodispersion, respectively. If any of the

dispersion processes in equation (1.14) dominate the diffusion term, theoretical limits cannot be obtained and equation (1.12) will not be valid. In this case, only minimal improvements in efficiency and resolution can be obtained by increased voltage.

1.3.4.2. Joule heating

The main advantage of performing electrophoresis in narrow-bore capillaries is reduction of the effects of heating which have traditionally limited electrophoretic techniques. Heating is problematic since it can cause non-uniform temperature gradients, local changes in viscosity, and subsequent zone broadening. While the theoretical equations for efficiency and resolution advocate the use of as high electric fields as possible, Joule heating ultimately limits the benefit of this approach, regardless of capillary dimensions and temperature control measures.

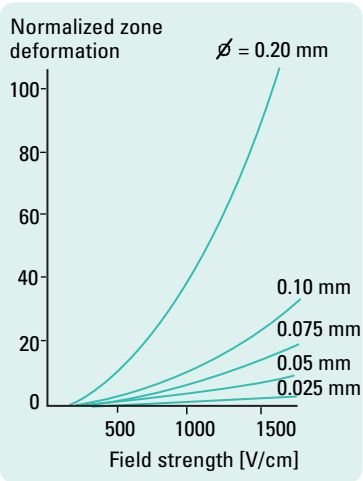

Figure 1.12
Effect of Joule heating and temperature gradients on solute zone deformation[8] (Ø = capillary id).

The heat generated by the passage of an electric current through a conductor is called Joule heat. The temperature increase depends on the power (product of voltage and current) generated and is determined by the capillary dimensions, thermal conductivity of the buffer, and the applied voltage. Significantly elevated temperatures will result when the power generation exceeds dissipation. Typical power generation ranges from 0.5 to 5 W/m. Temperature increases of 10 °C are not uncommon, although 70 °C and higher can occur.

While the absolute rise in temperature is generally not detrimental, temperature gradients are. Thermal dissipation of the heat through the capillary walls can result in higher temperatures in the center than at the wall. These temperature gradients cause viscosity differences of the running buffer over the cross section of the capillary and give rise to zone deformation. This is illustrated in figure 1.12 for a variety of inner diameter capillaries. Control of temperature differentials is critical since a one degree change in temperature results in a 2 to 3 % change in viscosity (and therefore a 2 to 3 % change in mobility).

The thermal gradient between the center of the capillary and the surroundings is illustrated in figure 1.13. As shown in this figure, the temperature difference depends on the capillary inner radius (r_1 = 25 µm),

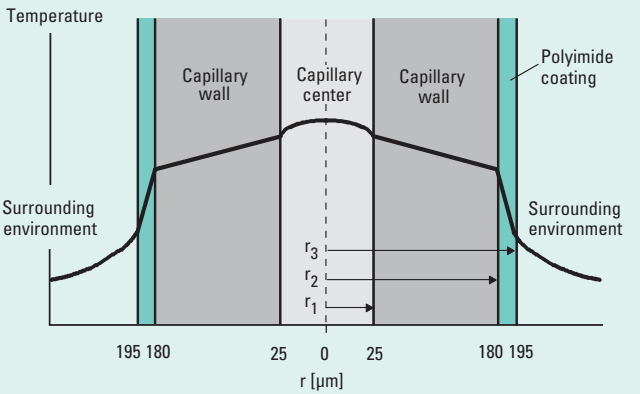

Figure 1.13
Schematic of temperature gradients from capillary center to the surroundings. Where r_1, r_2, and r_3 are the radii of the open channel, the fused silica wall, and the polymer coating, respectively. r_1 = 25 µm, r_2 = 180 µm, r_3 = 195 µm.

the thickness of the fused silica wall (155 µm), the thickness of the polyimide coating (15 µm), their respective thermal conductivities, and the heat transfer coefficient to the surroundings (h).

Theoretically this can be expressed by

1.15
$$\Delta T_T = \frac{Q r_1^2}{2}\left[\frac{1}{2\kappa_1} + \frac{1}{\kappa_2}\ln\left(\frac{r_2}{r_1}\right) + \frac{1}{\kappa_3}\ln\left(\frac{r_3}{r_2}\right) + \frac{1}{r_3}\left(\frac{1}{h}\right)\right]$$

where: $\Delta T_T = T_o - T_s$

T_o = temperature at the capillary center line

T_s = temperature of the surrounding environment

Q = power density

r = radius (subscripts 1, 2 and 3 refer to the radii as indicated in figure 1.13)

κ = thermal conductivity (subscripts 1, 2 and 3 refer to the thermal conductivities of the buffer, fused silica and polymer coating, respectively)

h = heat transfer coefficient from the capillary to the surrounding environment

One should realize that in most cases of practical interest, the magnitude of the overall temperature rise, $T_0 - T_s$, is dominated by the last term in equation (1.15)

1.16

$$T_o - T_s \approx \frac{Qr_1^2}{2r_3 h} = \Delta T_{w\text{-}s}$$

where: $\Delta T_{w\text{-}s}$ = temperature difference between outer capillary wall and surrounding environment

This results from the fact that the resistance to heat transfer (h) between the outside wall (w) of the capillary and the surrounding environment (s) is typically much larger than any of the other resistances.

The first term in equation (1.15) only describes the temperature difference between the capillary center line and the inside wall, being

1.17

$$\Delta T_{cap} = T_o - T_1 = \frac{Qr_1^2}{4\kappa_1} = \frac{EId^2}{16\kappa_1}$$

where: T_1 = the temperature at the inside capillary wall (with boundary condition: at $r = r_1$, $T = T_1$)

I = current density (A/cm^2)

d = capillary inside diameter

An example of the calculated temperature differences between the respective capillary interfaces (as indicated in figure 1.13 and formulated in equation (1.15) is given in table 1.4.

Table 1.4 clearly shows the validity of equation (1.16) and that under the specified conditions cooling of the capillary (with air or liquid) is absolutely necessary when an inner radius of ≥ 75 µm is used.

Equation (1.15) and table 1.4 indicate that it is advantageous to use narrow inner radii capillaries with large outer radii. As mentioned, the small volume limits the quantity of heat generated, even when several hundred

volts per centimeter are applied. In addition, the high inner surface-to-volume ratio helps dissipate the generated heat through the capillary wall. The large outer diameter is advantageous due to a reduction in the insulating properties of the polyimide and improvement of heat transfer to the surroundings. Although the polyimide coating is only a few microns thick, its low thermal conductivity significantly limits heat transfer.

There are a number of indicators that point at excessive heat generation and possible temperature gradients. These phenomena may be apparent when, with increasing voltage, a reduction in efficiency and/or a disproportionate, non-linear increase in EOF or solute mobility are observed.

Radius (µm)	Current (µA)	ΔT_{cap} (°C)	ΔT_{FS} (°C)	ΔT_{Pi} (°C)	$\Delta T_{w\text{-}s}$ (°C)	ΔT_T (°C)	T_0 (°C)
25	11.8	0.05	0.08	0.04	6.0 (h = 50)	6.2	31.2
					1.2 (h = 250)	1.4	26.4
					0.6 (h = 550)	0.8	25.8
50	47.1	0.19	0.19	0.16	24.0 (h = 50)	24.5	49.5
					4.8 (h = 250)	5.3	30.3
					2.2 (h = 550)	2.7	27.7
75	106.0	0.42	0.29	0.37	54.1 (h = 50)	55.2	80.2
					10.8 (h = 250)	11.9	36.9
					4.9 (h = 550)	6.0	31.0
100	188.5	0.75	0.33	0.66	96.3 (h = 50)	98.0	123.0
					19.3 (h = 250)	21.0	46.0
					8.8 (h = 550)	10.5	35.5
125	294.5	1.17	0.29	1.00	150.3 (h = 50)	152.8	177.8
					30.1 (h= 250)	32.6	57.6
					13.7 (h = 550)	16.2	41.2

Table 1.4
Calculated temperature gradients from capillary center to surrounding environment.
Conditions: E = 300 V/cm; I (current density) = 0.6 A/cm^2; i = I x πr_1^2 (capillary cross section), $\kappa_1$25° C (water) = 6.0 x 10^{-3}; κ_2 (FS) = 1.40 x 10^{-2}; κ_3 (Pi) = 1.55 x 10^{-3} (all in W/cm K), h (stagnant air) = 50; h (v_{air} = 2 m/s) = 250; h (v_{air} = 10 m/s) = 550 (W/m^2 K); v_{air} = velocity of the air over the capillary; FS (fused silica); Pi = polyimide (layer of polymer, coating the capillary outer surface), r_1 is a variable (from 25 to 125 µm), r_2 = 167 µm; r_3 = 187 µm; polyimide layer (Pi) = 20 µm.
Note *that in this calculations r_2 and r_3 are slightly different from the values indicated in figure 1.13!) at i = 0, $T_o = T_s$ = 25 °C.*

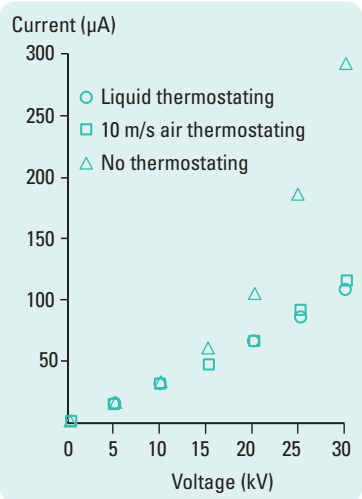

Figure 1.14
Ohm's law plots to monitor Joule heating.

Similarly, a non-linear increase in current with voltage (Ohm's law) indicates a temperature increase of the buffer in the capillary as depicted in figure 1.14.

A variety of methods to limit Joule heating are described in table 1.5. Equation (1.17) indicates that temperature gradients will be reduced with a reduction in power (Q). This can be accomplished by lowering either the applied voltage or decreasing the buffer conductivity by lowering the ionic strength ($I = 1/2 \sum_i c_i z_i^2$) or decreasing buffer ion mobility. The latter methods may be useful but have practical limitations. Reduced buffer concentration may decrease buffering capacity and may also lead to increased solute-surface interactions (see section 1.3.4.4.).

An alternative is the use of low mobility buffers that contain large, minimally charged ions, such as Tris, borate, histidine and CHAPS. Additional comments regarding buffer selection can be found in chapter 4.

A dramatic decrease in temperature differences can also be realized by reducing the capillary inner diameter (d) and therefore the electric current [$i = \kappa \cdot E \cdot (\pi d^2)/4$]. Capillaries with internal diameters as small as 5-10 µm have been used. However, such small inner diameters are not practical for routine use since difficulties in detection, sample loading and possibly capillary clogging have been described and discussed throughout the literature.

Removal of heat from the outer capillary wall, in order to decrease and stabilize the temperature difference between capillary center and its surrounding environment, is also extremely important. This can be accomplished by means of a cooling system, which thermostats the capillary with liquid or high velocity air circulation. Further details regarding temperature control can be found in chapter 3, section 3.3.

Variable	Effect
Decrease electric field strength.	Proportional decrease in heat generated. Reduces efficiency and resolution.
Reduce capillary inner diameter.	Dramatic decrease in current. Decreases sensitivity (pathlength, chapter 3). May increase sample adsorption.
Decrease buffer ionic strength or concentration.	Proportional decrease in current. May affect zone width (see 1.3.4.5). May increase sample adsorption.
Active temperature control.	Thermostat. Removes heat from capillary.

Table 1.5
Methods to control Joule heating and temperature gradients.

1.3.4.3. Injection plug length

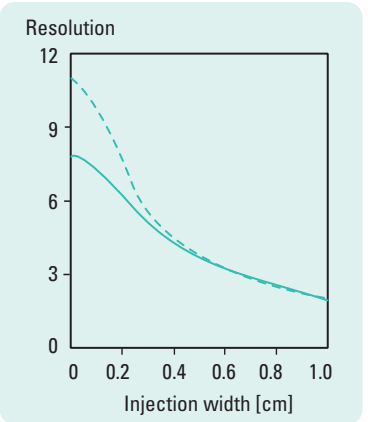

Figure 1.15
Effect of injection plug length on resolution.[9]
Calculation using:
Upper curve = 20 kV,
lower curve = 10 kV,
$\mu_{e1} = 3.0 \times 10^{-4}$ cm^2/Vs,
$\mu_{e2} = 3.15 \times 10^{-4}$cm^2/Vs,
$\mu_{EOF} = 3.0 \times 10^{-4}$ cm^2/Vs,
diffusion coefficients = 7×10^{-5} cm^2/s.

During injection it is important that the sample plug length be minimized. If the length is longer than the dispersion caused by diffusion, efficiency and resolution will be sacrificed. This is illustrated in figure 1.15.

Assuming that the sample solution enters the capillary as a rectangular plug, the contribution of injection to the total variance is given by

1.18
$$\sigma^2_{inj} = \frac{w_i^2}{12}$$

where w_i = injection plug length

Ideally, the sample plug length should be less than the standard deviation due to diffusion, $(2Dt)^{1/2}$. The exact length depends both on the diffusion coefficient of the solutes and on the analysis time. Macromolecules can have diffusion coefficients 100 times lower than small solutes and will necessitate smaller sample plugs. The relationship between injection plug length and diffusion coefficient and their effect on efficiency is illustrated in table 1.6.

Injection length (mm)	N (D=10^{-5} cm^2/s)	N (D=10^{-6} cm^2/s)
1	238,000	1,400,000
2	164,000	385,000
10	81,000	112,000

Table 1.6
Effect of injection length and diffusion coefficient on efficiency.

A practical injection length should be limited to less than 1 to 2 % of the total capillary length. For a 70-cm capillary, a 1 % length corresponds to 7 mm (or 14 nL for a 50 µm id). While current instrumentation can load these small volumes reproducibly, under typical conditions detection limit constraints often necessitate longer injection lengths. Methods to improve detection limits without degrading efficiency are discussed in chapter 3.

1.3.4.4. Solute-surface interactions

Interaction between the solute and the capillary wall has a detrimental effect on efficiency in CE. Depending on the extent of interaction, peak tailing and even total adsorption of the solute can occur. The primary causes of adsorption to the fused silica walls are ionic interactions between cationic solutes and the negatively charged wall, along with hydrophilic and hydrophobic interactions. The large surface area-to-volume ratio of the capillary, which is beneficial for heat transfer, in fact increases the likelihood of adsorption. Significant adsorptive effects have been noted especially for large peptides and proteins primarily because these species possess numerous charges and hydrophobic moieties.

In essence, these interactions can be regarded to be of chromatographic nature and are treated as such below. The variance due to adsorption can be given by

1.19

$$\sigma^2_{ads} = \frac{k' v_{EOF} l}{(1 + k')^2} \left(\frac{r^2 k'}{4D} + \frac{2}{K_d} \right)$$

where
- k' = capacity factor
- v_{EOF} = electroosmotic flow velocity
- D = solute diffusion coefficient
- l = capillary effective length
- K_d = first order desorption rate constant
- r = capillary inner radius

The capacity factor is defined like in liquid chromatography

1.20

$$k' = \frac{t_r - t_0}{t_0}$$

where
- t_r = elution time of a retained solute
- t_0 = elution time of an unretained solute

Equation (1.19) describes both radial diffusion (that is, across the capillary) and adsorption-desorption kinetics (K_d). The variance is strongly dependent on the magnitude of the capacity factor. As shown in figure 1.16 and table 1.7, small interactions can have dramatic effects on efficiency. Capacity factors even less than 0.1 can be detrimental. In practice, protein separations typically exhibit capacity factors between 0.01 to 0.1. Thus, plate counts between 10^6 to 10^4 may be expected.

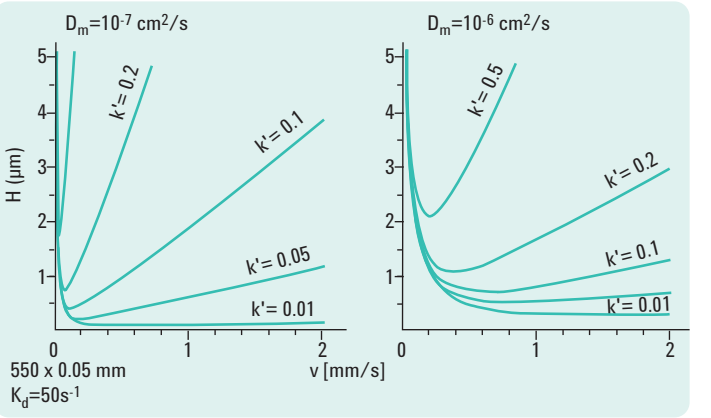

Figure 1.16
Effect of protein-wall interactions on HETP. Left panel: diffusion coefficient 10^{-7} cm²/s. Right panel: diffusion coefficient 10^{-6} cm²/s.

k'	H (µm)	N
0.001	0.04	1.3×10^7
0.005	0.24	2.3×10^6
0.010	0.55	1.0×10^6
0.050	5.4	1.0×10^5
0.100	16.2	3.4×10^4

Table 1.7
Impact of adsorption on efficiency.
Conditions: D = 10^{-6} cm²/s; v_{EOF} = 1 mm/s; l = 55 cm; L = 60 cm; K_d = 50 s^{-1}; r = 25 µm.
Note: *the mean desorption time of the adsorbed molecules is expressed as $t_d = 1/K_d$. Thus for $K_d = 50\ s^{-1}$ $t_d = 0.02$ seconds and for $K_d = 10\ s^{-1}$, $t_d = 0.1$ seconds.*

There are a variety of strategies employed to reduce solute wall interactions. These are in depth discussed in chapter 4.

1.3.4.5. Electrodispersion[10]

In this section the phenomenon of electrodispersion in CE is discussed in a qualitative way.

In CE, the capillary contains a buffering solution or back ground electrolyte (BGE) in which analyte ions are separated, under the influence of the electric field, since the zones are migrating with different velocities. The BGE should provide constant conditions for the analyte ions during their separation. This means that these conditions should be independent of the sample composition and only then can a sample be identified by its migration time.

The velocity of an analyte zone is the product of the effective mobility (μ_e) of the analyte ion and the local electric field strength (E) in this zone. The role of the BGE is to keep these two factors constant. The effective mobility of an ionic species is kept constant when the pH of the BGE remains constant. That's why the BGE is a buffering solution in which not only weak acids or bases (for which μ_e is a function of pH) are separated but also strongly acidic and basic compounds. For the latter compounds the pH should be constant and stable in order to maintain a constant EOF from run to run.

The presence of analyte ions in a zone will influence the local electric field in that zone. This arises from the observation that the electric current (i) is proportional to the local field strength and the electrical conductivity κ_e in the solution as expressed by

1.21

$$\mathbf{i = A \,.\, \kappa_e(x) \,.\, E(x)}$$

where A = cross section of the capillary $[(\pi d_c^2)/4]$
$\kappa_e(x)$ = local electrical conductivity
E(x) = local electric field strength

The current will be constant over the length of the capillary. This means that at a position (in a zone) where the conductivity is higher than that of the pure BGE, the local field strength will be lower and vice versa. Analyte ions in a zone will almost inevitably change the local conductivity to some extent and the difference in conductivity with that of pure BGE

will increase with the concentration of the analyte. This causes a dependence of the velocity of an analyte zone on its concentration. However, a suitable buffer solution (as the BGE) will keep this effect as small as possible.

The dependence of the local field strength on the concentration of the analyte ion within a zone may lead to broadening of the zone by a process called electrodispersion.

This phenomenon is illustrated in figure 1.17. By first assuming that the conductivity of the analyte solution increases with increasing analyte concentration (figure 1.17A), the field strength, and therefore the electrophoretic velocity of the analyte ions, will be relatively low in that part of the zone with a high analyte concentration.

A zone with an originally symmetric, triangular or Gaussian concentration profile will be deformed, since the front end will migrate at a higher velocity than the apex (peak maximum), while the tail of the original symmetric

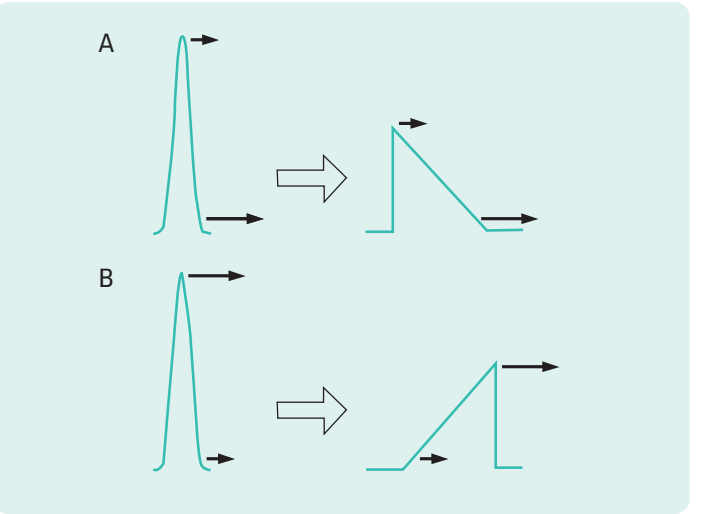

Figure 1.17
Zone broadening and peak deformation when the migration velocity decreases (A) or increases (B) with the concentration of the analyte.[10]

peak will catch up with the apex. In this manner a triangular concentration profile will develop with a sloping front and a steep backside. During electrophoresis the distance between the fast moving front and the slower moving peak maximum will steadily increase. The second situation in which the conductivity of the analyte solution decreases with analyte concentration (for example since the mobility of the analyte ions is lower than the BGE ions) is depicted in figure 1.17B. Here, the front end of the zone is overtaken by the peak maximum, while the tail lags continuously further behind during electrophoresis. A triangular peak with a sharp front and a sloping back side will develop. In both cases this will result in broadening zones.

Electrodispersion is a general phenomenon in CZE, and its effect is more pronounced with increasing sample amounts so that it is also called sample overloading.

Overloading can be recognized from the following indicators:

- with increasing analyte amount symmetrical peaks are deformed into tailing or fronting triangular peaks; in one electropherogram both tailing and fronting peaks may be observed.
- the width of a triangular peak increases with the amount of analyte injected
- peak heights do not increase proportional with the amount of analyte injected; due to increasing peak widths
- migration times of peak maxima are slightly shifted with increasing injected amount
- overloading effects decrease with a higher salt concentration in the BGE

Electrodispersion is particularly evident with complex samples containing solutes with a wide range of effective mobilities. An example of the separation of inorganic ions and organic acids is illustrated in figure 1.18.

Note *the fronting and tailing shapes of the peaks with high and low effective mobilities, respectively.*

Many important features of CE, such as electrodispersion, sample stacking and indirect photometric detection (see chapter 3), can be predicted theoretically by means of moving boundary equations that describe mass

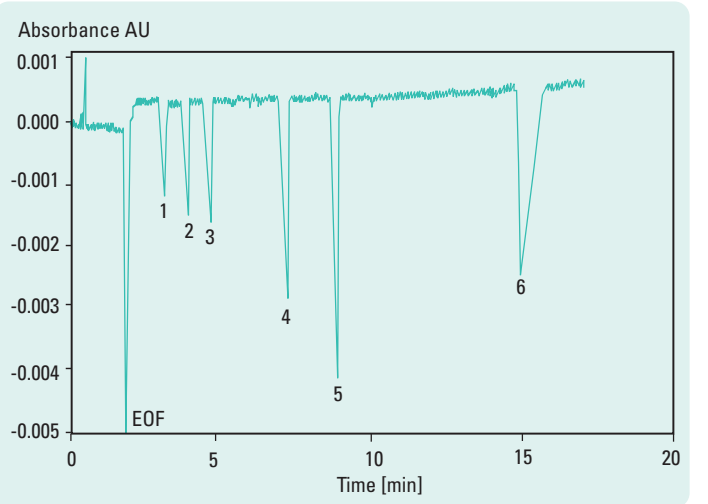

Figure 1.18
Fronting and tailing of solutes due to electrodispersion.[11]
Peaks: 1) Chloride, 2) Chlorate, 3) Fluoride, 4) Acetate, 5) Proprionate, 6) MES.
Conditions: Detection = Indirect UV, buffer = 0.01 M benzoic acid adjusted to pH 8 with Tris and addition of 0.05 % MHEC to suppress EOF, sample concentration = $5x10^{-4}$ M, detection wave length = 254 nm, V = -25 kV, l = 50 cm, L = 57 cm, id = 75 µm.

tranport during electrophoresis. For systems containing multiple ionic species, a derivation of these equations with an elegant general solution was submitted by Friedrich Kohlrausch[12] in 1897. This general solution is now called the Kohlrausch Regulation Function (KRF) and expressed as

1.22

$$\sum_i \frac{|z_i|\, c_i}{\mu_i} = \omega$$

where z_i = valence of ion i
c_i = concentration
μ_i = mobility
ω = constant (Kohlrausch value at any point in the buffer solution)

The KRF and descriptions given in this chapter have laid base for modelling and simulation of CE separations like PeakMaster by Gas *et al.* (http://www.natur.cuni.cz/~gas/).

1.3.4.6. Unleveled buffer reservoirs

As described in section 1.3.4 (table 1.3), maintaining equal liquid levels in the buffer reservoirs is important to both efficiency and migration time reproducibility. Siphoning from capillary inlet- to outlet-reservoir, or vice versa, will superimpose hydraulic flow in the capillary. This is not only disadvantageous to reproducibility but also to the efficiency. The influence of non-equal level reservoirs is dependent on the diameter and length of the capillary and the viscosity of the buffer. Clearly, wide-bore, short capillaries run at elevated temperatures would exhibit the most deleterious effects. It has been shown that a liquid height difference of 2 mm in one of the reservoirs can change migration time 2 to 3 % in a 50-µm id capillary. This increases to about 10 % in a 100-µm id capillary.

An automated buffer leveling system will accurately deliver liquid to a user-specified level during replenishment. It can also be used to re-level liquids in the running reservoirs caused by EOF, without emptying them first.

1.3.4.7. Detector

The output of the detector represents a signal that is averaged over a finite volume (the detector cell). The variance introduced in this manner (σ^2_{det}) is the same as that from a finite injection plug

1.23

$$\sigma^2_{det} = \frac{w_d^2}{12}$$

where w_d = the length of the detection cell

For CE applications, this contribution to the total variance of the system (σ^2_T in equation 1.16) can usually be neglected if w_d is roughly 3 times smaller than the incoming sample zone length.

1.3.5. Resolution

Resolution of sample components is the ultimate goal in separation science. Resolution is most simply defined as

1.24

$$R = \frac{2(t_2 - t_1)}{w_1 + w_2} = \frac{t_2 - t_1}{4\sigma}$$

where t = migration time
w = baseline peak width (in time)
σ = temporal standard deviation
subscripts 1 and 2 refer to the two solutes

The numerator in equation (1.24) describes the separation process in terms of differential migration and the denominator the zone broadening processes acting against it. Separation in CZE is primarily governed by efficiency, not selectivity. This is in contrast to liquid chromatography in which the opposite is usually true. Due to very sharp solute zones, small differences in solute mobility (< 0.05 % in some cases) are often sufficient for complete resolution. Of course, the extent of zone broadening is immaterial if sufficient mobility differences are realized.

The resolution of two components can also be expressed with respect to efficiency

1.25

$$R = \frac{1}{4} N^{1/2} \left(\frac{\Delta\mu_a}{\bar{\mu}_a} \right)$$

where $\Delta\mu = \mu_{a2} - \mu_{a1}$

$$\bar{\mu}_a = \frac{\mu_{a2} + \mu_{a1}}{2}$$

*(**Note:** time or velocity can be substituted for mobility). Substituting equation (1.12) into equation (1.25) yields a commonly cited theoretical equation for resolution (1.26) that does not require explicit calculation of efficiency, N. This equation also describes the effect of EOF on resolution.*

1.26 $$R = \left(\frac{1}{4\sqrt{2}}\right)(\Delta\mu_a)\left(\frac{V}{D(\bar{\mu}_a + \mu_{EOF})}\right)^{1/2}$$

In contrast to efficiency, which increases linearly with applied voltage (equation 1.T4), a similar gain in resolution is not found, due to the square root relationship. The voltage must be quadrupled to double the resolution. The generation of Joule heat often limits the benefits gained from this action. It is evident from equation (1.26) that infinite resolution will be obtained when μ_a and μ_{EOF} are equal but opposite. That is, when the ion migrates in the opposite direction and at the same rate as the EOF. In this case, however, the analysis time approaches infinity. Clearly, the operational parameters should be controlled so as to balance resolution and analysis time.

1.4. Characteristics of capillary electrophoresis

- Electrophoresis is performed in narrow-bore (25- to 75-µm id), fused silica capillaries
- High voltages (10 to 30 kV) and high electric fields (100 to 500 V/cm) are applied across the capillary
- High electrical resistance of the capillary limits current generation and internal heating
- High efficiency ($N>10^5$ to 10^6) and short analysis time
- Detection performed on-capillary (DAD, CCD, LIF), with an external detection cell (DAD) or on-line MS
- Small sample volume required (1 to 50 nL injected)
- Numerous modes to vary selectivity and wide application range
- Operates in aqueous and non-aqueous media
- Simple methods development
- Automated instrumentation

Chapter 2

Modes of Operation

Modes of operation

The versatility of capillary electrophoresis is derived from its numerous modes of operation. This is very much in analogy to liquid chromatography. In essence the different CE operation modes are to some extent equivalent to the basic separation modes used in liquid chromatography. This is illustrated in the table 2.1 below.

Liquid Chromatography	Electrophoresis
Elution: Separation based on partition between a mobile and stationary phase. Reversed phase, ion exchange, normal & polar bonded phase, hydrophobic interaction.	**Elution:** Separation based on differences in zone velocity. Capillary zone electrophoresis (CZE), micellar electrokinetic chromatography (MEKC), capillary electrochromatography (CEC).
Molecular Sieving: Separation based on movement through a stationary phase according to size and shape. Size exclusion chromatography (SEC).	**Molecular Sieving:** Separation based on movement through a stationary or immobile phase (gel) according to size and shape. Capillary gel electrophoresis (CGE).
Chromatofocussing: Separation based on pH gradient delivered by mobile phase through an ion exchange stationary phase.	**Capillary Isoelectric Focussing (CIEF):** Separation by movement through a stationary pH gradient in the run buffer.
Displacement Chromatography: Separation based on moving a strong adsorbing zone (displacer) through a stationary phase. Sample molecules move as zones in front of the displacer with the solvent velocity.	**Capillary Isotachophoresis (CITP):** Separation based on a moving electric field gradient from leading to terminating electrolyte causing all sample molecules to move as connected zones with constant concentration with the same velocity.

Table 2.1
Modes of operation.

Despite the principle analogy of HPLC and CE separation modes, the underlying mechanisms are different, in particular regarding the "elution" modes of CE. Therefore, the selectivity of separation, that is the order in which the sample components elute, will be strongly deviating when comparing an HPLC with a CZE, MEKC or CEC separation. The separation mechanisms are orthogonal and therefore complimentary information is obtained about a sample. For example substances that co-elute in HPLC will be separated in CE.

In contrast to liquid chromatography, where partitioning and size exclusion chromatography is ubiquitously used, in capillary electrophoresis all modes

are used in practice. It is however imperative to understand the abilities and strengths of each individual CE mode and where a particular mode is best used for.

For the most part, the different modes are accessed simply by altering the buffer composition. Modern instrumentation supports the modes by providing specific settings.

In the previous chapter (1) the fundamentals of movement of charged molecules in an electrical field applied along the axis of a capillary filled with an electrolyte, has been explained. Factors affecting the speed, shape and width of the charged molecule zone have been discussed. In the next sections the basis for separation in the different modes will be described with emphasis on basic operation and relevant applications.

2.1. Capillary zone electrophoresis (CZE)

Capillary zone electrophoresis (CZE) is the simplest form of CE. In CZE a capillary is filled with an electrolyte (run buffer), the sample is introduced at the inlet and the electrical field is applied. As shown in figures 2.1 and section 1.11, separation occurs because solutes migrate at different velocities and in discrete zones.

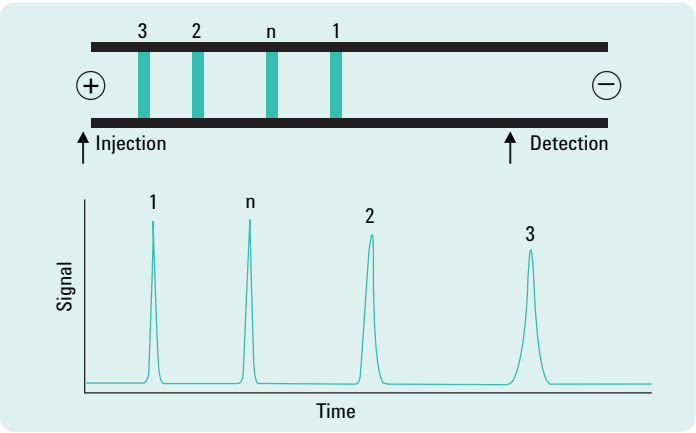

Figure 2.1
Differential solute migration superimposed on electroosmotic flow in capillary zone electrophoresis. The cationic analyte (1) has the highest mobility followed by the neutrals (n) and two anionic analytes (2, 3).

The velocity of each solute is given by equation 1.1. As explained in section 1.3.1., the electrophoretic mobility is a substance specific property depending mainly on the charge/size ratio of the ion. Small, highly charged ions move fast, large, lowly charged ions move slow. Solutes move towards the electrode of opposite charge that is anions move to the anode, cations move to the cathode.

Besides by electrophoretic movement, the solute zones are also moved through the capillary by the EOF (see section 1.3.2.). Direction of the EOF will be aligned with the direction of movement of either the anions or cations and will be towards the point of detection (figure 2.1).

Therefore separation of both anionic and cationic solutes is possible by CZE in one analysis. Ions moving in opposite direction of the EOF are swept to the detector since the EOF is in most cases significantly larger than the electrophoretic mobility. Neutral solutes all move with the EOF and are not separated (see section 2.2 and 2.3 for a solution).

It is thus essential for CZE to have control over the electrophoretic mobility of the solutes and over the electroosmotic flow. That is all the factors introduced in chapter 1 that effect ion mobility, EOF, and zone width come into play in order to optimize and control separation in CZE. That is both the time of analysis, the order of separation and reproducibility of separation are crucial parameters for the overall method.

Factors influencing EOF have been given in table 1.1. Electrophoretic mobility is influenced by all factors that affect the charge/size ratio. That is by adjusting the pH of the electrolyte (run buffer), the degree of ionization of the ions can be altered. Therewith the charge to size ratio changes and the electrophoretic mobility changes (see figure 1.3.). Alternatively the type of buffer (inorganic, organic, zwitter ionic) used or presence of organic solvents will strongly affect mobility and EOF. Some of these effects will be dealt with in chapter 4.4.1.

Wall interactions that affect zone broadening can be suppressed by operating at pH extremes. That is at low pH (< 2 to 3) the weakly acidic silanol groups at the fused silica inner capillary surface, will be protonated and uncharged. Zeta potential (see 1.3.2.) will be minimal and therefore

the EOF will be nearly zero. Since proteins (and other species) will also be protonated and positively charged at low pH, they will migrate towards the cathode without coulombic attraction to the neutral capillary surface. Conversely, at high pH (>8 to 10), both the wall and the sample will be deprotonated and negatively charged, and solute-wall interactions will be limited by charge repulsion. This behavior is illustrated in figure 2.2 with a highly efficient separation of proteins.

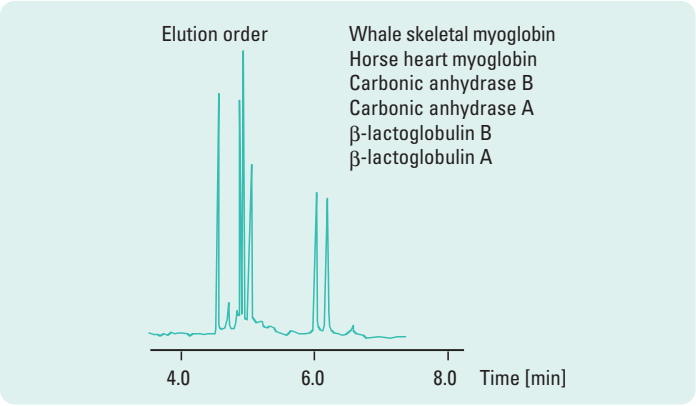

Figure 2.2
CZE of proteins using buffer pH above solute pI.[13]
Conditions: 20 mM borate pH 8.25, V = 30 kV, l = 55 cm, L = 101 cm, id = 52 µm, i = 38 µA.

2.2. Micellar elektrokinetic chromatography (MEKC)

Micellar electrokinetic chromatography (MEKC) is a hybrid of electrophoresis and chromatography. Introduced by Terabe[14] in 1984, MEKC is now a widely practiced CE mode in (bio)pharmaceutical analysis and increasing in food-, environmental- and clinical analysis. Its main strength is that it is the only electrophoretic technique that can be used for the separation of neutral solutes as well as charged ones.

The separation of neutral species by MEKC is accomplished by the use of surfactants in the running buffer. At concentrations above the critical micelle concentration (8 to 9 mM for sodium dodecyl sulfate (SDS), for example), aggregates of individual surfactant molecules, micelles, are

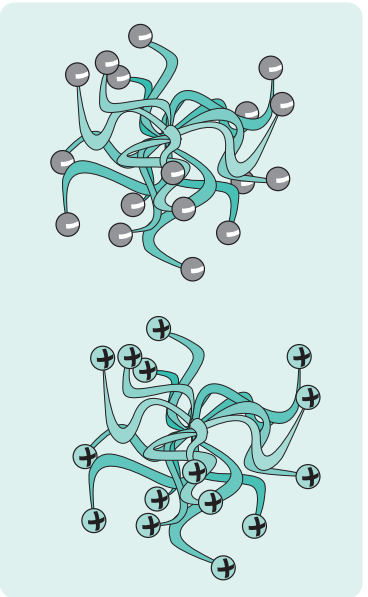

Figure 2.3
Schematics of cationic and anionic micelles.

formed. Micelles are often spherical with the hydrophobic tails of the surfactant molecules oriented towards the center, and the charged heads oriented outside towards the buffer. A representation of micelles is depicted in figure 2.3.

The surfactant and thus the micelles are usually charged and migrate either with or against the EOF (depending on their charge). Anionic surfactants such as SDS migrate toward the anode, that is, in the opposite direction to the EOF. Since the EOF is generally faster than the migration velocity of the micelles at neutral or basic pH, the net movement is in the direction of the EOF. During their electrophoretic migration, the solutes partition between the micelles and the running buffer in a chromatographic manner through both hydrophobic and electrostatic interactions. The micelles act as a stationary phase like in chromatography. In contrast to chromatography though, this stationary phase is moving!

For neutral species, only partitioning in and out of the micelle effects the separation. The stronger the solute interacts with the micelle the longer is its migration time since the micelle carries it against the EOF. When the solute is not in contact with the micelle it is simply carried with the EOF. The more hydrophobic compounds interact more strongly with the micelle and are "retained" longer. It is this differential interaction between micelles and neutral species that causes a separation. The overall MEKC separation process is depicted schematically in figure 2.4.

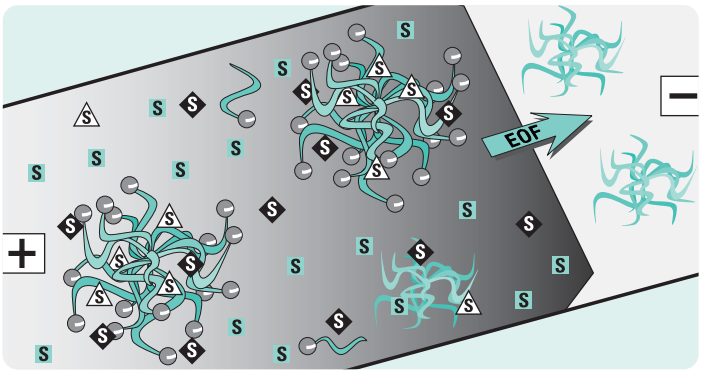

Figure 2.4
Separation in MEKC (s = solute).

The separation mechanism of neutral solutes in MEKC is essentially chromatographic and can be described using modified chromatographic relationships.

The ratio of the total moles of solute in the micelles, the pseudo-stationary phase, to those in the mobile phase, the capacity factor (k'), is given by:

2.1

$$k' = \frac{(t_r - t_0)}{t_0\left(1 - \frac{t_r}{t_m}\right)} = K\left(\frac{V_S}{V_M}\right)$$

where
- t_r = retention time of the solute
- t_0 = retention time of unretained solute moving at the EOF rate (or "dead time")
- t_m = micelle retention time
- K = partition coefficient
- V_S = volume of the micellar phase
- V_M = volume of the mobile phase

This equation is modified from the normal chromatographic description of k' to account for movement of the pseudo-stationary phase. Note that as t_m becomes infinite, if the micelle becomes truly stationary, the equation reduces to its conventional chromatographic form. Resolution of two species in MEKC can be described by

2.2

$$R = \left(\frac{N^{1/2}}{4}\right)\left(\frac{\alpha - 1}{\alpha}\right)\left(\frac{k'_2}{k'_2 + 1}\right)\left(\frac{1 - \left(t_0/t_m\right)}{1 + \left(t_0/t_m\right)k_1}\right)$$

Efficiency | Selectivity | Retention

where $\alpha = k_2' / k_1'$

From equation (2.2), resolution can be improved by optimizing efficiency, selectivity, and/or the capacity factor. With regard to the capacity factor,

this can be most easily adjusted by varying the concentration of the surfactant. Generally, the capacity factor increases linearly with concentration. A potential problem with the use of ionic surfactants, especially at high concentrations, is the increase in generated current. Power generation exceeding 5 to 10 W/m at moderate field strengths can develop. Even with narrow bore capillaries (25 to 50 µm) the use of extremely high electric fields is often avoided and efficient capillary thermostating is necessary (see section 3.3).

In MEKC the solutes elute between t_0 and t_m. Resolution is improved by extending the elution range or time window. In the separation of neutral solutes, all solutes elute between t_0 and t_m (figure 2.5). Hydrophilic solutes that do not interact with the micelle elute with the EOF and those that are totally retained by the micelles (Sudan III, for example) elute with the micelles. While the time window is often fairly small, the peak capacity can be very high due to the high efficiency. It is therefore desirable to employ conditions that open the time window, that is, moderate EOF and micelles exhibiting high mobility.

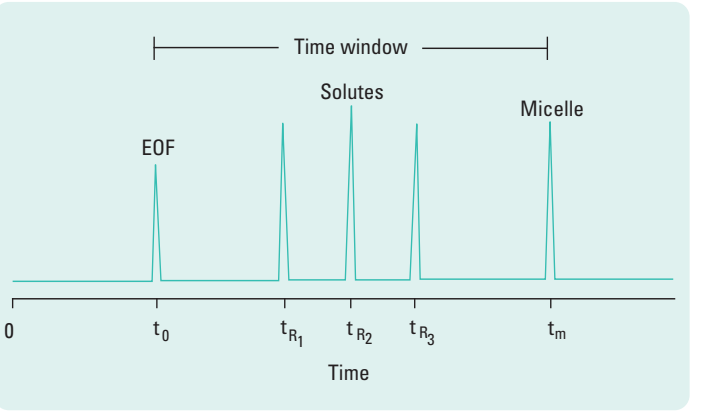

Figure 2.5
Elution time window for neutral solutes in MEKC.

Selectivity can easily be manipulated in MEKC. Varying the physical nature of the micelle such as size, charge or geometry by using different surfactants can yield dramatic changes in selectivity, similar to those obtained by

changing the stationary phase in LC. Surfactants can be anionic, cationic, non-ionic, zwitterionic, or mixtures of each (table 2.2). In each category, alkyl chain length or structure can also be varied. In addition, MEKC can be performed using bile salts or microemulsions, oil in water (o/w) and water in oil (w/o)[15]; (called micro-emulsion electro-kinetic chromatography (MEEKC)). In all cases, variations in buffer concentration, pH, temperature, or use of additives such as urea, metal ions, or chiral selectors can also be used to affect selectivity.

	Biological detergents	CMC (mM)	Aggregation number
Anionic	SDS	8.2	62
Cationic	DTAB	14	50
	CTAB	1.3	78
Non ionic	Octylglucoside	—	—
	n-Dodecyl-β-D-maltoside	0.16	—
	Triton X-100	0.24	140
Zwitterionic	CHAPS	8	10
	CHAPSO	8	11
Bile salt	Cholic acid	14	2 – 4
	Deoxycholic acid	5	4 –10
	Taurocholic acid	10 –15	4

Table 2.2
Surfactants used in MEKC.

Note: *the CMC of surfactants in buffer solutions is usually lower than that in water as indicated in the table; for example CMC of SDS is 8 mM in water but down to 3 mM in common buffer solutions.*

Like in chromatography, organic modifiers can be added to manipulate solute-micelle interaction. Modifiers, such as methanol, acetonitrile, and 2-propanol have all been used successfully. Added to the running buffer in concentrations from a few percent up to 50 % (v/v) can lessen hydrophobic interactions between the solute and micelle, allowing more rapid chromatographic kinetics.

Surfactants used for MEKC can also interact with the capillary wall and have dramatic effects on the EOF as well as solute-wall interactions (see chapter 4, section 4.1). The direction of solute and micelle migration varies

and depends on the micelle charge and the rate of EOF. Generally, high pH buffers are used to maintain reasonable EOF and ensure migration direction.

For (bio)pharmaceuticals, MEKC has been used for the determination of active drugs in tablets, creams, and injectable formulations. The separation of the active ingredients of a cold-relief preparation using SDS micelles is illustrated in figure 2.6.

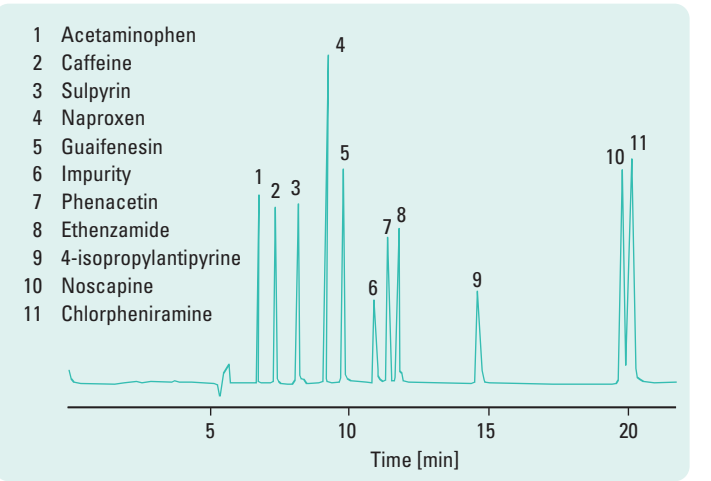

Figure 2.6
MEKC separation of cold-relief medicine constituents.
Conditions: 20 mM phosphate-borate, 100 mM SDS, pH 9.0, V = 20 kV, L = 65 cm, id = 50 µm, λ = 210 nm.

It should be noted that especially in MEKC and MEEKC temperature control is extremely important due to its effects on both CMC and the distribution coeficient (K). Increase in temperature causes an increase in CMC and hence a decrease in the micellar concentration ($C_{micelles}$), affecting k′. The distribution coefficient (K) decreases with increasing temperature.

2.3. Capillary electro-chromatography (CEC)

Capillary electrochromatography (CEC), is a form of miniaturized liquid chromatography, which uses an electric field to pump liquid (EOF) through a packed chromatography column. The original idea came from Pretorius in 1974[16], but was neglected until revived by Jorgenson and Lukacs in 1981.[17] However, at that time, CEC was overshadowed by the rapid development of capillary electrophoresis. In the late 80's Knox and Grant[18,19] undertook a detailed study of the main parameters of CEC, and from that time onwards, CEC has undergone exponential expansion, with a doubling period of about two years.

In CEC, a stationary phase packed in a fused silica capillary, with an id of 50-200 µm, is used to obtain separation. HPLC type silica based reversed phase particles, 1-5 µm, have been mainly used as a stationary phase. Mobile phases, typical for RP-type separations, such as organic solvent/ aqueous buffer mixtures, are used. On application of an electrical field along the axis of the packed capillary, an electro-(endo)-osmotic flow is established (see section 1.3.2.), which transports the solutes and the mobile phase through the packed bed. When the solutes are uncharged, separation is obtained by differential partitioning of the solutes between mobile and stationary phase. When the solutes to be separated are charged, they will have an additional, electrophoretic velocity component which will contribute to (or counteract) separation. The technique is very similar to CZE. Therefore, the equipment used for capillary electrophoresis can be used to execute CEC without major modification. A simple schematic of a system for CEC is given in figure 2.7.

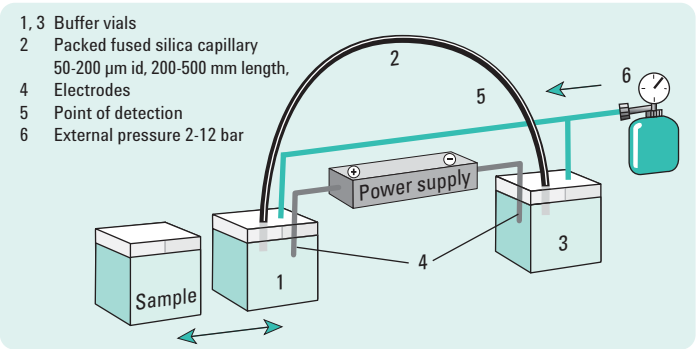

Figure 2.7
Schematic description of a system for CEC.

In section 1.3.2. it was discussed how the bulk flow of liquid (EOF) through a capillary, resulted from the application of an electric field on the solution double-layer at the wall (redepicted in figure 2.8).

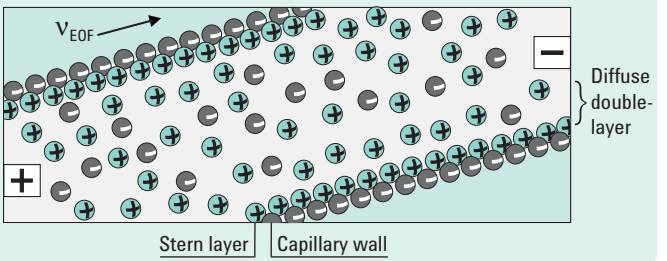

Figure 2.8
Illustration of the solid/liquid interface in a fused silica capillary filled with an electrolyte solution.

The velocity of this flow (v_{EOF}) is formulated by

2.3
$$v_{EOF} = \frac{\varepsilon\zeta E}{\eta} \approx \frac{\varepsilon\psi_0 E}{\eta} = \frac{\sigma^* E}{\delta\eta}$$

where
- ε = solution dielectric constant
- ζ = zeta potential $\approx \psi_0$ (wall potential)
- σ^* = charge density at surface of shear (where ζ imposes its influence)
- δ^{-1} = double layer thickness
- η = solution viscosity
- E = electric field strength

and the inverse double layer thickness (δ) is expressed by

2.4
$$\delta = \sqrt{\frac{\varepsilon RT}{2F^2 I}}$$

where
- R = gas constant
- T = temperature
- F = Faraday's constant
- I = ionic strength ($= 1/2\ \Sigma\ C_i\ z_i^2$; C_i = buffer concentration and z_i = ion valence)

When the capillary is packed with silica based particles a double-layer is also formed in and around the particles. Upon application of an axial electric field, the solvent starts to move in the direction of the cathode. This is illustrated in figure 2.9.

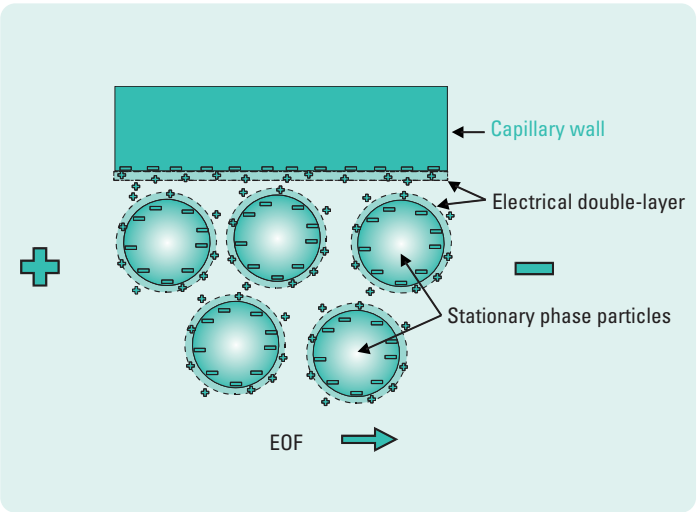

Figure 2.9
Depiction of the generation of electroosmotic flow in a packed capillary.[20]

Inserting reasonable values for the parameters in equation (2.3) for example 100 mV for the zeta potential which is typical for an unmodified silica surface in an aqueous buffer solution at pH 4, an EOF should be attained with a velocity from 0.8 mm/s at 100 V/cm to 3.2 mm/s at 400 V/cm. In order to avoid outgassing and bubble formation in the column at high currents, buffer vials on inlet and outlet side are pressurized at 2-12 bar. As experimental proof, the EOF obtained with a CEC column was measured and the results given in figure 2.10.

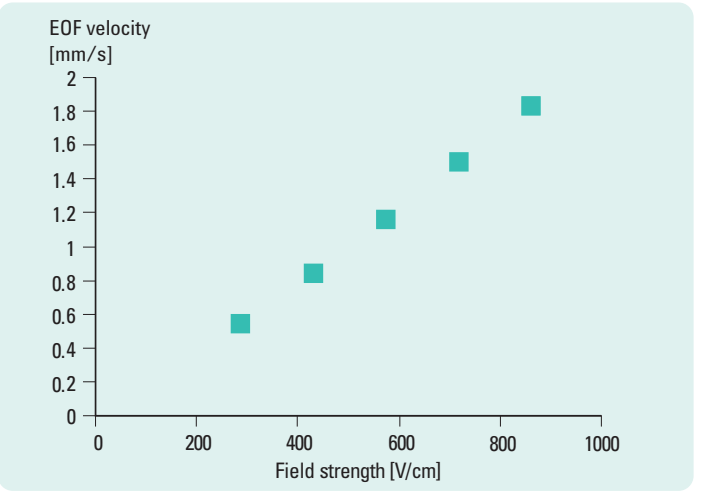

Figure 2.10
Experimental verification of the magnitude of the EOF in a packed capillary in dependence of the applied field.[21]
Conditions: Column: CEC-Hypersil C18, 3 µm, 250(335) x 0.1 mm; mobile phase: acetonitrile/morpholino-ethylsulfonic acid (MES) 25 mM pH 6 80/20, temperature: 20 °C.

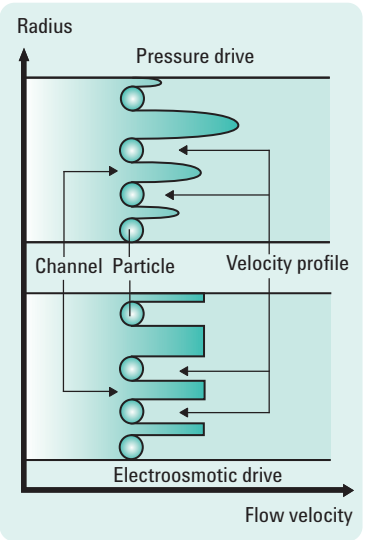

Figure 2.11
Depiction of the flow velocity profile in a packed bed in electro drive and pressure drive.

The generated EOF in the particle packed capillary has a velocity flow profile identical to that in an open-tubular capillary (figure 1.7A, section 1.3.2.) and is shown in figure 2.11.

The velocity of pressure driven flow varies with the diameter of the channels. Solutes may find fast and slow flow paths through the column, resulting in zone broadening. In an electrically driven system, the flow velocity is largely independent on the channel width, such that solutes changing from one channel to the other do not experience a change in flow velocity. This results in much lower zone dispersion.

The net result of this is a 30-60 % reduction of the HETP of a capillary HPLC column driven by electrical force compared to pressure driven mode, depending on the particle size, capacity ratio and velocity. This is illustrated by the chromatogram of figure 2.12 where the individual peaks have an efficiency of 60-70,000 plates. In the HPLC mode the column will generate 25-30,000 plates, maximally.

The electrical force on the solvated cations is exerted equally over the length of the column in contrast to the hydraulic force, which is applied to the inlet of the column and dissipates linearly over the length of the column. The hydraulic pressure needed to drive the liquid, at a particular velocity through the packed capillary, increases with the inverse of the square of the particle diameter. The pressure also increases linearly with the length of the packed bed. As a result, the attempt to increase the efficiency of an HPLC separation by reducing the particle size and/or increasing the column length is penalized by a severe increase in pressure or decrease in speed of analysis.

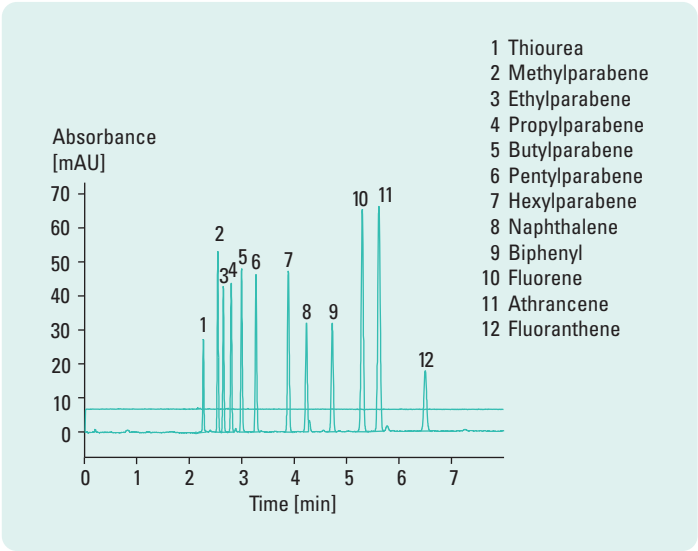

Figure 2.12
Example of a CEC separation. Conditions as in figure 2.10. Voltage is 25 kV. Sample injection electrokinetic.[21]

In the electro-driven case this does not occur. Therefore longer columns with smaller particles can be used in CEC than feasible in HPLC. As an example, a chromatogram obtained on a column with 40 cm bed length and packed with 3 µm particles is given in figure 2.13.

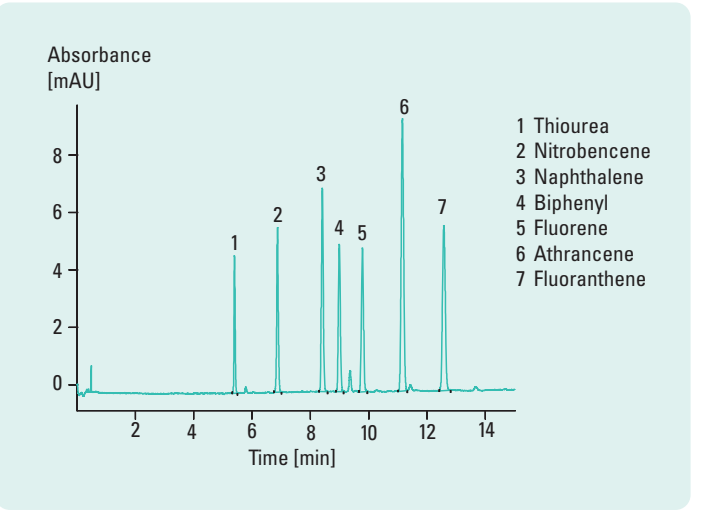

Figure 2.13
The 100,000 plates column.
Conditions: Column: Spherisorb ODS1, 3 µm, 400(485)x0.1 mm;
mobile phase: acetonitrile/Tris 50 mM, pH 8, 80/20; voltage 30 kV, temperature: 20°C.[22]

On average, all peaks have an efficiency of 100,000 plates.

The better solvent transport mechanism in the electrodrive case thus leads to less zone broadening and the absence of back pressure. As a result, it can be predicted that in CEC a 3-10x better separation efficiency than in HPLC can be eventually achieved, leading to columns that generate 250,000-1,000,000 plates per meter in the same time as current HPLC separations. It must be emphasized that the above treatment applies to solutes that are neutral and separate only by partitioning between mobile and stationary phase. If the solutes are charged, they will undergo an accelaration or deceleration of their velocity depending on their actual net charge. Therefore CEC is a technique which can be best used for high efficiency separation of neutral or weakly acidic/basic solutes. Capillary zone electrophoresis (CZE) is then the method of choice for strongly charged solutes like strong acids and bases.

In summary:
The electroosmotic flow in a packed capillary differs from pressure driven laminar flow in three important aspects:

a) It has a plug flow velocity profile in the channels between the particles and the velocity is independent of the channel width. Therefore, in a packed bed there is much less cross-sectional flow velocity difference in electrical driven flow than in hydraulic flow.

b) Flow velocity is virtually independent of the particle size. No column backpressure is generated.

c) The presence of an electrical double-layer on the packing is a prerequisite for the generation of the EOF. The magnitude of the flow will therefore depend on the stationary and mobile phase used. These factors have a highly favorable effect on the zone broadening (HETP) that occurs in a CEC column when compared to an HPLC column.

Extensions of CEC from particle packed capillaries to open tubes with coated stationary phases[23] and monolithic phases in fritless capillaries[24, 25] have been described. For more theoretical details regarding these CEC considerations, see references 20, 21.

2.4. Capillary gel electrophoresis (CGE)

Slab gel electrophoresis has been employed in molecular biology research for the size-based separation of macromolecules such as proteins and nucleic acids. In order to separate proteins according to size they first have to be denatured, that is saturated with sodium dodecyl sulfate (SDS). The size separation is then obtained by electrophoresis of the solutes through a suitable polymer, which acts as a "molecular sieve".

This form of zonal electrophoresis in the capillary format (CGE) is illustrated in figure 2.14.

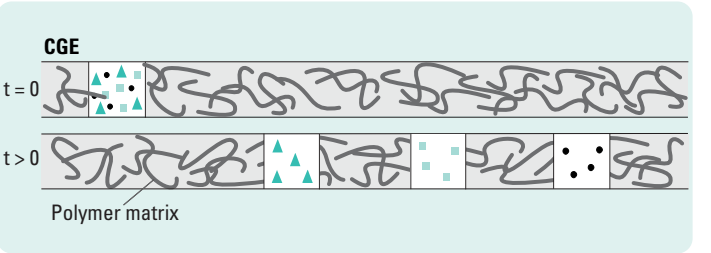

Figure 2.14
Size separation in CGE.

As charged solutes migrate through the polymer network they become hindered, with larger solutes hindered more than smaller ones. Macromolecules such as DNA and SDS-saturated proteins cannot be separated without a gel since they have invariable mass-to-charge ratios. That is, with DNA for example, each nucleotide appended to a DNA chain adds an equivalent unit of mass and charge and does not affect the mobility in free solution.

Capillary gel electrophoresis is directly comparable with traditional slab or tube gel electrophoresis since the separation mechanisms are identical. The capillary format offers a number of advantages over the traditional slab gel format for electrophoresis, including the use of 10x to 100x higher electrical field without the deleterious effects of Joule heating, on-capillary detection, and automation. In addition, due to the anti-convective nature of the capillary (that is no convective mixing due to the absence of a large radial temperature gradient) it is not necessary to use a gel that is itself anti-convective. An anti-convective gel needs a rigid structure and shape, which can only be obtained at a certain concentration and composition of its constituents. These requirements can therefore be abandoned in the capillary format, allowing the application of newly created "gels". The capacity to run preparative separations, considered a major advantage of the slab gel, can also be accomplished to a certain extent in CE by the use of wide-bore capillaries (internal diameters >100 to 200 µm) and low electric fields. The multi-lane capacity slab gels (previously used in DNA sequencing) are becoming displaced by capillary arrays filled with replaceable sieving "gels".

Traditionally, crosslinked polyacrylamide and agarose have been used in the slab or tube format. The former usually has smaller pore sizes and is applied for protein separations. The larger pores of agarose gels make them more suitable for DNA.

Use of the term "gel" in CGE is somewhat ambiguous. A gel usually implies a solid-like structure as used in slab gel electrophoresis. Since many of the "gels" used in CGE do not (and need not) possess this property, a more suitable term may be "polymer network". Polymers in CGE can be covalently crosslinked, hydrogen bonded or just dissolved in buffer solutions (such as uncrosslinked polyacrylamide, methylcellulose etc.). Although the polymer structure of the uncrosslinked gel is radically different from that of crosslinked gels, the mechanism of separation is identical. Subsequently, macromolecules can be size-separated using either gel type (table 2.3).

Polymer	Concentration	Application
Crosslinked polymers		
Polyacrylamide/bis- acrylamide	2– 6 % T, 3 – 6 % C_0	Oligonucleotides, DNA sequencing, native and SDS-bound proteins.
Linear polymers		
Polyacrylamide	< 0.1– 6 %	Restriction fragments.
Hydroxylalkylcellulose, polyvinylalcohol, dextran	6 –15 %	Oligonucleotides, DNA sequencing, proteins.
Agarose	0.05 –1.2 %	Restriction fragments, proteins.

Table 2.3
Polymer matrices for CGE.

To date, linear polyacrylamid (LPA) and polydimethylacrylamide (PDMA) are popular separation matrices for DNA sequencing and are now commonly used on commercial sequencers and genetic analyzers).

In situ preparation of crosslinked polyacrylamide in capillaries requires extreme care and appears to possess too many disadvantages for practical CGE. This type of gel has now been displaced by linear polymers.

Since they are essentially polymer solutions, they are much more flexible. The linear polymer solutions may also be polymerized *in situ*, but it is not

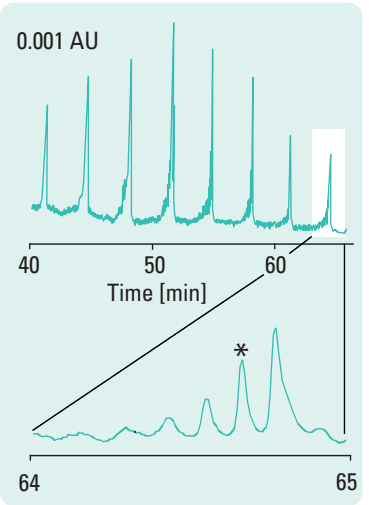

Figure 2.15
CGE separation of polydeoxythyamidylic acid mixture, p(dT)20-160 using crosslinked polyacrylamide.[26]
Conditions: Bis-crosslinked polyacrylamide (6 % T, 5 % C), 100 mM Tris, 25 mM borate, 7 mM urea, PH 7.6, E = 200 V/cm, i = 8.2 mA, l = 100 cm, id = 75 µm, λ = 260 nm, polyacrylamide coated capillary.

necessary. Pre-polymerized polymer can be dissolved in buffer and hydrodynamically loaded into the capillary. For polyacrylamide, a wide range of gel concentrations can be used (that is, below 1 % to more than 20 %). Generally, the polymer concentration necessary is inversely proportional to the size of the analyte.

With low viscosity polymer solutions, pressure can be used for sample injection and they can be repeatedly filled into the capillary (depending on concentration and viscosity). They are also less susceptible to bubble formation and other failures. While they possess more stability in these respects, the less viscous the gel the more dependent the system is on the integrity of the wall coating (if used). With either type, the capillary wall is usually coated to eliminate EOF.

Resolution and efficiency in CGE are virtually identical to that in CZE since they are both "zonal" electrophoretic techniques. One notable difference is the ultra high efficiency achievable for DNA separations. Figure 2.15 illustrates that over 10^7 plates/m can be realized for single-stranded oligonucleotides using crosslinked polyacrylamide.

An example of uncrosslinked polyacrylamide in PCR product analysis is shown in figure 2.16. Here, the analysis of a single-stranded DNA prepared by asymmetric PCR is depicted. The peaks were identified by a calibration curve obtained using DNA size standards. Note that the single-

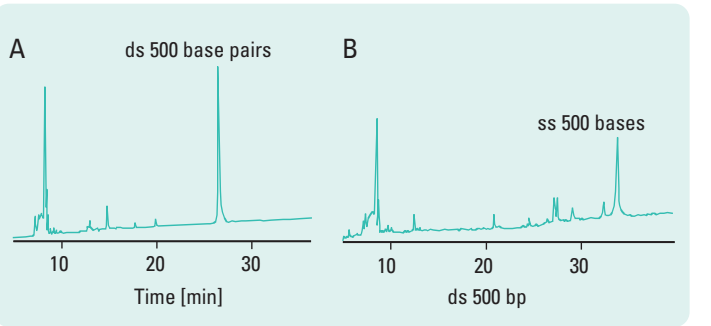

Figure 2.16
PCR analysis of single- and double-stranded DNA.[26]
Conditions: Uncrosslinked polyacrylamide (9 % T), 100 mM tris-borate, pH 8.3, E = 300 V/cm, i = 9 µA, l = 20 cm, L = 40 cm, id = 75 µm, λ = 260 nm, PA coated capillary wall.

stranded DNA migrates slower than the double-stranded DNA of the same size due to increased random 3-dimensional structure. In addition, the lack of specificity of asymmetric PCR yields more by-products than normal PCR.

As in CZE, selectivity in CGE can be altered by the addition of chiral selectors, ionpairing reagents, or another complexing agent (such as ethidium bromide for DNA and SDS for proteins). These species can be covalently bound to the gel or simply added to the running buffer.

2.5. Capillary isoelectric focusing (CIEF)

Capillary isoelectric focusing (CIEF) is a "high resolution" electrophoretic technique used to separate peptides and proteins on the basis of their isoelectric point (pI). CIEF can be used to separate proteins that differ by ≈ 0.005 pI units. Similar to CGE, this is a well-established slab gel electrophoretic technique adapted to the CE format.

In CIEF a pH gradient is formed within the capillary using ampholytes. Ampholytes are zwitterionic molecules that contain both an acidic and a basic moiety and can have pI values that span the desired pH range of the CIEF experiment (pH 3 to 9, for example). After filling the capillary with a mixture of solute and ampholytes, the pH gradient is formed. With a basic solution at the cathode and an acidic solution at the anode, upon application of the electric field the charged ampholytes and proteins migrate through the medium until they reach a region where they become uncharged (at their pI). This process is known as "focusing". The protein zones remain narrow since a protein which enters a zone of different pH will become charged and migrates back. The overall separation process is depicted in figure 2.17.

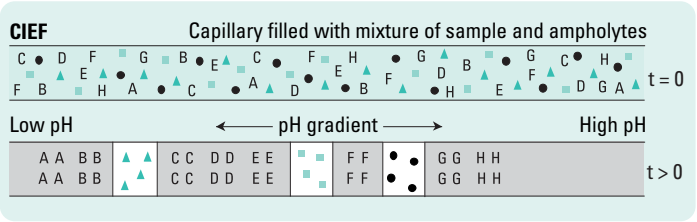

Figure 2.17
Illustration of CIEF. A, B, C, D, E, F, G, H represent ampholyte molecules. Symbols ▲, ■, and ● represent solute molecules for example peptides, proteins.

The status of the focusing process is indicated by the current. Once complete, a steady-state is reached and current no longer flows. After focusing, the solutes and ampholytes are mobilized by hydraulic pressure (while retaining electric field) and the zones pass through the detector. Besides by hydraulic pressure, mobilization can be accomplished by the addition of salt to one of the reservoirs or by providing both reservoirs with an acid or a base.

The zone width, 4σ (σ being the standard deviation), in CIEF is given by

$$\sigma = \left[\frac{D}{\left(\frac{d\mu}{dpH}\right)\left(\frac{dpH}{dx}\right)} \right]^{1/2} \quad (2.5)$$

and the resolution with respect to pI difference is given by

$$\Delta pI = 3 \left[\frac{D\left(\frac{dpH}{dx}\right)}{E\left(\frac{-d\mu}{dpH}\right)} \right]^{1/2} \quad (2.6)$$

where D = diffusion coefficient (cm^2/s)
E = electric field (V/cm)
dpH/dx = pH gradient at the zone
dμ/dpH = mobility slope at the pI (which depends on the charge of the protein near its pI)

As described by equation (2.6) high resolution is obtained with high electric fields, a high mobility slope at the isoelectric point, and a shallow (small range) pH gradient over the capillary length.

EOF needs to be reduced or eliminated in CIEF since the flow could flush the ampholytes from the capillary before focusing is complete. Reduction of EOF can be accomplished by the use of dynamic or covalent surface coatings of the capillary wall. The dynamic coatings have the advantage

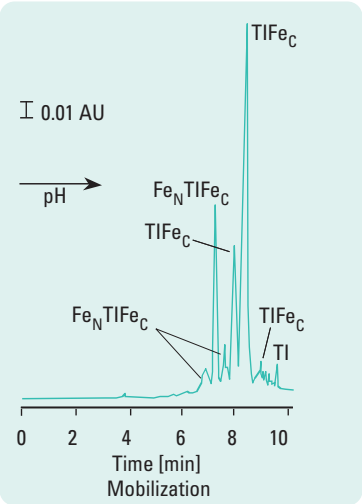

Figure 2.18
CIEF of transferrin isoforms.[27]

of simplicity, but obtaining reproducible EOF is often difficult. The coating, either dynamic or covalent, is also helpful in limiting protein adsorption to the capillary walls.

Since the solute is loaded on to the capillary during filling with the amphoteric solution, it is possible to load significantly larger volumes than in most other CE modes. However, at its pI, the solubility of a zwitterionic molecule is very low. At the same time at the focusing point, the concentration of the solute is at maximum. Therefore precipitation, is the limiting factor in sample loading.

CIEF has been used successfully to measure protein pI and for the separation of isoforms, and other protein species problematic by other methods, including immunoglobulins and hemoglobins, and analysis of dilute biological solutions. An example of the use of CIEF for the separation of transferrin isoforms is shown in figure 2.18.

Recently whole-column imaging CIEF technology[28, 29] has been commercialized. The method typically uses 50 mm (long), 100 µm inner diameter fused silica capillaries with an UV absorption-imaging detector operated at 280 nm.

2.6. Capillary isotachophoresis (CITP)

Capillary isotachophoresis (CITP) is a "moving boundary" electrophoretic technique. In CITP, a combination of two buffer systems is used to create a state in which the solutes all move as connected, separate bands and at the same velocity. The zones remain sandwiched between so-called leading and terminating electrolytes. In a single CITP experiment either cations or anions can be analyzed.

For anion analyses, for example, the buffer must be selected so that the leading electrolyte contains an anion with an effective mobility that is higher than that of the anionic solutes. Similarly, the terminating anion must have a lower mobility than that of the solutes. When the electric field is applied the anions start to migrate towards the anode. Since the leading anion has the highest mobility it moves fastest, followed by the anion with the next highest mobility, and so on. In CITP the individual anions migrate in joined zones, but all move at the same velocity, as defined by the velocity of the leading anion. The separation process is illustrated in figure 2.19.

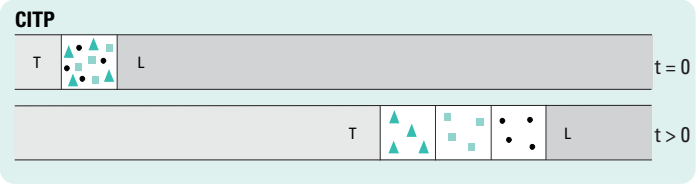

Figure 2.19
Illustration of CITP. T terminating electrolyte, L leading electrolyte, ▲, ■, and ● represent solute molecules.

The steady-state velocity in CITP occurs since the electric field varies in each zone. The field is self-adjusting to maintain constant velocity (that is, velocity = mobility x field), with the lowest field across the zone with highest mobility. This phenomenon maintains very sharp boundaries between the zones. If an ion diffuses into a neighboring zone its velocity changes and it immediately returns to its own zone.

Another interesting feature of CITP is the constant concentration in each zone, determined by the concentration of the leading electrolyte. Since CITP is usually performed in constant current mode, a constant ratio must exist between the concentration and the mobility of the ions in each zone (the so called, Kohlrausch Regulating Function (KRF)[30], see also section 1.3.4.5.). Zones that are less (or more) concentrated than the leading electrolyte are sharpened (or broadened) to adapt to the proper concentration. The solute-concentrating principle of CITP has been used as a preconcentration step prior to CZE, MEKC, or CGE (see section 3.2.3.). In most cases, a true CITP steady-state is not obtained since the modes are mixed. Nonetheless, up to 30 to 50 % of the capillary can be filled with sample while maintaining good separation quality. A difficulty often arises with finding buffer systems that contain both leading and trailing ions and also form the desired pH. An additional limitation is that only cations or anions can be sharpened, not both simultaneously.

Zone sharpening can occur upon the addition of a high concentration of leading and/or trailing electrolytes to the sample (that is, addition of salt to the sample). An example of such improvements is illustrated in figure 2.20. Here, the sample contains a high concentration of chloride (≅ 110 mM) in addition to the solutes of interest. The earliest eluting peaks exhibit over 10^6 plates, significantly more than described by simple theory. This example also illustrates how CITP effects can inadvertently occur, especially with complex samples.

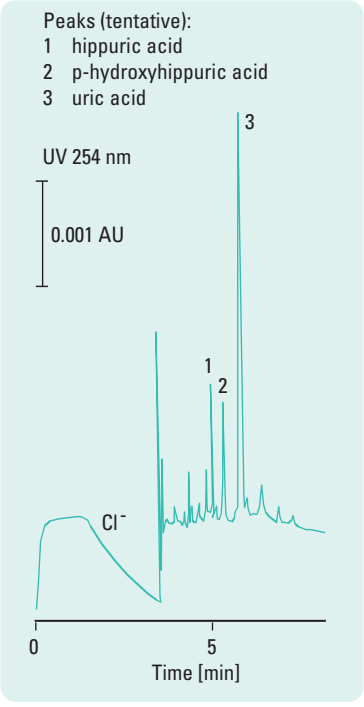

Figure 2.20
CITP-stacked uraemic sera, separation by CZE.[31]
Conditions: 10 mM MES, histidine, pH 6.05, 0.05 % methyl hydroxyethyl cellulose, constant current = 35 µA, l = 25 cm, id = 200 µm, PTFE capillary.

Instrumentation

Instrumentation

3.1. High voltage power supply

In capillary electrophoresis a dual polarity (DC) power supply is used to apply up to about 30 kV and current levels of 200 to 300 mA. Stable regulation of the voltage (± 0.1 %) is required to maintain high migration time reproducibility. When bare fused silica capillaries are used, the EOF will be in the direction of the cathode (see 1.3.2). Since the point of detection will be at the end of the capillary, the cathode will be at that end. In this case, the inlet side of the capillary becomes the anode and sample injection is made from this end.

The power supply should have the capability to switch polarity. If the EOF is reversed (for example by a cationic wall coating or pH change), it is necessary to change the direction of the field by reversing polarity of the electrodes; that is, to switch the cathode to the injection end.

Since the inlet and outlet ends of the capillary are predetermined by the location of the point of detection near the outlet end, polarity switching must be performed at the power supply. This can best be accomplished by use of a DC power supply. With such a power supply it is important to realize that the high voltage electrode and the ground electrode remain positional fixed. That is, the high voltage electrode is driven either positive or negative with respect to the ground electrode.

While constant voltage analyses are most common, it is often beneficial to use either constant current or constant power modes. Constant current or power mode is particularly useful for isotachophoretic experiments or when capillary temperature is not adequately controlled. With regard to the latter, temperature changes alter buffer viscosity and migration time in constant voltage mode. In constant current mode, these viscosity changes are compensated by proportional changes in the applied voltage, maintaining constant migration time. The high voltage power supply should therefore have the ability to run in constant current or constant power mode. Another power supply feature is the ability to run voltage, current, or power gradients (also called field programming) during an analysis. Field programming can be used to ramp the voltage at the beginning of an analysis to avoid rapid heating, causing thermal expansion of buffer, and expulsion of sample from the capillary. Field programming is also particularly useful for decreasing the analysis time of complex samples and is often necessary for fraction collection. Since manipulation of narrow,

closely spaced solute zones (for example 5 to10 seconds) is difficult under high field conditions, reduction of the field immediately prior to collection increases the time window and relaxes the stringent timing problems associated with precise collection (see section 3.5).

3.2. Sample introduction

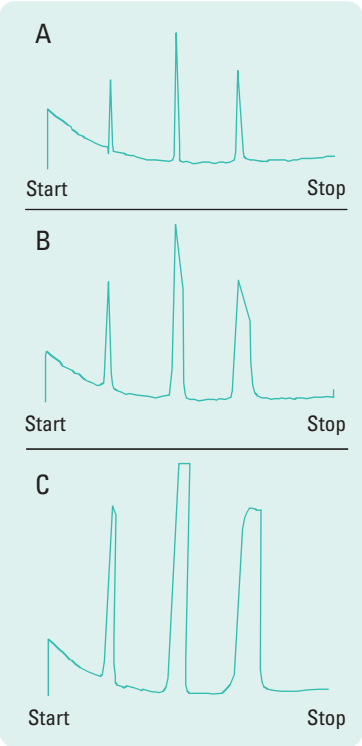

Figure 3.1
Effect of sample overloading on peak shape. Starting zone widths: A = 0.6 cm, B = 2.0 cm, C = 3.0 cm.

In CE only minute volumes of sample are loaded into the capillary. These small volumes are, of course, governed by the small volume of the separation capillary (0.025 - 0.15 mm id, 150 -1000 mm length). As a rule of thumb, the sample zone length should be less than 1 to 2 % of the total length of the capillary. This corresponds to an injection length of a few millimeters (or 1 to 50 nL), depending on the capillary inner diameter. This is an advantage when sample volumes, as small as 5 µL, are sufficient to perform numerous injections. Conversely, these small volumes seriously hamper sensitivity when the samples are extremely dilute.

Sample overloading can have two significant effects, both detrimental to resolution (figure 3.1). First, injection lengths longer than the diffusion controlled zone width (an example of how to calculate the maximum injection length will be given under section 3.2.1, hydrodynamic injection) will proportionally broaden peak width. Secondly, it can worsen peak shapes by field inhomogeneities, due to mismatched conductivity between the running buffer and the sample zone.
Quantitative sample injection can be accomplished by a number of methods. The two most common are hydrodynamic and electrokinetic injection (figure 3.2). In either case, the sample volume loaded is generally not a known quantity, although it can be calculated. Instead of volume, the quantifiable parameters are pressure x time for hydrodynamic injection, or voltage x time for electrokinetic injection, as described in detail in the next two sub-sections.

3.2.1. Hydrodynamic injection

Hydrodynamic sample injection is the most widely used method. It can be accomplished by application of pressure at the injection end of the capillary, vacuum at the exit end of the capillary, or by siphoning action obtained by elevating the injection reservoir relative to the exit reservoir (figure 3.2). With hydrodynamic injection, the quantity of sample loaded is nearly independent of the sample matrix.

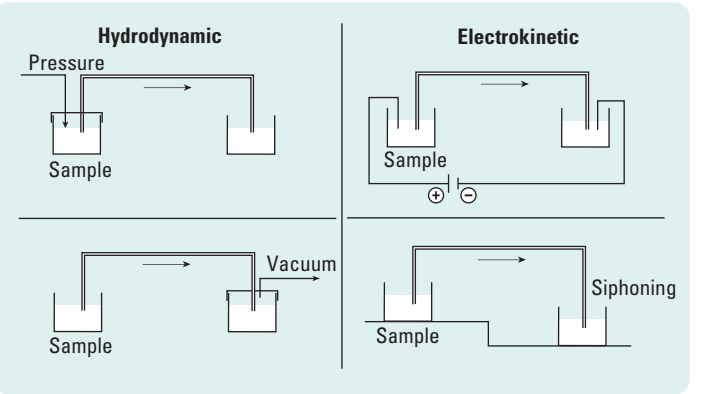

Figure 3.2
Methods of sample injection.

The volume of sample loaded (V_{Inj}) will be a function of the capillary dimensions, the viscosity of the buffer in the capillary, the applied pressure, and the time. This volume can be calculated using the Hagen-Poiseuille equation.

3.1

$$V_{inj} = \frac{\Delta P d^4 \pi t_{inj}}{128 \eta L}$$

where ΔP = pressure difference across the capillary
d = capillary inside diameter
t_{inj} = injection time
η = buffer viscosity
L = total capillary length

Typical injection pressures and times range from 25 to 100 mbar and 0.5 to 5 seconds, respectively. Using equation (3.1), the sample plug

volume and length loaded, as a function of applied pressure, time, and capillary dimensions, is given in table 3.1.

Capillary id Inj. pres. x time, (mbar x s)	**10 µm** V_p (nL), l_p (mm)	**25 µm** V_p (nL), l_p (mm)	**50 µm** V_p (nL), l_p (mm)	**75 µm** V_p (nL), l_p (mm)	**100 µmA** V_p (nL), l_p (mm)
25	0.0008, 0.01	0.03, 0.06	0.5, 0.25	2.6, 0.59	8.2, 1.04
50	0.0016, 0.02	0.06, 0.12	1.0, 0.50	5.2, 1.18	16.4, 2.08
75	0.0024, 0.03	0.09, 0.18	1.5, 0.75	7.8, 1.77	24.6, 3.13
100	0.0032, 0.04	0.12, 0.24	2.0, 1.00	10.4, 2.26	32.8, 4.16
150	0.0048, 0.06	0.18, 0.36	3.0, 1.50	15.6, 3.54	49.2, 6.26

Table 3.1
Injection volume and plug length as a function of pressure, time and capillary id.
V_p = plug volume (nL); L = 75 cm; η = 1cP; T= 20 °C, l_p = plug length (mm).

In order to calculate the maximum injection length, w_i^{max}, that will not significantly disturb resolution, the following assumption with respect to total zone broadening in the separation system (σ^2_T in equation 1.16, chapter 1) is made:

Neglect all zone broadening factors except molecular diffusion (σ^2_{Dif}) and sample injection (σ^2_{Inj}), total zone broadening will then be compressed into

$$\sigma_T^2 = \sigma_{DIF}^2 + \sigma_{INJ}^2 = 2Dt_D + \frac{w_i^2}{12} \qquad (3.2)$$

When, due to injection, a 10 % loss in resolution (which roughly equals to a 20 % loss in theoretical plates) is accepted, the relationship between the standard deviations of the two terms in equation (3.2) can be calculated as

$$\sigma_{INJ} \approx 0.5\sigma_{DIF} \qquad (3.3)$$

Combining equations (3.2) and (3.3) with equation (3.1), it follows that

3.4
$$w_i^{max} = \sqrt{6Dt_D} = \frac{\Delta P t_{inj} d^2}{32\eta L}$$

From equation (3.4), the maximum injection width can now be calculated from an estimated analyte's migration time and its diffusion coefficient in the running buffer, which then leads to the proper hydrodynamic injection parameter ($\Delta P \times t_{inj}$). The result is shown in table 3.2.

D (cm^2/s)	t_D (s)	w_i^{max} (mm)	L (cm)	id (µm)	V_{inj} (nL)	$\Delta P \times t_{inj}$ (mbar x s)
10^{-5}	500	1.73	50	75	7.7	49.3
				50	3.4	110.9
				25	0.9	443.4
	200	1.10	20	75	4.8	12.5
				50	2.2	28.0
				25	0.5	112.2
10^{-6}	500	0.55	50	75	2.4	15.6
				50	1.1	35.1
				25	0.3	140.2
	200	0.35	20	75	1.5	3.9
				50	0.7	8.9
				25	0.2	35.5

Table 3.2
Maximum injection plug length as a function of estimated diffusion coefficient and migration time of analyte in correlation with determining injection parameter, capillary dimensions and buffer viscosity (η = 1 cP at 20 °C).

This table clearly shows that large molecules (small D) need narrower injection zones, when short and small id capillaries are used, than smaller molecules.

For siphoning injection, the pressure differential for use in equation (3.1) is given as

3.5
$$\Delta P = \rho g \Delta h$$

where ρ = buffer density
g = standard acceleration of gravity (9.807 m/s^2)
Δh = height differential of the buffer reservoirs

A typical siphoning injection is obtained by raising the sample reservoir 5 to 10 cm relative to the exit reservoir for 10 to 30 seconds, depending on the conditions. Siphoning is typically used in systems without pressure injection capabilities. If sensitivity is not limiting, the smallest injection lengths possible should be used. However, injection reproducibility is usually diminished with short injection times due to instrumental limitations. This is especially true when short and/or wide-bore capillaries are employed or when concentrated samples are used. Reproducibility can be improved significantly by use of an integrated pressure x time profile with active feedback control to compensate for system rise time effects and variations in the applied pressure.

Finally, to avoid unwanted sample injection by siphoning it is important that the liquid levels of the sample and buffer reservoirs should be equal. Siphoning can cause poor peak area reproducibility and even overloading. It has also been found that simply placing the capillary in a sample reservoir will cause an injection due to capillary action. This phenomenon has been called a zero-injection effect. While often insignificant, with concentrated samples the injected amount can be quantifiable and should be considered during quantitative analysis.

From an instrumental standpoint, injection reproducibility can be better than 1 to 2 % relative standard deviation (RSD). Reproducibility of peak area, however, can be affected by other phenomena, including sample interaction with the capillary wall, variations in temperature, integration of peaks with low signal-to-noise ratios, (see factors affecting reproducibility of peak area and mobility in chapter 4).

Precise temperature control (± 0.1°C) of the capillary is necessary to maintain constant injection volume. As with migration time, viscosity of the buffer in the capillary and thus the injected quantity varies 2 to 3 % per °C. Note that sample viscosity does not significantly affect injection volume since the sample plug is only a very small volume relative to the total liquid volume in the capillary.

3.2.2. Electrokinetic injection

Electrokinetic or electromigration injection is performed by replacing the injection-end buffer reservoir with the sample vial and applying the voltage (figure 3.2). Usually field strengths 3 to 5 times lower than that used for separation are applied with injection times of 10-30 seconds. In electrokinetic injection, analytes in the sample enter the capillary by both migration and by the pumping action of the EOF. A property of electrokinetic injection is that the quantity of each analyte loaded is dependent on the electrophoretic mobility of the individual solutes. Discrimination occurs for ionic species since the more mobile ions are loaded to a greater extent than those that are less mobile.

The quantity injected (Q) [grams or moles], can be calculated by

$$Q = \frac{(\mu_e + \mu_{EOF})\, V \pi r^2 C t_{inj}}{L} \qquad (3.6)$$

where
- μ_e = electrophoretic mobility of the analyte
- μ_{EOF} = EOF mobility
- V = voltage
- r = capillary radius
- C = analyte concentration
- t_{inj} = injection time
- L = capillary total length

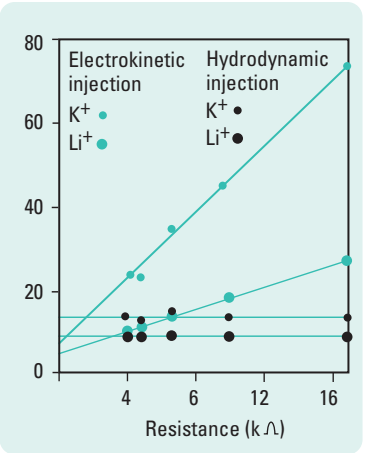

Figure 3.3
Quantity of sample loaded as a function of sample resistance for hydrodynamic and electrokinetic injection.[32]

As described by equation (3.6), loading is dependent, besides injection time, on the EOF, solute concentration, and solute's mobility. Variations in sample conductivity, which can be due to matrix effects such as a large quantity of a dissolved salt, result in differences in sample resistance (induces a change in electric field: E = V/L) and therefore quantity loaded as depicted in figure 3.3. Due to these phenomena electrokinetic injection is generally not as reproducible as its hydrodynamic counterpart.

Despite quantitative limitations, electrokinetic injection is very simple, requires no additional instrumentation, and is advantageous when viscous media or gels are employed in the capillary rendering hydrodynamic injection less effective.

3.2.3. On-capillary sample concentration

Several techniques have been described to enhance sensitivity by on-capillary sample concentration during or just after sample injection. These injection methods can be regarded functionally equivalent to solid phase extraction (SPE) and solid phase micro extraction (SPME) techniques used in HPLC. In capillary electrophoresis they are based on field strength differences between the sample zone and the running buffer, and are called "stacking methods".

3.2.3.1. Field amplified sample stacking (FASS) and field amplified sample injection (FASI)

In the first chapter (electro-dispersion, section 1.3.4.5.) it was demonstrated that when the sample conductivity is higher than that of the running buffer (= back ground electrolyte (BGE); often also indicated as back ground solution (BGS)), the sample zone is smeared out during the first part of the separation. However, the opposite may also occur. Sample zones are compressed when the conductivity of the sample matrix is significantly lower than that of the running buffer the BGE. This focusing effect may be used to increase the loadability of the CE system.

With samples having a low salt content (solution ion strength), the sample volume can be much larger before excessive zone broadening comes in to play. This technique of preconcentration is called field amplified sample stacking (FASS), when the injection is performed *hydrodynamically* or field amplified sample injection (FASI), when injection is performed by *electrokinetic injection*.

For analyte ions migrating in the same direction as the osmotic flow (usually cations), electrokinetic injection can be combined with simultaneous sample preconcentration. When the sample conductivity is low enough (for example, when the sample matrix is pure water) the normal injection time (10-30 seconds) can be applied as still a large amount of sample cations are introduced into the capillary by the field amplification effect. Stacking (zone sharpening) occurs automatically at the interface between the sample solution and the BGE. It is often recommended to first introduce a small amount of water in order to take care of possible disturbances of the stakking process on the boundary between the BGE and the sample. Finally, the sample vial is replaced by the buffer vial and electrophoresis started. In figure 3.4 the field amplification effect with *electrokinetic injection* is illustrated.

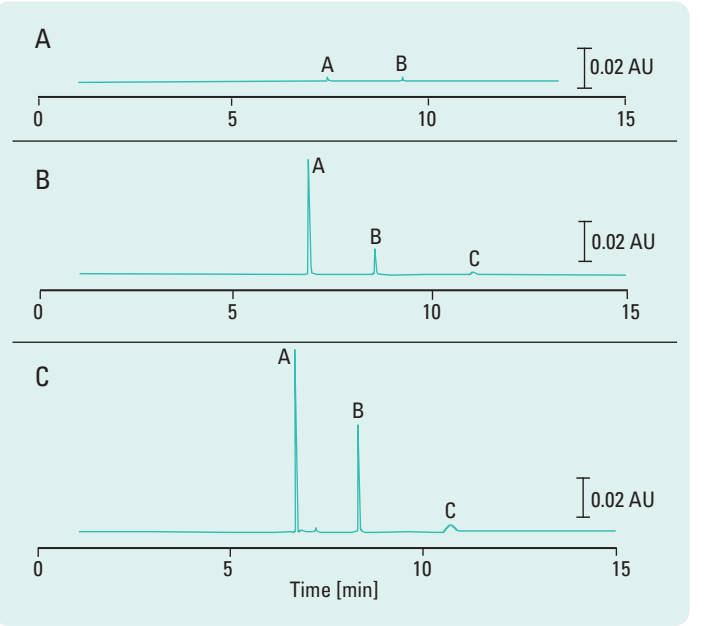

Figure 3.4
Field amplified sample injection.[33] A) sample dissolved in buffer; B) sample dissolved in water; C) short plug of water injected before sample in B.

A disadvantage of the *electrokinetic* field amplification method is that the amount of introduced sample ions strongly depends on the actual sample conductivity. When this conductivity cannot be controlled, results will be unreliable.

Therefore, *hydrodynamic* stacking methods are more often applied. In this method, a long plug of a low conductivity sample solution is introduced by a time controlled pressure difference. Due to the difference in conductivity, analyte zones are sharpened in the first stage of the separation after application of the electric field.

When the conductivity of a particular sample is not as low as expected, the resulting peak resolution will be affected but the peak areas are still

reliable. The schematics of field amplified sample stacking by *hydrodynamic injection* (FASS) is shown in figure 3.5.

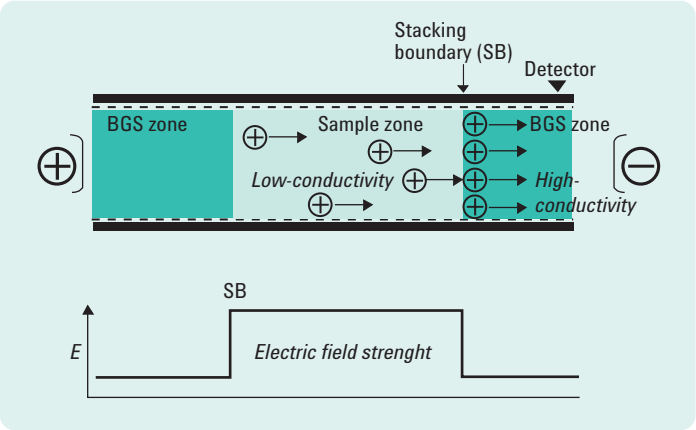

Figure 3.5
Schematics of the principle of FASS.

The amount of sample that can be injected before the efficiency of the separation starts to deteriorate, is often more than a 100-fold higher than without stacking. The enrichment factor that can be realized by stacking, without compromising the separation, depends in the first place on the upper limit of the sample conductivity. However, there are also some other limitations. In the first place, the Joule heating in the sample plug should be considered. When the conductivity of the sample matrix is much lower than that of the BGE, a relative large part of the applied high voltage drop is over the sample plug so that the field strength in this part of the capillary is much higher than average. This may result in excessive heat generation in the sample plug, causing degassing and/or boiling. This excessive heat generation is especially strong when the low conductivity sample plug is relatively short, which means that the stacking possibilities are not fully exploited. Significantly elevated temperatures in the sample zone, even with capillary thermostatting, have been reported and an example of this phenomenon is depicted in figure 3.6.

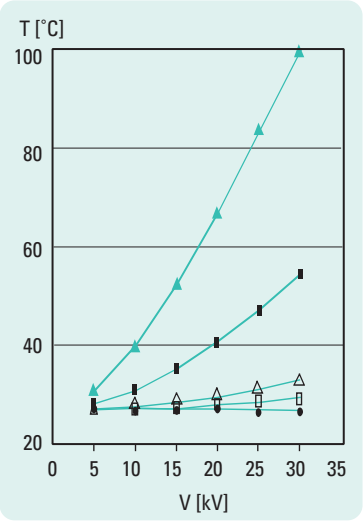

Figure 3.6
Estimated temperature of sample zone and running buffer under stacking conditions[35] closed symbols = sample zone; open symbols = buffer.
Conditions: 10 mM tricine, pH 8.0, containing 0 mM NaCl (●), 25 mM NaCl (■), 50 mM NaCl (▲)

Another limitation for sample stacking is related to differences in electro-osmotic flow velocities occurring between the part of the capillary

containing the sample solution and the remainder of the capillary containing the BGE. In the low conductivity sample plug the field strength is higher than in the rest of the capillary. Moreover, the electroosmotic mobility is usually increasing with decreasing salt concentration. Both effects cause the electroosmotic velocity in the sample plug to be higher than in the BGE. This causes a pressure difference between sample plug and buffer zone resulting in parabolic flow velocity profiles superimposed on the plug like osmotic flow velocity profiles in both parts of the capillary. These superimposed parabolic flow velocity profiles are a source of zone broadening in both sample plug and BGE during the actual separation. When the difference in electroosmotic velocity is large and the sample zone is relatively long, the obtained plate number will be decreased. Manipulation of the electroosmotic mobility in either the sample plug or in the BGE, to create a better match, may help to decrease peak broadening and to increase the sample volume that can be loaded.

When the analytes are weak cations or anions, sample stacking can also be realized by pH manipulation (a dynamic pH junction).[34] This occurs when the pH of the sample is different from that of the BGE so that the effective mobilities of the analyte ions can also be different. The pH of the sample and BGE should therefore be chosen such that the mobilities in the sample are much higher than those obtained in the BGE. In this way, a large sample plug can also be introduced by pressure and will henceforth be compressed during the first stage of the separation.

3.2.3.2. Isotachophoretic sample stacking

Discontinuous buffer systems have been used for the stacking of samples that do not have a low conductivity. In these cases, the stacking is based on isotachophoretic principles. In ITP (as described in section 2.6) a sample solution is sandwiched between a leading (L) and a terminating (T) electrolyte solution. The leading electrolyte contains a co-ion that has a higher mobility than any of the analyte ions. The terminating electrolyte has one that is slower than the analyte ions. During electrophoresis, in such a system, the analyte ions cannot overhaul the leading ion and the terminating ion not the analyte ions. The result is that sharp (pure) zones of analytes are formed, which all migrate with the same velocity between the two electrolytes in a sequence according to their respective mobilities. The

concentrations of the pure analyte zones in ITP are determined by the composition of the leading and terminating electrolytes (following the Kohlrausch regulation function), and not by their original concentrations in the sample solution. Therefore, sample enrichment or stacking is a common phenomenon in ITP.

A practical implementation of (on-capillary) ITP-CZE for the stacking of *cations* is illustrated in figure 3.7.

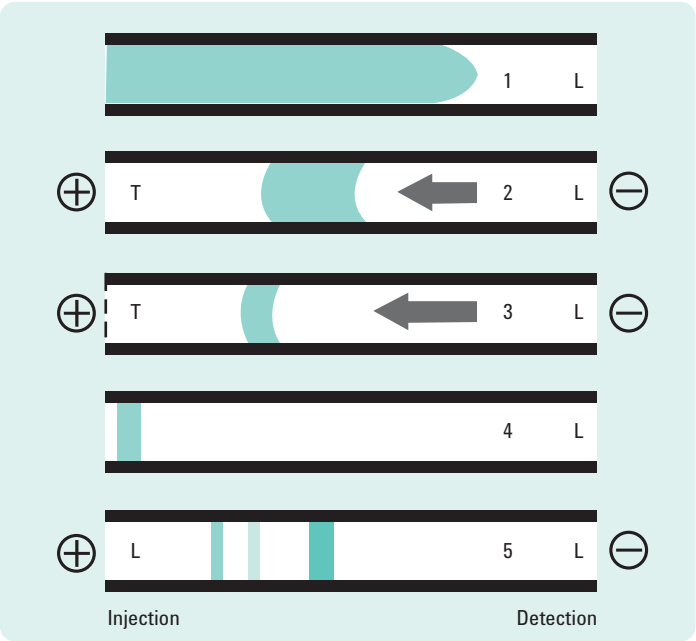

Figure 3.7
Diagram showing the procedure of on-capillary ITP-CZE for cations with hydrodynamic back pressure.[36]

The background electrolyte for the CZE separation serves as the leading electrolyte (L), which has been chosen such that its co-ion has a higher mobility than any of the analyte ions. First the capillary is flushed with L. Then a large plug of the sample solution is injected hydrodynamically. Next, the capillary inlet is placed in a vial containing the terminating electrolyte (T), and a voltage applied for isotachophoretic focusing of

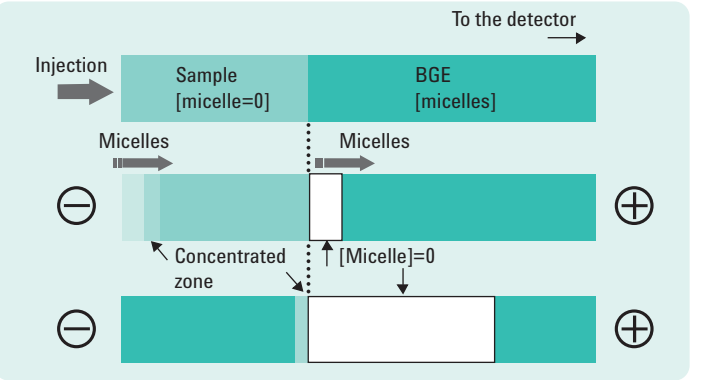

Figure 3.8
Schematics of the principle of sweeping under suppressed EOF conditions.

the analyte zones. A hydrodynamic pressure is applied on the outlet side of the capillary to prevent too much of T to enter the capillary by electro-osmosis. When focusing is complete, the remainder of T is removed from the capillary by a higher back pressure than used before, and the capillary inlet is placed in a vial with L. Then, the actual zone-electrophoretic separation of the stacked analytes can start. The zone-electrophoretic separation can also be performed with T as the BGE by using a slightly different ITP-procedure. Similar schemes have been developed for anionic analytes. In theory, orders of magnitude in concentration can be obtained by ITP-CZE if introduction of the other electrolyte (not used for the CZE separation) can be avoided. If this electrolyte is still present, the started CZE mode will lead to destacking of the analyte zones and subsequently to broadened and shifted peaks in the electropherogram.

The length of the swept zone is given by[37]

3.7
$$l_{sweep} = l_{inj}\left(\frac{1}{1+k'}\right)$$

where l_{sweep} and l_{inj} are the lengths of the sample zone after and before sweeping, respectively, and k' the capacity factor in the sample matrix, which is different from that in the BGE

It should be kept in mind that the maximum injection length should be less than 90 % of the effective capillary length as some length must be still be available for separation.

In order to maximize k', additives such as organic solvents or cyclodextrins (used to improve resolution and kinetics) should not be added to the sample matrix. Especially under suppressed EOF conditions, sweeping can result in concentration efficiencies generating detector signals that are roughly 3 orders of magnitude higher than a conventional injection will produce. An example of this powerful sample concentration is given in figure 3.9.

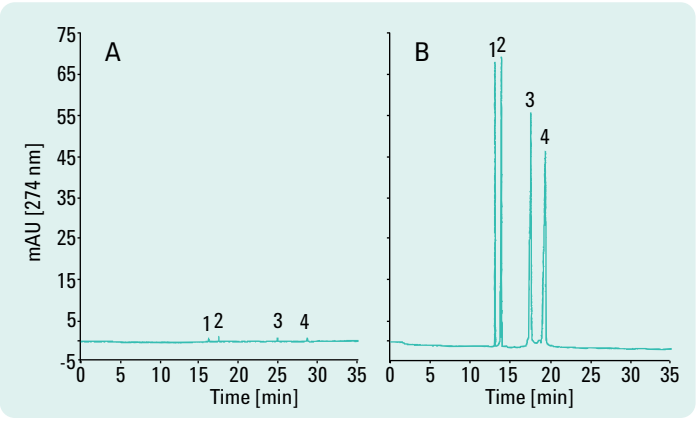

Figure 3.9
Sweeping in a neutral capillary (virtually no EOF) with a basic buffer.[37]
Conditions: BGE: 50 mM SDS/20 mM borate (pH 9.3) + 20 % MeOH; sample: steroids in borate buffer adjusted to the conductivity of the BGE; injected length: 0.64 mm (A), 42 cm (B); -30 kV; concentration of analytes: ~ 20 ppm (A), 2 ppm (B); peaks: 1) progesterone, 2) testosterone, 3) hydrocortisone, 4) cortisone; capillary: celect N, L_{eff} = 57 cm, L_{tot} = 65.5 cm.

Besides neutral analytes, charged species (ions) can also be concentrated by the sweeping technique when the micelle has a counter-charge with respect to the analyte. In this manner, large capacity factors (k', s) are warranted due to strong electrostatic interactions. Therefore cationic analytes should be concentrated with SDS micelles and anionic analytes (aromatic sulfonates or carboxylates) with CTAB micelles. The concentration efficiency of sweeping was further demonstrated with pseudostationary

phases (charged cyclodextrins, CD's and microemulsions) and the use of complexation reactions (metal ions and sugars swept by ethylene diamine tetra-acetic acid (EDTA), or borate, respectively).

3.2.3.3. High-salt stacking

This mechanism of analyte preconcentration is also applied in MEKC by stacking of micelles (for example sodium cholate, SC) at the side of the injected sample plug that faces the negative electrode (or detector side). In order to stack micelles the conductivity of the sample zone should be roughly 1.5 - 2.5 x that of the BGE. The result is that the electric field in the BGE is higher than that in the sample zone ($E_{BGE} > E_{SZ}$). Upon application of the separation voltage the micelles concentrate at the detector side of the sample zone where the cationic analytes are collected and further transported by the usual MEKC mechanism with strong EOF. This stacking mode is illustrated in figure 3.10.

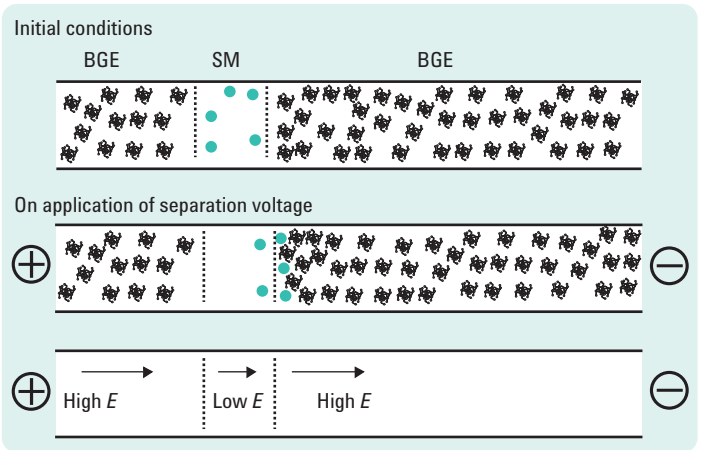

Figure 3.10
Mechanism of high-salt stacking; the ionic strength of the sample matrix is adjusted so that it is 1.5-2.5 x the ionic strength of the BGE.

The effectiveness of high-salt stacking of alkaloid analytes is shown in figure 3.11. In this example, components 1 and 2 are as well stacked demonstrating the efficiency of high-salt stacking for analytes with low k's.

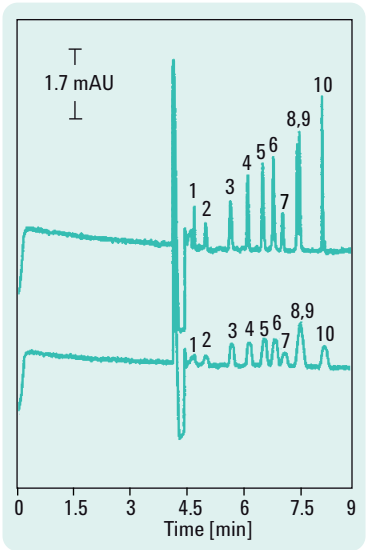

Figure 3.11
Separation of 10 alkaloids by high-salt stacking.[38]
Bottom trace: Sample matrix is BGE; top trace: sample matrix is 150 mM NaCl; peaks: 1) nicotine, 2) aconitine, 3) colchicoside, 4) strychnine, 5) thiocolchicoside, 6) colchicine, 7) benzoinmethyl ether, 8) yohimbine, 9) thiocolchicine, 10) emetine.
Conditions: BGE: 10 mM $Na_2B_4O_7$/80 mM sodium cholate; L_{eff} = 50 cm, L_{tot} = 60 cm; inj = 10 mm (690 mbar x s); 25 kV (47 µA); 50 µm id; λ = 214 nm.

3.3. Temperature control

Effective control of capillary temperature is important for reproducible operation. Temperature control to ± 0.1 °C is beneficial due to the strong viscosity dependence (2-3 % per °C) of sample injection (which also requires a good temperature control of buffers and sample vials in the autosampler) and migration time. Furthermore, the system should isolate the capillary from changes in ambient temperature. The two approaches generally used are to bath the capillary in a high velocity air stream or in a liquid. While liquid thermostating is theoretically more efficient ($k_{Liquid} > k_{Air}$), forced air thermostating at ≈ 10 m/s air velocity is usually sufficient for the quantity of heat generated in CE. As shown in the Ohm's law plots (figure 1.14 and table 1.4), efficiency of the two systems is similar up to a power of about 5 W/m. Although the liquid system is more effective at higher power generation, CE experiments are not usually performed under such conditions. A benefit of the air thermostating system is instrumental simplicity and ease of handling the separation capillary.

Although the primary purpose of thermostatically controlling capillary temperature is to maintain constant temperature by removing Joule heat, temperature control can also be used as a parameter in optimizing a CZE separation. Elevated or reduced temperatures alter viscosity, EOF, and analysis time. It can also be used to affect chemical equilibria and kinetics.

3.4. Detection

Detection in CE is a significant challenge as a result of the small dimensions of the capillary. Although CE requires only nanoliter volumes of sample, it is not a "trace" analysis technique since relatively concentrated analyte solutions or pre-concentration methods are often necessary. A number of detection methods have been used in CE to meet this challenge, many of which are similar to those employed in liquid column chromatography. As in HPLC, UV-visible detection is by-far the most common. Table 3.3 contains a list of many of the detection methods investigated, along with attainable detection limits, and advantages/ disadvantages.

Method	Mass detection limit (moles)	Concentration detection limit (molar)*	Advantages/ disadvantages
UV-vis absorption	$10^{-12} – 10^{-15}$	$10^{-5} – 10^{-7}$	"Universal". DAD offers spectral information.
Fluorescence	$10^{-15} – 10^{-17}$	$10^{-7} – 10^{-9}$	Sensitive. Usually requires sample derivatization.
Laser induced fluorescence	$10^{-18} – 10^{-20}$	$10^{-9} – 10^{-12}$	Extremely sensitive. Usually requires sample derivatization. Expensive.
Amperometry	$10^{-18} – 10^{-19}$	$10^{-10} – 10^{-11}$	Sensitive. Selective but useful only for electroactive analytes. Not robust.
Conductivity	$10^{-15} – 10^{-16}$	$10^{-6} – 10^{-7}$	Universal.
Mass spectrometry	$10^{-16} – 10^{-17}$	$10^{-8} – 10^{-9}$	Sensitive. Structural information. Interface between CE and MS complicated.
Indirect UV, -fluorescence, -amperometry	10 – 100 times less than direct method.	–	Universal. Lower sensitivity than direct methods.

Table 3.3
Key metrics of detection methods.[39] *Assume 10 nL injection volume.

3.4.1. UV-vis spectrophotometric detection

UV-visible absorption is the most widely used detection method primarily due to its nearly universal detection nature. With fused-silica capillaries, detection below 200 nm up through the visible spectrum can be used. The high efficiency observed in CE is due in part to on-capillary detection. Since the optical window is directly in the capillary there is no broadening of the zone as a result of dead-volume or component mixing. In fact the separation is still occurring while in the detection window. As with all optical detectors, the axial detection path length should be short relative to the width of the solute zone entering the detector to maintain high resolution. This is best accomplished with an optical slit designed for specific capillary dimensions. Since peaks in CE are typically 2 to 5 mm wide, slit lengths should be maximally one third of this figure.

3.4.1.1. Noise, sensitivity, linear detection range

Detector design is critical due to the short optical path length. The optical beam should be tightly focused directly into the capillary to obtain maximum throughput at the optical slit and to minimize stray light reaching the detector. These aspects are important to noise, sensitivity and linear detection range.

Sensitivity is defined as the slope of the calibration curve (detector response / sample concentration). A steeper slope indicates better sensitivity. For absorptive detectors the absorbance of a solute is dependent on optical path length (b), concentration (C), molar absorptivity (ε), as defined by Beer's law

$$A = b\,C\,\varepsilon \qquad (3.8)$$

The short path length (b), is the factor that mainly limits sensitivity [A/C in equation (3.8)] in CE. Due to the curvature of the capillary, the effective optical path length (b_e), in the capillary is less than the inner diameter, d_c, ($b_e \approx 0.8\ d_c$) since only a fraction of the light passes directly through the center. The actual path length can be determined by filling the capillary with a solute of known concentration and molar absorptivity.

Higher sensitivity can often be realized by use of low-UV detection wavelengths. Peptides and carbohydrates, for example, have no strong chromophores but can be adequately detected at 200 nm or below (figure 3.12). Detection at these low wavelengths necessitates the use of minimally UV-absorbing running buffers since high background absorbance increases baseline noise and decreases signal. Phosphate and borate are useful in this respect. Many biological buffers such as N-2-hydroxyethylpiperazine-N´-2-ethanesulfonic acid (HEPES), 3-[cyclohexylamino]-1-propane-sulfonic acid (CAPS), and tris(hydroxymethyl)aminomethane (Tris) are inappropriate for use below about 215 nm. [Note: the pH of a Tris buffer is highly temperature dependent, $\approx$ - 0.01 pH unit / °C increase].

Deviations from Beer's law ultimately limit quantitative analysis. High analyte concentrations lead to a deviation, called absorbance saturation, which results in a lower sensitivity (A/C) that will ultimately define the linear detection range. Ideally, all light should pass through the center of the capillary, not through the wall.

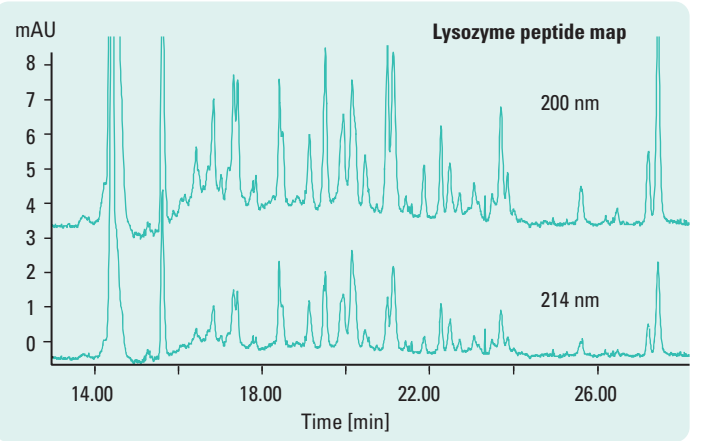

Figure 3.12
Use of low detection wavelengths to increase signal-to-noise ratio.

A good detector design has a narrow optical slit allowing a narrow light beam to pass through the center of the capillary. In this case the effective optical path length equals the inner diameter of the capillary ($b_e = d_c$) and the maximal sensitivity of detection (A/C^{max}) can be predicted with equation (3.8). A disadvantage of such a narrow light beam is that a small amount of photons reaches the photodiode, which results in a high base-line noise.

Increasing the light throughput, by increasing the slit width, the amount of light to the photodiode is increased thereby decreasing both baseline noise and sensitivity (but the effective path length also decreases).
However, if the slit allows stray light through the capillary walls, the sensitivity will further decrease and the linear detection range will be compromised. The interdependent relationship between noise, sensitivity and linear detection range is shown in figure 3.13.

If the slit is increased along the length of the capillary, resolution can be reduced. Depending on the analysis, slit size (width and/or length) can be chosen to optimize sensitivity, linear detection range and/or resolution. Note that the linear detection range in CE is significantly lower than that observed in LC (0.4 to 0.7 AU in CE versus 1.2 to 1.5 AU in LC) due to the small size and curvature of the capillary.

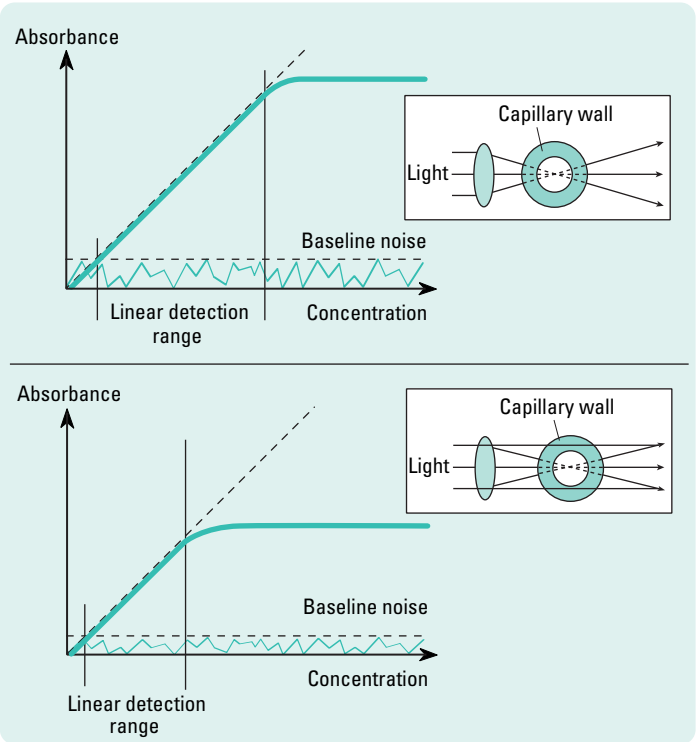

Figure 3.13
Dependence of sensitivity (A/C), linear detection range and baseline noise on light path through the capillary.

3.4.1.2. Extended path length flow cells

Sensitivity and linear detection range can usually be improved by increasing the inner diameter of the capillary.

This approach is limited, however, by the increase in current and subsequent heating within the capillary. For example, a two-fold increase in diameter will yield a two-fold increase in absorbance but a four-fold increase in current. Special capillary designs can be used to extend the optical pathway without increasing the overall capillary inner diameter. Three of these designs are shown in figure 3.14.

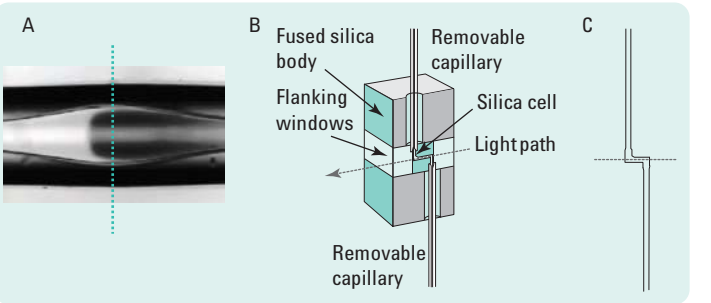

Figure 3.14
Designs of flow cells with an extended path length. A = bubble cell with a dye front passing through the extended light path; B = high-sensitivity cell; C = Z-cell.

The bubble cell offers a unique method to extend the pathway with nearly no degradation of separation efficiency and resolution. It is made by forming an expanded region, a bubble, directly within the capillary. Since the bubble is located only in the detection region no increase in current occurs. In the region of the bubble the electrical resistance is reduced and thus the field is decreased. Concomitant to this is a proportional decrease in flow velocity due to the expanded volume of the bubble. When the zone front enters the bubble its velocity decreases and the zone concentrates or "stacks" in a manner similar to electrophoretic stacking during injection. As the sample zone expands radially (across the capillary) to fill the increased volume, it contracts longitudinally (along the capillary). Thus the sample concentration remains constant but the path length increases (figure 3.15). Figure 3.14A shows a photograph of the zone front of a dye in the expanded region of the bubble cell.

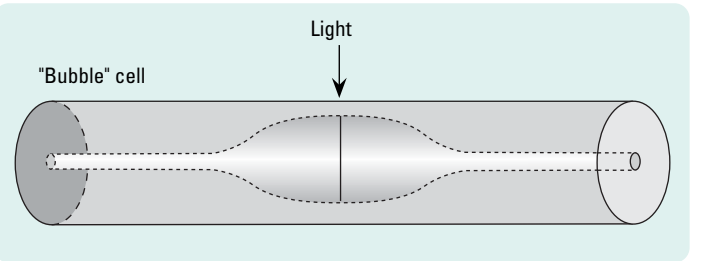

Figure 3.15
Schematic of extended light path capillary (bubble cell).

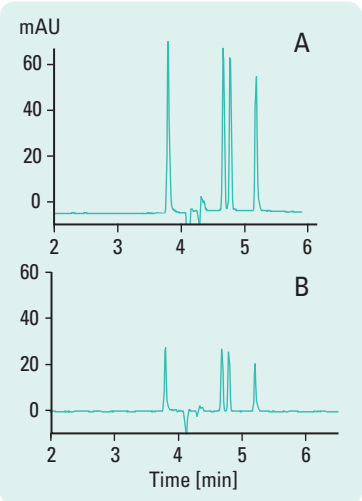

Figure 3.16
Peptide analysis using: A) the extended light path capillary, and B) a normal straight capillary.
Conditions: A) id = 50 µm with 150 µm detection cell; B) id = 50 µm.

The performance of the bubble cell is illustrated in figure 3.16 for the separation of neuropeptides. Here the bubble is three times larger than the inner diameter (150-µm id bubble in a 50-µm id capillary). This yields nearly a 3-fold increase in signal relative to the straight capillary with a inner diameter of 50 mm. This figure also shows that there is virtually no measurable band broadening. In addition, a lower limit of detection and a larger linear detection range are achieved due to the increased light absorbance in the bubble cell.

Another example to extend the path length of a flow cell is depicted in figures 3.14C.

In this design, the capillary is bent into a Z-shape and the transverse part used as the optical cell. The coupling and focusing of light into this cell is performed by a sapphire ball lens. A part of the light escapes or is trapped in the fused silica while the remaining part is transmitted through the solution in the bore of the capillary by multiple total reflection on the silica/air surface. The capillaries are pre-aligned and fixed in a capillary holder that can be manufactured for different instruments.

The length of the transverse section of the capillaries is 3 mm, which is large relative to the solute zone in CE separations. Guiding of light through this type of cell by refraction and reflection appears to be delicate as the refractive index of the solution has a large influence on the optical properties of these axially illuminated capillaries and part of the light travels the capillary wall and not the solution. The effective optical path length will be shorter than 3 mm.

The inherent disadvantages of such a Z-shaped flow cell are removed in a cell design as depicted in figures 3.14B and 3.17.

This cell design incorporates a fused silica body with flat flanking windows and a black fused silica cell that reduces stray light. It has an optical path length of 1.2 mm (12x longer than a bubble cell with a path length of 100 mm and therefore more sensitive) which establishes a well defined detector cell volume of 12 nL. The flat windows flanking the cell will improve spectral analysis.

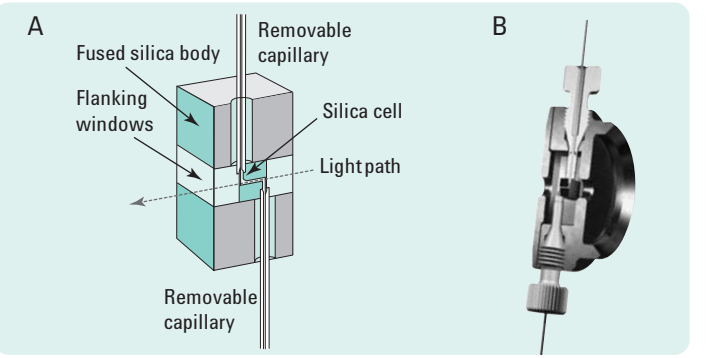

Figure 3.17
High-sensitivity cell used in micro-HPLC and CE. A) schematic configuration, B) representative example of a real high-sensitivity cell.

The high-sensitivity cell profoundly increases the practical linear detection range (deviation from linearity < 1 % up to 1400 mAU and < 3 % up to 2200 mAU) and signal-to-noise ratio (S/N), from 62.5 on a capillary with 75 mm id to 650 on the high-sensitivity cell, as is shown in figures 3.18 and 3.19, respectively.

In this example, a S/N increase of 16 (path length ratio of both cells) is expected instead of the obtained factor 10. This is caused by the fact that a higher absorbance (signal) in the high-sensitivity cell is accompanied by a proportional increase in noise.

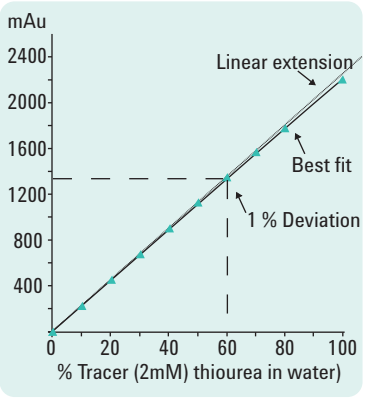

Figure 3.18
Determination of the linear detection range of a high sensitivity cell with thiourea in water.

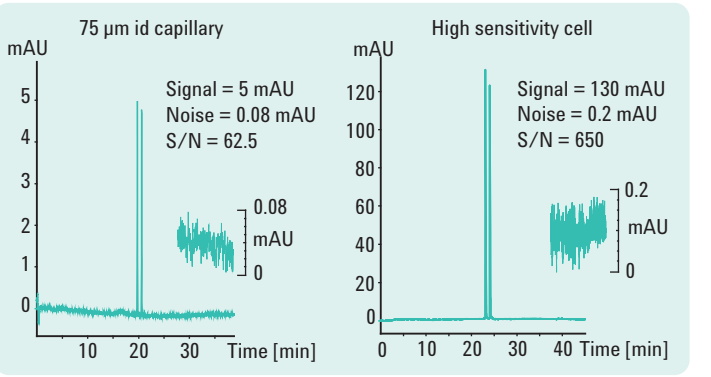

Figure 3.19
Comparison of signal-to-noise ratios of a high-sensitivity cell with a capillary of 75 µm inner diameter.

The inherent sensitivity of this type of cell really comes to fruition when enantiomeric excess in a drug component has to be determined; as is shown in figure 3.20.

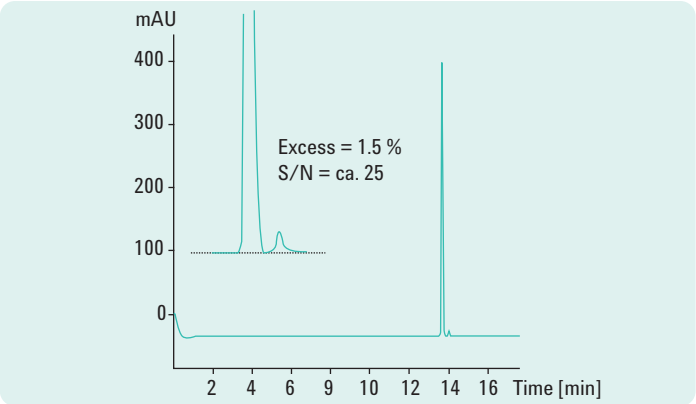

Figure 3.20
Determination of enantiomeric access.
Conditions: Main peak (+/-) epinephrine (100 µM); 20 mM dimethyl-ß-cyclodextrin/ 50 mM tris-phosphate pH 2.4; L_{eff} = 40 cm; id = 75 µm; injection: 150 mbar x s; 30 kV; 20 °C; λ = 200 nm high sensitivity detection cell.

3.4.1.3. Application of spectral data

As in HPLC, multi-wavelength UV detection can be applied in CE for the purpose of peak identification and the assessment of peak purity. However, the requirements for the rate of data collection are more severe in CE. With migration times of a few minutes and plate numbers of several hundreds of thousand, a total peak width of less than a second is not unusual. With the present diode-aray detectors (DAD) the cycle time (that is polling all available diodes) is ≤ 10 ms and this is certainly enough to allow the registration of peak shapes and spectra without bias.[40]

The schematics of a DAD, with a wavelength range (190-600 nm) and diodes on an array is illustrated in figure 3.21.

The DAD allows continuous acquisition of spectra in the UV-visible region of the spectrum; since all wavelengths are acquired simultaneously, there

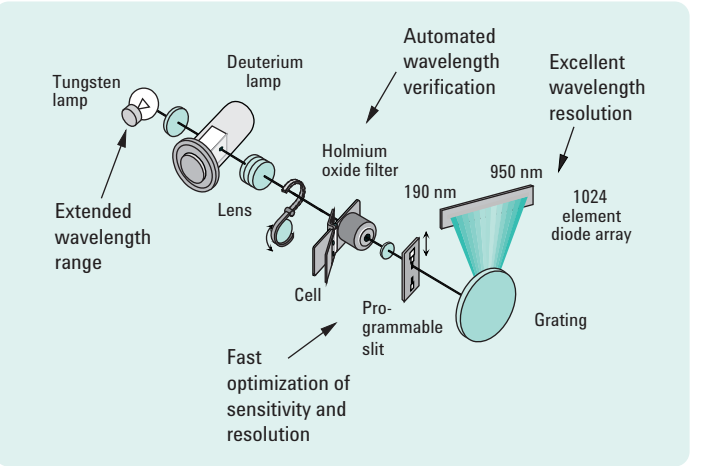

Figure 3.21
Optical design of a diode-array detector.

is no loss of sensitivity during spectral acquisition. When suitable conditions for peak separation have been developed, the spectral data can be processed in several ways:

- to extract electropherographic signals from spectral data to determine the optimum detection wavelength for each peak,
- to perform spectral library searches to obtain a qualitative identification,
- to calculate ratios of electropherographic signals to evaluate peak purity, and
- to perform peak purity checks to discover (hidden) impurities.

One way to present peak intensity (absorbance) versus wavelength and time is in a 3-dimensional (3D) plot (figure 3.22), from which the highest peak intensities at a particular wavelength can be determined.

Another, more practical, way to present spectral information is as a contour map, also called iso-absorbance plot. This technique plots the spectral information as a series of iso-absorptive, concentric lines in a wavelength and time plane (2D-plot, as is often also depicted on geographical maps to indicate lines of equal height). This presentation allows a simultaneous inspection of all spectral information as depicted in figure 3.23.

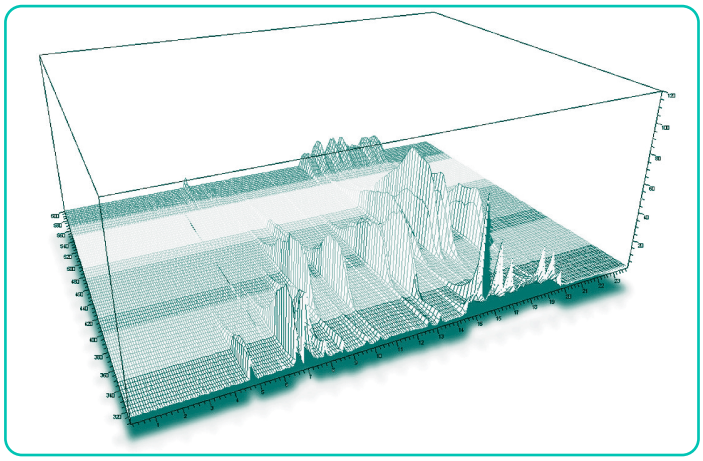

Figure 3.22
3D-plot of an electropherogram.

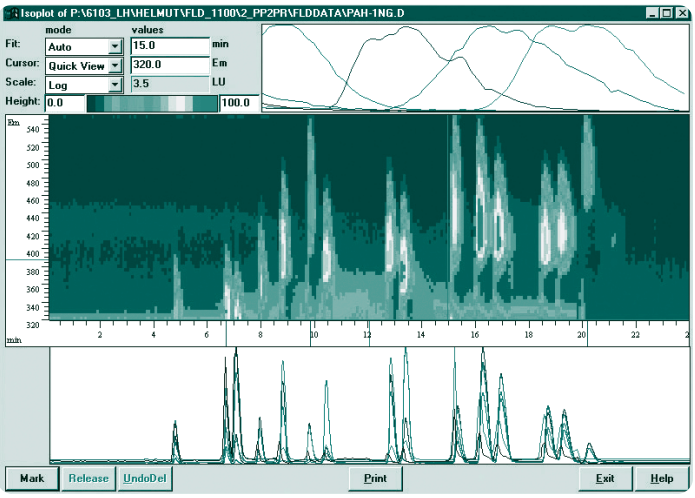

Figure 3.23
Iso-absorbance plot of spectral information with additional information on optimum intensity and single compound spectra.

This display can be broken down into three parts. The center of the display is an iso-absorbance plot, which gives a top-down view of the entire analysis. Different colors indicate absorbance levels from low to high.

The lower section of the display shows three electropherograms, which represent three cuts of the iso-absorbance plot along the horizontal line shown in the iso-absorbance plot. This allows the selection of the optimal wavelength for each peak in the electropherogram The upper section is a graphic display of the single spectra that can be obtained by moving the vertical line on the iso-absorbance plot to a specific contour of a peak. In this manner, a compound can be qualified by its spectrum.

To qualify an unknown compound by its spectrum, it has to be compared with spectra stored in one or more libraries. This is usually performed by normalization of the spectra to be compared. Normalization means, that both spectra are changed to a fixed value by setting the highest intensity to unity. Spectra can then be overlaid for visual comparison. As this is not very suitable for automated operations, statistics are applied to calculate the similarity (match factor or correlation coefficient) of a standard compound's spectrum with that of the unknown.

An example of such a peak purity check is shown in figure 3.24, in which spectra have been acquired at the upslope, the apex and the downslope of the peaks and normalized (normalization of these spectra compensates for the changing concentration of the eluting component passing through the detector). Both visual comparison and calculated purity match factor

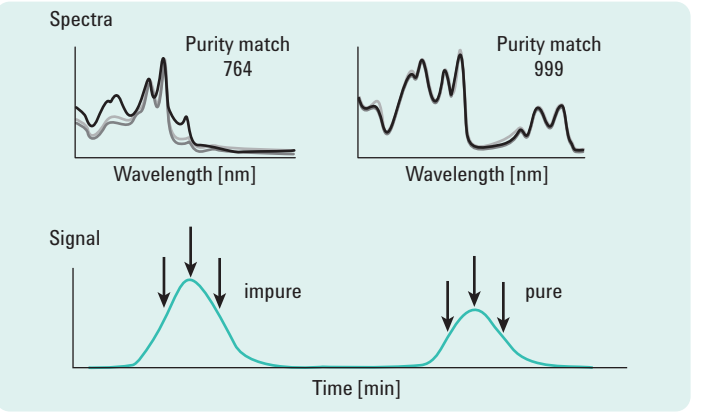

Figure 3.24
Comparing spectra of pure and impure peaks by spectral overlay and calculated match factor.

clearly show the difference between the pure and impure peak. For increased precision a calculation of the match factor on 3, 5, 7, 9, or all spectra across a peak can be calculated.

Note: *a match factor above 990 generally indicates that spectra are similar. Values between 900 and 990 indicate that there is some similarity, but the result should be interpreted with care. All values below 900 indicate that the spectra are different.*

Another technique to establish peak purity is to plot absorbance ratios at two or more wavelengths over the concentration profile of the peak. For any given compound the ratio (R) is constant irrespective of peak height. Thus, a plot of this ratio across the peak profile takes on a rectangular shape (if the component is pure) with the height of the rectangle equal to the absorbance ratio. If the wavelengths are chosen carefully, this ratio can be quite compound specific. An example of this is illustrated in figure 3.25, where the measured ratios of 1.5, 5.3 and 2.8 help to identify peaks 1, 2 and 3 as components B, C, and A, respectively.

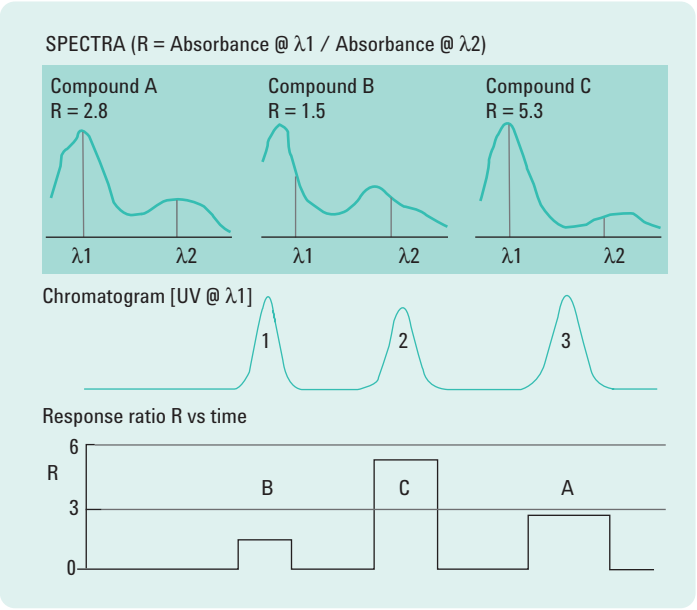

Figure 3.25
Ratio signal plot in peak purity detection.

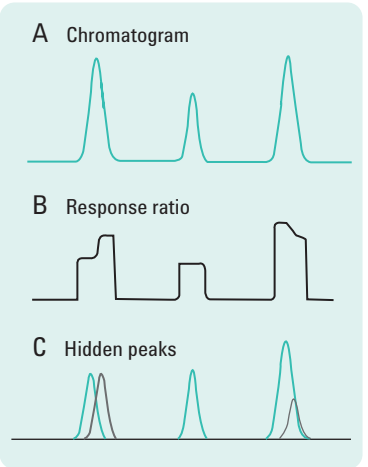

Figure 3.26
Ratio signal plot revealing unresolved hidden peaks.

Response rationing can also reveal unresolved hidden peaks. Shown in figure 3.26 is a chromatogram (or electropherogram) [A] recorded at λ1 which appears to have three peaks. The λ1 /λ2 response ratio in [B] does not show the expected rectangular shape for peaks 1 and 3. The reason for the irregular response ratios is the presence of unresolved hidden peaks shown in [C].

When peak purity is sufficiently established, the compound can be identified by searching for an identical spectrum in one of the available libraries. An example of this is shown in figure 3.27, where the spectrum of a CE peak is shared with the HPLC compound library.

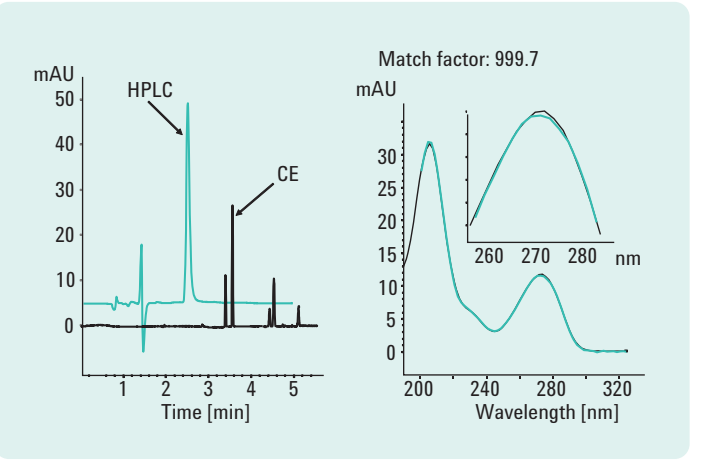

Figure 3.27
Identification of a CE peak by interrogation of an HPLC compound library.

3.4.1.4. Indirect photometric detection

In CE, the application of indirect photometric detection of non-UV absorbing analytes, that are otherwise difficult to measure with direct spectroscopic techniques, was introduced by Hjertén.[41] Examples of analyte types often detected indirectly are inorganic and simple organic ions, and sugars. These compounds generally do not absorb UV light, except in the extremely short wavelength range (< 190 nm).

For indirect photometric detection, an ionic compound with advantageous detection properties (such as a high UV absorbance intensity) is used as the monitoring ion, which is at the same time one of the constituents of the BGE. The presence of any non-absorbing analyte in a zone causes a change in the concentration of the BGE ions. When this analyte zone passes through the detector it will be detected by the accompanied change of the monitoring ion concentration as illustrated in figure 3.28

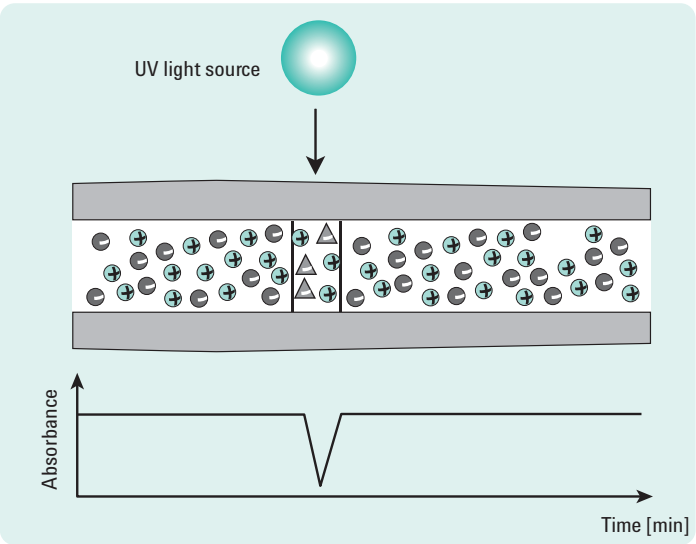

Figure 3.28
Schematic representation of indirect UV detection in CE.

Indirect detection is universal but non-selective. Its mechanism is explained as the displacement of one monitoring ion by one analyte ion of the same charge, on the basis of maintaining electroneutrality. This explanation is an

oversimplification that can be refuted when the equations, describing the electrophoretic transport processes, are diligently solved by applying the Kohlrausch Regulation Function (KRF, see section 1.3.4.5.).

The KRF mathematics show that the displacement ratio (number of BGE ions displaced by one analyte ion) can be higher than one and that even analyte ions with a charge opposite to that of the monitoring ion can be detected. It should be noted that the displacement ratio for a specific analyte-BGE combination is often also called: transfer ratio (TR).

The transfer ratio is defined as the change in concentration of the monitoring ion (C_m) through the presence of an analyte (a) in a zone, relative to the analyte concentration[42]:

3.9 $$\mathbf{TR = -\frac{\Delta C_m}{C_a}}$$

In this equation, the minus sign is added as in almost any practical application a decrease in the baseline signal is observed when analyte is present (figure 3.28).

Through the monitoring of a change in C_m, the transfer ratio is in fact a measure of the sensitivity that will be obtained in a particular application. Optimization of the BGE composition with respect to the transfer ratios is of importance in trace analysis. When lower detection limits are not so important, because the expected analyte concentrations are reasonably high, it is often better to optimize the BGE with respect to the sample capacity.

The ability to determine the concentration limit of detection (CLOD) for indirect UV detection depends on both sensitivity (TR) and baseline noise. If the BGE has no light absorbing components the noise is called system noise. When a UV absorbing BGE is present, every fluctuation in the monitoring ion concentration is detected as noise. The latter effect is mainly due to unequal heat dissipation at isolated spots on the capillary. This baseline noise is therefore dominant in indirect UV detection and proportional to C_m. When the BGE is only constituted of a monitoring ion with its counter ion, then $C_m = C_{BGE}$. With such a simple BGE the CLOD can be expressed by

3.10

$$\text{CLOD} = \frac{\text{Noise}}{\text{Sensitivity}} = \frac{N}{TR} \approx \frac{C_{BGE}}{TR} = \frac{A_{BGE}}{\varepsilon_{BGE}\, b_e\, TR\, DR}$$

where A_{BGE} = absorbance of the BGE = $\varepsilon_{BGE}\ b_e\ C_{BGE}$
DR = dynamic reserve = A_{BGE} / baseline noise
b_e = effective path length of the detector
ε_{BGE} = molar absorptivity of the BGE

An overview of the above mentioned characteristics is depicted in figure 3.29.

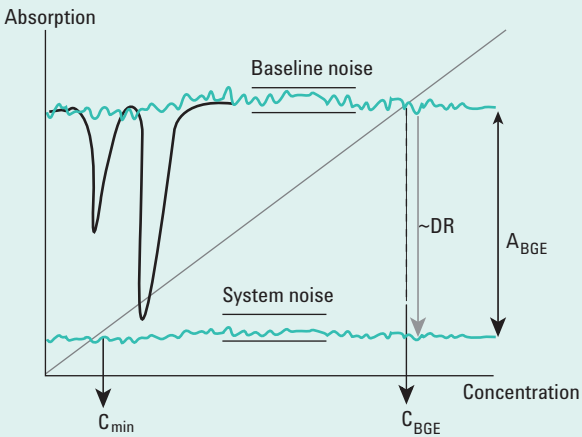

Figure 3.29
Characteristics of indirect UV detection.

Equation 3.10 clearly shows that optimization of CLOD depends on TR and DR. The optimization of TR (>1) is not easy as this requires a considerable knowledge of how to match analyte with monitoring ion. In contrast to TR, the optimization of DR boils down to finding a BGE with a high molar absorptivity of the BGE (ε_{BGE}), so that C_{BGE} can be kept as low as possible (a high BGE concentration will allow a higher sample capacity but this also leads to a higher noise level and a chance that the linear range of the

detector will be exceeded). Therefore, one always has to find the best compromise between a low limit of detection (low C_{BGE}) and a high sample capacity (high C_{BGE}). In many practical applications, typical monitoring ion concentrations of 5-10 mM are used, which can lead to detection limits of 10^{-4} - 10^{-5} M.

For the BGE, a salt of a small, UV absorbing ion can be chosen. For the detection of anions, monitoring ions such as chromate, benzoate, phthalate or sorbate can be used. For cations, imidazole and pyridine are usually recommended. Addition of other ionic compounds to the BGE should be kept to a minimum as both TR and DR can be affected.

Compared to indirect UV detection, indirect fluorescence detection can provide lower detection limits (~ 10x). This is mainly due to the difference in noise characteristics of the two detection methods.

Note: *Besides these two indirect photometric detection techniques, an indirect contactless conductivity detection method has also been described in the literature (see section 3.4.3.).*

3.4.2. Laser induced fluorescence (LIF)

In UV-vis spectrophotometric detection, the molecule of interest absorbs a discrete package of energy (photon with energy, $h\nu_{0,1}$) to reach a higher energy level S1 (S0 → S1: excitation). If the molecule would immediately emit this photon and fall back to its lower energy level S0, the original lower intensity of the transmitted light would directly be compensated and no absorbance would be measured. Fortunately, this effect does not happen as the molecule loses its extra energy through collisions with its nearest neighbors, which are molecules of the solution. The photon energy of the incident light beam is thus converted into heat.

In some cases, this conversion of energy does not take place. The molecule maintains its extra potential energy for some time (in general during a very short time, roughly 10^{-6} seconds) before it, indeed now, emits a photon with energy $h\nu_{0,1}$. This phenomenon is called fluorescence and is in general restricted to molecules with a particular rigid planar structure, such as aromatic ring systems.

However, during the short time that the molecule stays in its higher electron energy level, it also has the chance to fall back to some of its lower energy levels. First, a part of the absorbed energy is dissipated radiation less until the lowest singlet energy level (S1) of the electronic state is reached, and subsequently, after typically 1 – 100 ns, the molecule falls back to one of the vibrational energy levels of the electronic ground state (S0).

In general, this means that the emitted photons have a random direction and that the fluorescence radiation does not have the same wavelength as the absorbed radiation so that a complete fluorescence spectrum is emitted, which resembles its absorption spectrum but has shifted to higher wavelengths (lower photon energies). An example of this process is depicted in figure 3.30.

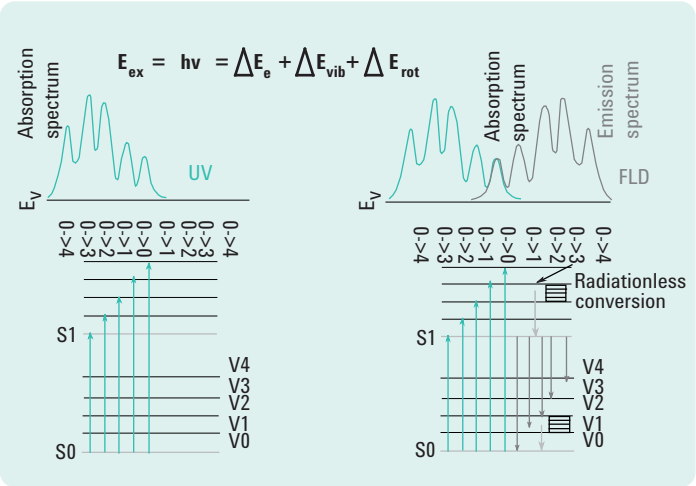

Figure 3.30
UV absorption spectrum of a molecule in solution and its emitted fluorescence spectrum (V0 through V4 are vibrational energy levels of the electronic ground state (S0), or of the next higher singlet electron energy level: S1).

When the zone of a fluorescent compound passes the detection window, the expected signal (S) is approximately given by:

3.11

$$S \approx k\ I_0\ V_{ill}\ \Phi_i\ \varepsilon_i\ C_i$$

where
- k = collection efficiency of the optical system (fraction of emitted light directed onto the photosensor)
- I_0 = excitation light intensity in the optical cell
- V_{ill} = illuminated volume of the solution in the optical cell
- Φ_i = fluorescence quantum yield
- ε_i = molar absorptivity
- C_i = analyte concentration

Equation (3.11), suggests that the instrumental requirements for high sensitivity are a strong radiation source and an efficient collection of the emitted light. The fluorescent quantum yield of a compound, however, is difficult to predict. Although quantum yields of 1 have been observed, a compound with a quantum yield of 0.1 can already be regarded as "highly" fluorescent.

The fluorescence signal of the analytes is always measured on a certain background signal. This background is caused by scattering of the excitation radiation on the walls of the flow cell, by fluorescent impurities in the solvent and ultimately by Raleigh and Raman scattering of the solvent. To obtain a low background signal it is of special importance to discriminate the desired emission wavelength(s) by spectral filtering or spatial resolution against the excitation wavelength and overtones thereof. The noise of the background signal is the determining factor for the CLOD's that can be obtained. These detection limits can be one to three orders of magnitude lower than those obtained with absorbance detection.

In CE, a laser can be used as the excitation source, since with this light source a high light intensity can be directed on a part of the fused silica capillary, which acts as the optical cell with a small detection volume. The disadvantage of the small volume scale in CE (the low value of V_{ill} required to preserve separation efficiency) can be counteracted by an increase in intensity of the excitation light on the detection window and/or using cells with an expanded illuminated volume (bubble and high-sensitivity cell).

Laser induced fluorescence detection (LIF) has been introduced in CE by Gassman *et al.* in 1985[43] and by Burton *et al.* in 1986.[44] Several, lamp based, optical fluorescence detector designs that are still compliant with lasers, formed the basis for today's LIF detectors.

A further development of this, lamp based, optical design to the application of lasers is shown in figure 3.31. A laser beam is focused on the capillary by means of a ball lens. An identical separation of the excitation position from the collection of the emitted light, as shown before, ensures that a high fraction of emitted light is collected and adequately filtered so that high signal-to-noise ratios can be achieved.

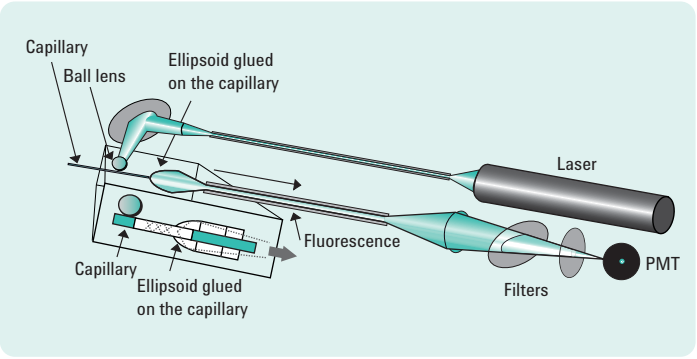

Figure 3.31
Non-collinear optical design for LIF. The ball lens has a very large aperture and maximizes the fluorescence intensity by optimizing the illumination of the inner part of the capillary cell by the laser. The ball lens also precisely focuses the excitation radiation onto the flow cell. An ellipsoid collects the emitted radiation for transmission to the emission filters and the PMT (reproduced with permission of Picometrics SA).

A careful arrangement of this optical design with a replaceable capillary LIF-cassette system avoids refocusing of the laser and re-alignment of the emitted light beam with the photomultiplier tube when capillaries and/or lasers are changed.

The advantages of the application of lasers are obvious:
- The light produced by the laser is monochromatic, which allows an optimal excitation selectivity.
- The parallel beam of a laser is easy to focus on the capillary, so that a high irradiance in the detection cell can be realized.

For LIF applications, the power of the laser does not have to be extremely high. A line power of several milliwatts is sufficient to obtain a high sensitivity. With higher applied power, signal-to-noise ratios are, in general, not further improved. This is caused by several factors. First, with very high light intensities the fluorescent compounds have a tendency to get saturated (the majority of the molecules is already in the excited state). An increase in light intensity is then not producing a higher response. A second factor is the possible photodegradation of the fluorescent analytes. With some photosensitive compounds the absorption of a photon may lead to a decomposition of the molecule. When this happens, there is an upper limit to the emission intensity and the use of a less intense excitation light beam is then mandatory. A third factor that limits the signal-to-noise ratios when the intensity of the excitation light is increased, is the instability of the light source (laser). Since the signal as well as the noise on the background are proportional to the excitation light intensity, a further increase of the irradiance does not help to obtain higher signal-to-noise ratios.

Since fluorescence is a rather rare phenomenon, the applicability of this detection mode based on natural fluorescence is limited. However, in order to profit from the inherent selectivity and sensitivity, a large number of reagents have been developed with which certain classes of compounds can be made fluorescent before they are separated by HPLC or CE. Most of these pre-column derivatization schemes involve the covalent addition of a fluorescent moiety to a specific functional group on the analyte molecules.

A large number of labeling reagents are commercially available. Some of the more frequently used reagents, together with their optimal excitation and emission wavelengths, are listed in table 3.4.

Functional group	Reagent	λ_{ex} [nm]	λ_{em} [nm]
Primary amine	O-phthalic aldehyde (OPA),	325/340	455
	fluorescamine, 3-(4-carboxybenzoyl-2-quinoline-carboxyaldehyde (CBQCA),	390	475
	5-furoylquinoline-3-carboxyaldehyde (FQ)	442 488	550
Primary or secondary amine	Dansyl chloride, fluoronitrobenzooxadiazole (NBD-F)	350	530
	9-fluorenylmethyl chloroformate (FMOC)	470	530
	fluorescein isothiocyanate (FITC)	260, 488	305, 525
Hydroxy	Naphtyl isocyanate	310	350
	anthroylnitrile	370	470
Aldehyde or ketone	Reductive amination APTS	365	505
	dansylhydrazine (Dns-H)		
Carboxylic acid	Anthryldiazomethane (ADAM)	365	412
Thiol	N-acridinyl maleimide (NAM)	355	465
	OPA	340	455
Arginine residues	Benzoin	325	440
Tyrosine residues	4-methoxy-1,2-phenylenediamine	325	438
Phe, Tyr, Trp	Native fluorescence	257 280	305, 325

Table 3.4
Reagents for pre-column fluorescence labeling.

Pre-column derivatization procedures from HPLC have often been applied directly in CE. In other cases special labeling reagents have been developed for CE. A special reason for this can be that the derivatives should be suited for a particular type of laser to be used for LIF, with an excitation wavelength compatible with a line of the laser spectrum. An example of such a derivatization reagent is naphthalene-2,3-dicarboxaldehyde (NDA), which can be used as an alternative for the well known OPA reagent (but reacts slower). NDA shows a strong absorbance (and high fluorescence intensity) when excited with the 442 nm line of a HeCd laser.[45,46] Another reason to choose a special derivatization reagent can be that certain electrophoretic properties of the derivatives are required. The complete resolution of similar compounds is often easier to accomplish when they migrate against the EOF. Therefore, in a BGE with an EOF towards the negative electrode, negatively charged derivatives have some advantage. An example of such a derivatization reagent is 1-aminopyrene-3,6,8-trisulfonate (APTS), which has been used for the derivatization of oligosaccharides.[47] Since the derivatization label caries three strongly acidic groups, a wide pH-range is available for the separation of the sugar derivatives.

3.4.3. Contactless conductivity detection (CCD)

In early work on electrophoresis in narrow tubes (1967-1980) conductivity was used as a standard detection device. However, with the emergence of CE in fused silica capillaries (1981) it was experienced that spectrophotometric detection (UV and fluorescence) was almost ideal, and conductivity detection was neglected for quite some time (up to 1987). Nevertheless, there are some strong points for the use of conductivity detection in CE. First, the method is in principal universal and therefore especially suited for compounds that are otherwise difficult to detect, such as inorganic ions. Secondly, the small volume scale, required for the detector, is no obstacle to obtain low detection limits.

In the following decade, several serious and promising attempts were made to revive conductivity detection in CE. With sensing electrodes in the capillary[48,49], end column detection[50,51] (one sensing electrode at the capillary exit, the other grounded with the HV supply) and end column detection with an "open architecture". In the last construction (1996)[52], capillaries are easily interchangeable whereas the detection volume remains precisely defined. With this type of end column detection, 10 x lower detection limits (10^{-5} - 10^{-6} M ≈ 1 ppm - 100 ppb) than with indirect UV detection were obtained for inorganic ions. But this construction did not hold up in CE practice which was mainly due to the emergence of contactless conductivity detection (CCD), which wiped out all problems encountered with electrodes contacting the BGE.

The contactless conductivity detector was introduced into the electromigration separation techniques by Gaš *et al.* in 1980.[53] Eighteen years later, Zemann *et al.*[54] constructed a coaxial CCD for CE. With this detector, two stainless-steel tubes act as electrodes mounted around the capillary at a defined distance from each other. By applying an oscillating frequency (30-600 kHz) to the actuator electrode, a capacitive transition occurs between this electrode and the liquid inside the capillary. After having passed the detection gap between the electrodes (which acts as an ohmic resistor), a second capacitive transition between the electrolyte and the pickup electrode takes place. When, due to passing analytes, the conductance (= 1/resistance) in the gap changes, this will be sensed by the pickup electrode.

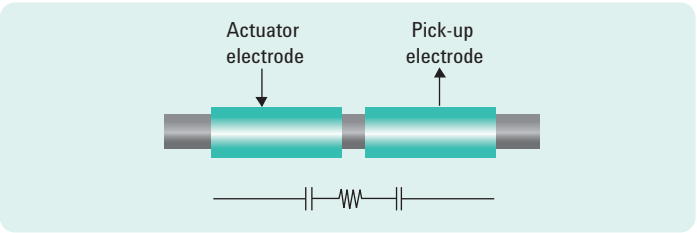

Figure 3.32
Schematic of CCD principle. Lower diagram; electrical equivalent, capacitor, ohmic resistor, capacitor.

The simple, mechanical construction of the CCD's cylindrical metal electrodes around the separation capillary is shown in figure 3.32.

The advantages of the CCD are obvious:
- On-capillary detection
- No electrode fouling
- No necessary connections
- Hyphenation with other detection systems (UV, LIF, MS)
- Ability to work with packed capillaries (CEC)
- Besides fused silica, other materials (Peek, PTFE) can be used
- Limits of detection for inorganic and small organic ions in the ppm → ppb region

To achieve optimal sensitivity, the difference in conductance between an analyte zone and the BGE should be as high as possible. This condition, however, leads to one of the inherent problems with conductivity detection as a bulk property of the BGE is measured. Fluctuations of the BGE composition or its temperature are directly translated into baseline instabilities. Furthermore, a high background conductivity of the BGE will be associated with a high noise level and will thus negatively affect detection limits. On the other hand, a low conductivity of the BGE can easily lead to overloading (see section 1.3.4.5., electrodispersion, in chapter 1). A compromise for conductivity detection can therefore be found in the use of amphoteric buffers at relatively high concentrations (MES, CAPS, amino acid zwitter ions and mixtures thereof).

Two examples of the separation of anionic and cationic ions, detected by a CCD are shown in figures 3.33 and 3.34, respectively.

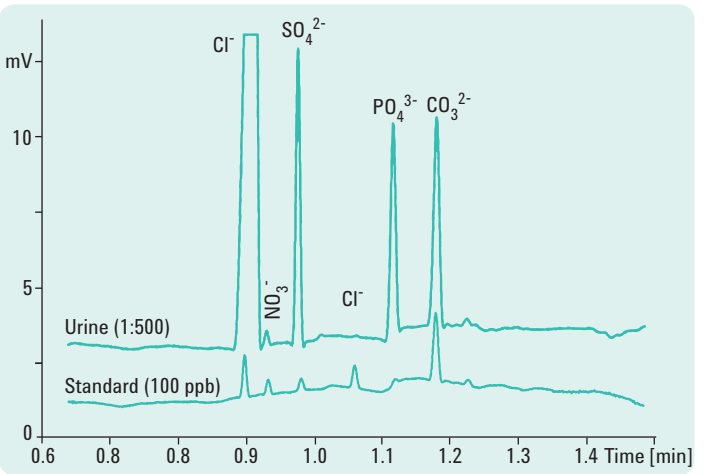

Figure 3.33
CZE of anions in a urine sample (500x diluted).
Conditions: Buffer: 7 mM sorbic acid/15 mM arginine + 0.001 % hexadimethrin hydroxide (HDB), pH 9.0; L_{tot} = 50 cm; L_{eff} = 37 cm; id = 50 µm; injection: 200 mbar x s; applied voltage: 30 kV.

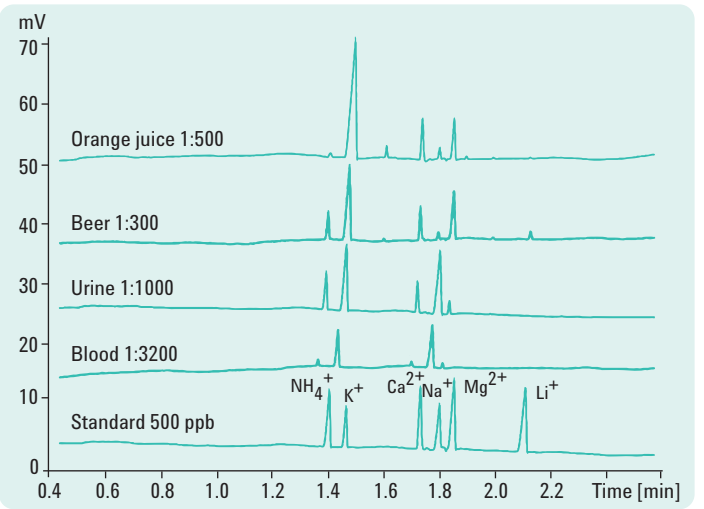

Figure 3.34
CZE of cations in several diluted real samples.
Conditions: Buffer: 25 mM MES/25 mM histidine + 1 mM 18-crown-6-tetracarboxylic acid, pH 6.1; L_{tot} = 50 cm; L_{eff} = 46 cm; id = 10 µm; injection: 840 mbar x s; applied voltage: 30 kV.

The standard trace in this electropherogram shows that low ppb detection limits of anions are feasible. Figure 3.34 illustrates the separation and detection of cationic ions, of several diluted real samples, on a capillary with an id of 10 µm.

In this example, the crown ether complexes with the cations to obtain separation of K^+ and NH_4^+ ions. The standard trace also indicates that detection of cations can be achieved for ppb amounts, which seems hardly feasible with UV detection on a 10 µm id capillary.

More recently, the CCD has been used to fruition in the separation of mono- and disaccharides[55], underivatized essential amino acids[56], haloacetic acids in water[57] and metal ions.[58]

One example of these applications is given in figures 3.35 A and B where the separation profiles of underivatized amino acids with CZE-CCD in real samples such as beer and yeast are presented. Due to elimination of EOF in the separation capillary a significant migration time reproducibility was obtained (RSD < 0.3 %) for all amino acids. The detection limits of individual amino acids were in the range of 9.1 to 29 µM (~ 1-3 ppm).

It should be noted that in the separation of haloacetic acids in water[57], it was demonstrated that several buffer systems can be chosen (based on the PeakMaster simulation program, see section 4.4.1.1.) so that these compounds can not only be detected by direct CCD but also by indirect CCD. Quantitation of these compounds, by both detection methods, could be established at a 0.1 ppm level.

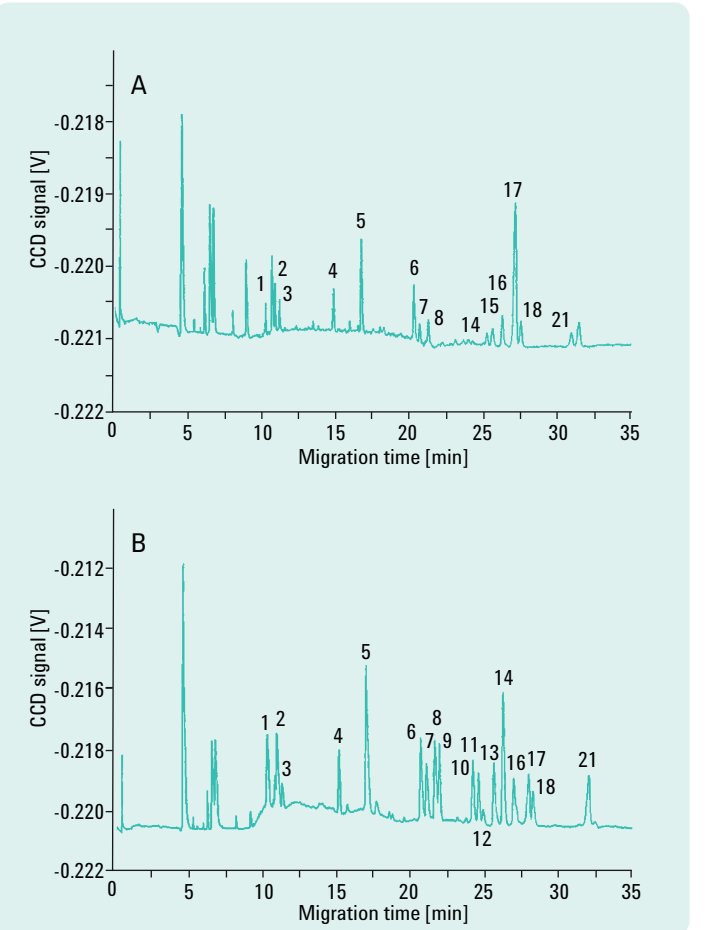

Figure 3.35
Profiles of amino acids measured by CZE-CCD in (A) Budvar beer; (B) Pangamin yeast.[56]
Conditions: 2.3 M acetic acid (pH 2.1) + 0.1 % HEC; L_{eff} = 66.5 cm; L_{tot} = 80 cm; id = 50 µm; injection: 300 mbar x s; voltage: + 30 kV; current: 15.4 µA; temperature: 25 °C; detection: CCD; peaks: 1, Lys; 2, Arg; 3, His; 4, Gly; 5, Ala; 6, Val; 7, Ile; 8, Leu; 9, Ser; 10, Thr; 11, Asn; 12, Met; 13, Gln; 14, Trp; 15, Glu; 16, Phe; 17, Pro; 18, Tyr; 21, Asp.

3.5. Fraction collection

Although CE is in essence a miniaturized separation technique, there is a continued interest in its preparative possibilities due to its unsurpassed separation efficiency and the fact that it can be performed in free solution. Bulk production of desired compounds is marginal but the technique remains still attractive for the production of small amounts of purified components. The separated, tiny fractions can therefore be collected for the following purposes:

- sequencing of DNA fragments or peptides,
- off-line identification by MS and molecular weight determination by MALDI-TOF,
- establishing biological activity in a single substance, or
- checking the purity of a collected peak by reinjection.

When sufficient material cannot be obtained in one run, automated multiple collections can be programmed. An example of a preparative CE run is shown in figure 3.36A, where a tryptic digest of a recombinant protein (GroEs) was separated on a 100 µm id capillary under overloaded conditions. Reinjection of one of the collected fractions on a 50 µm id capillary confirmed the purity of the product (figure 3.36B).

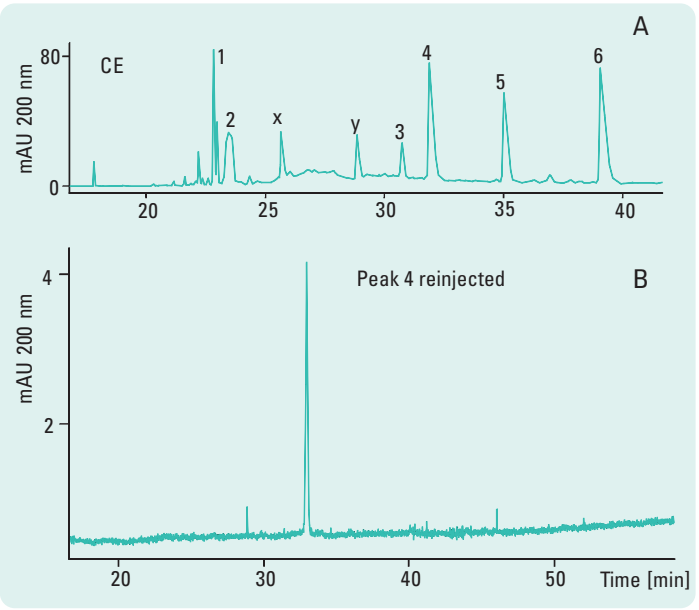

Figure 3.36
Preparative separation by CZE of a tryptic digest of recombinant GroEs (A) and a purity check of the collected fraction (B).
Conditions (A): Buffer: 105 mM phospate, pH 2.0; sample: tryptic digest of recombinant GroEs protein; effective length: 87.5 cm; total length: 96 cm; id: 100 µm; temperature of capillary and sample tray: 15 °C; voltage gradient, 0-3 min: 0-10 kV, 3-10 min: 10-20 kV, 10-20 min: 20-25 kV, 20-40 min: 25-30 kV; injection: 350 mbar x s.
Conditions (B): Same buffer; sample: peak 4 from (A); effective length: 56 cm; total length: 62.5 cm; id: 50 µm; id at point of detection: 150 µm; temperature of capillary and sample tray: 15 °C; voltage: 30 kV; injection: 200 mbar x s.

The schematic of a sample collection, during a preparative CE run, is illustrated in figure 3.37.

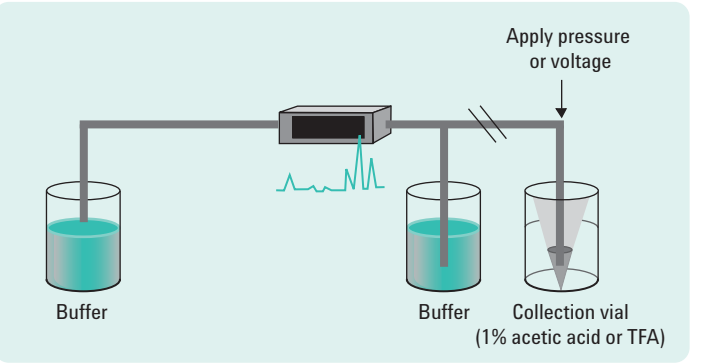

Figure 3.37
Schematic of sample collection.

Before collecting samples, several important things have to be considered:

- Use 75 or 100 µm id capillaries; multiple collections are usually needed with 75 µm id, but with a 100 µm id capillary a single collection often suffices.
- Calculate time from detector to end of capillary and program a switch from buffer to collection vial.
- Load as much sample as possible (overloading limits are discussed below).
- Stable migration times are mandatory for multiple collections.
- Collect in conical micro vials with a minimal volume of 5-50 µL.
- Decrease voltage during elution to increase temporal peak width and simplify collection of narrow zones.
- Use buffer (or diluted buffer) in collection vial to maintain electrical connection during electro-kinetic elution.

In order to predict the temperature increase in the preparative capillary, an estimate of the electrical conductivity (κ_e) was made from several identical buffer conditions found in the literature and by applying: $\kappa_e = i/E\,A$ (where i, E, and A are current, electric field strength and capillary cross section, respectively [equation (1.23), section 1.3.4.5.]. When correcting to 15 °C, the result is: $\kappa_e 15\ °C \approx 0.005\ \Omega^{-1}cm^{-1}$.

With this value table 3.5 was generated for the highest applied voltages (20, 25 and 30 kV, respectively) on the preparative capillary (100 µm id). For the sake of comparison, the calculated data for the analytical capillary (50 µm id) are also given.

Voltage (kV)	Electric field (V/cm)	Current (µA)	Current density (A/cm^2)	ΔT_{cap} (°C)	$\Delta T_T \approx \Delta T_{w\text{-}s}$ (°C)	T_0 (°C)	V_{inj} (nL)	L_{inj} (mm)	N_{est}
Preparative capillary									
							81.3	10.4	40,000
20	208.3	81.8	1.04	0.22	2.5	17.5			
25	260.4	102.2	1.30	0.34	4.0	19.0			
30	312.5	122.7	1.56	0.50	5.7	20.7			
Analytical capillary									
30	480	47.1	2.4	0.30	3.4	18.4	4.5	2.3	90,000

Table 3.5
Calculated values for the temperature differences between capillary center line and inside wall (ΔT_{cap}), capillary center line and surrounding environment (ΔT_T) and the elevated temperature at the capillary center line (T_0) under the experimental conditions of the preparative and analytical capillary (figure 3.36, A and B, respectively). (For explanation of the temperature calculations, see section 1.3.4.2., Joule heating).

That a 350 mbar x s injection on the preparative capillary leads to injection overloading is clear from the calculated volume of 81.3 nL (at 15 °C) with a plug length of 10.4 mm (which is ~ 12 % of the effective length) and an estimated plate number (N_{est}) of ~ 40,000. In contrast to these numbers, the analytical capillary generates at 200 mbar x s an injection volume of 4.5 nL with a plug length of 2.3 mm (which is ~ 0.4 % of the effective length!) and an estimated plate number of ~ 90,000.

If diffusion is the only source of band broadening, it can be expected that the analytical capillary will generate, for the specific tryptic digest peptide of peak 4 in figure 3.36B (MW = 1012 Da, determined by off line MALDI - TOF and with an estimated diffusion coefficient: $D^{20\,°C} \approx 3.10^{-6}$ cm^2/s), a plate number: $N = L^2_{eff}/2Dt \approx 250{,}000$. As the experimentally estimated plate number for a symmetrical peak of this type of compound is only ~ 90,000, it is obvious that other dispersion sources (see section 1.3.4.) must have contributed. The most likely culprits are therefore: joule heating

(ΔT_{cap} = 0.3 °C, table 3.5), some wall adsorption and probably siphoning from inlet to collecting outlet reservoir.

Sacrificing plates to enhance collected product, as shown on the preparative capillary, can only be performed when resolution is not at stake!
Figure (3.36, A) and table 3.5 show that in this preparative separation example, injection overloading leads to a severe plate number loss with respect to the analytical capillary (~ 50,000 plates or ~ 56 %). However, this does not lead to peak overlapping or extreme peak deformation, but a radial temperature gradient [ΔT_{cap} (max) = 0.5 °C], due to Joule heating, (at an operational temperature of 15 °C) could not be avoided.

Apart from a loss in separation efficiency, due to radial temperature gradients, siphoning and an overloading injection plug length, a more serious efficiency loss is usually encountered when a high concentration (compared to that of the BGE) of analyte ions is injected. A high concentration of analyte ions in a zone will disturb the local field strength, causing electrodispersion (see also section 1.3.4.5.). In this case, the apparent mobility of the analyte in the zone (μ_a) becomes a function of its concentration and triangular concentration profiles are developed that can be described by:[59]

3.12
$$\mu_a(c) = \mu_0 . \left(1 + \beta_E . \frac{c}{c_b}\right)$$

where
- c = local analyte concentration in the zone
- c_b = salt concentration of the BGE
- μ_0 = analyte mobility at infinite dilution
- β_E = electromigration constant

Increasing the amount of analyte will lead to a wider range of the analyte concentration within the zone, larger differences in apparent mobilities and thus to a wider zone. The (dimensionless) electromigration constant ($ß_E$) describes the susceptibility of an analyte/BGE combination for overloading.[60] Electrodispersion can be minimized by a proper choice of the BGE composition. However, in practice it will usually not be possible to avoid it completely; under optimized conditions values of $ß_E$ in the order of 0.1 to 1 are realistic.

On the basis of equation (3.12), it can be derived that under overloading conditions the obtained plate number is inversely proportional to the concentration of analyte injected. An approximate expression that relates the maximum amount of analyte (Q_i^{max}, in moles) that can be purified in one run to the plate number required for the separation (N_{req}) is:[59]

3.13

$$Q_i^{max} \approx \frac{8}{N_{req}} . \frac{1000\, c_b}{\beta_E} . \frac{1}{4} \pi d_c^2 . L$$

where the BGE salt concentration (c_b) is in mol/L (M) and d_c and L are the capillary inner diameter and total length, respectively

According to equation (3.13), maximizing the sample capacity of a CE system, one should:

- tune the composition of the BGE with the electrophoretic properties of the sample component to be purified, in order to obtain a low susceptibility to overloading (low value of $ß_E$),
- use a high BGE concentration, within the limits set by the solubility of the buffer or the sample components (and not induce temperature elevations that can cause sample decomposition),
- apply a relatively low voltage, but high enough to reach the required number of plates,
- use a long capillary, within the limit set by an acceptable run time,
- select a capillary with a wide bore, within the limit set by the allowed temperature increase.

A bottle neck for preparative CE is often that some parts of the capillary can not efficiently be cooled (isolated conducts to capillary cassettes, bottles and so forth) so that the power that can be applied is limited to the maximum allowed temperature in these parts.

In table 3.6, the operating conditions and performance of a typical analytical application of CE are compared to those of a (hypothetical) preparative application, optimized in the manner presented above. Compared to the analytical system, the mass capacity per run (Q_i^{max}) of the preparative

system is increased by a factor of 100 and the production rate (mol/s) by a factor of 10.

Parameter	Analytical	Preparative
V (kV)	25	10
L^{tot} (m)	0.5	1
d_c (µm)	50	100
C_b (mM)	10	125
t_{run} (min)	6	60
N^*_{max}	500,000	200,000
P (W/m)	0.5	1
ΔT_T (°C)	5	10
$Q_i^{max,**}$ (pmol)	2	200

Table 3.6
Comparison of operating conditions and performances of an analytical and a micropreparative CE system.
***Plate number obtained without overloading.**
****Maximum amount injected for N_{req} = 100,000.**

Note: *ΔT_T is proportional to the power per unit length (P), [$P = Q \cdot d_c^2/4$, in W/m, equation 1.17, section 1.3.4.2.]. When this parameter (P) is calculated from our experimental examples (figures 3.36, A and B), the result for the preparative capillary is: 30 kV (P = 1.2); 25 kV (P = 0.9); 20 kV (P = 0.5) and for the analytical capillary: 30 kV (P = 0.7).*

These calculations show that application of 30 kV, in both preparative and analytical experiment, leads to surpassing of power limits (table 3.6) without exceeding the indicated temperature limits (tables 3.5 and 3.6).

3.6. Capillary electrophoresis coupled with mass spectrometric detection and ICP-MS

Mass spectrometry (MS) has become very popular as a detection technique for capillary electrophoresis. Both techniques by themselves have large potential in separation, identification and quantitation of substances in complex mixtures. In their combination, limitations of the one technique are offset by properties of the other. For example solutes that are isobaric, means they have the same molecular weight, cannot be distinguished by MS. However a separation technique like CE may separate such substances easily so that they are identified easily in MS. Vice versa, solutes that co-elute in a separation method, may be easily distinguished in MS since they are of different molecular weight and may show dissimilar fragmentation.

However, like in liquid chromatography the challenge in coupling CE with MS detection is to combine a liquid phase separation with a vacuum detection technique. In case of CE to a certain extend this problem is alleviated by the very low amount of solvent needed in a CE separation. Coupling of the effluent of a CE separation to MS detection by electrospray ionization (ESI) therefore seems an ideal match. Especially since ionization yield and therefore sensitivity improves dramatically when one uses ESI at very low flow rates common in CE. An additional advantage of ESI is that it is particularly well suited to ionize polar and charged substances, which CE deals with mostly.

But a new challenge for coupling CE and MS appeared. Both CE and ESI are electrical field driven. In coupling, the end electrode of the CE separation device will be effectively shared with the electrode to establish the ESI field. Here is a strong mismatch though, since the CE and ESI current may differ by several orders of magnitude and the electrodes may be of opposite sign which mandates delicate electrical configuration (see 3.6.2).

Several methods to surmount these problems have been described in the literature and are commercialized.[61] The most important aspects of the coupling are discussed in the next paragraphs. In addition, many reviews have recently appeared and give up-to-date information about the status of the technology.[62-65]

3.6.1. Fundamentals of CE-MS interfacing

In order to move solutes from the liquid phase into the mass spectrometer they have to be transferred into gaseous ions. Subsequently, such ions may become radical ions by collision with electrons, photons or other charge-transfer processes in the source or in the MS itself (collision gas or other processes).

Electrospray ionization has become the dominant methodology in direct on-line coupling of a liquid flow from a separation column into the MS at atmospheric pressure and ambient temperature. A generalized schematic of ESI is given in figure 3.38.[66,67]

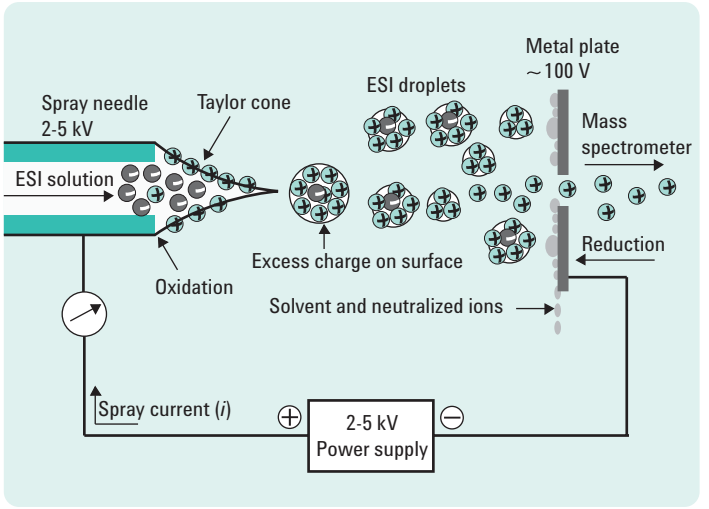

Figure 3.38
Pictorial description of the electrospray ionization process.

In an electrical field, solvent leaving the end of the capillary at nL/min flow rate forms very small droplets (spray). These droplets very readily loose neutral solvent molecules thereby decreasing in size and by which the surface charge increases rapidly. Eventually the droplets explode (coulombic fission) forming even smaller droplets in which the same process continues. Eventually gas phase solute ions remain, which may bear multiple charges, and which are drawn into the entrance of the MS.

In nanoflow HPLC this process is accelerated by putting the MS entrance at a high temperature, delivering a drying gas flow towards the needle tip and by using organic solvents like acetonitrile used for reversed phase HPLC. The direction of the electrospray field and the current is not critical in nanoESI. In contrast in coupling CE with MS, the direction in which the field is applied and the direction of the current, have large consequences for the electrical interfacing which will be described in the next paragraph.

3.6.2. Electrical interfacing

In CE a high voltage is applied to the inlet of the separation capillary. Therefore a stable electrode contact at the end of the separation capillary is required to provide a return path for the current carried by the solvent. Typically the outlet electrode is kept at ground (see 3.1).

In order to establish the electrospray, also a high electrical field is required between the outlet of the separation capillary and the inlet (capillary) of the MS. The simplest arrangement to establish this field is one in which the CE outlet capillary (or sprayer tip) is at ground and the electrospray voltage is applied from the MS. If this potential is negative, then positive ions will enter the MS; this is called positive ion mode. If the potential is positive, negative ions will enter the MS and this is called negative ion mode. MS vendors like Agilent Technologies and Bruker provide instruments with electrospray potential applied at the MS.

Vice versa, where the end of the capillary (or sprayer tip) is set at high voltage in CE-MS, important circuit considerations apply. In this situation an electrical current carried by the background electrolyte (BGE) is delivered from the HV power supply of the CE instrument to the end of the capillary (or sprayer tip). At the same time, the gaseous ions in the electrospray carry a current driven by the electrospray potential. These currents may differ by three orders of magnitude (μA versus nA). Therefore, the power supply for the electrospray generation may become damaged by a high incoming current from the CE BGE. In this case a ground path for the current needs to be provided via a resistor sink. It should be noted though, that in this case the effective voltage in the CE separation may be reduced or increased by the electrospray voltage depending on the sign of this potential. So if one switches polarity or changes this potential it will affect the CE separation.

The overall picture is given in figure 3.39.

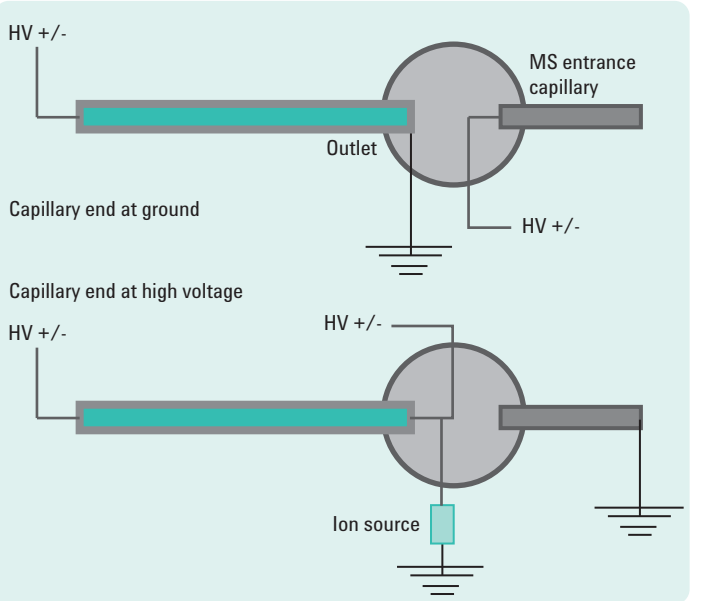

Figure 3.39
CE-MS electrical interfacing.

3.6.3. Hydraulic interfacing

As mentioned in 3.6.2 a robust electrical contact between the end of the CE capillary and the instrument's ground is required to provide a return path for the CE current. In a standard CE configuration this is achieved by the electrode in the vial at the end of the separation capillary. When one interfaces with a mass spectrometer, this vial is not used and the electrical contact between the background electrolyte and instrument ground needs to be established in another way.

Apart from closure of the electrical circuitry, a hydraulic flow rate is required to form the electrospray. The amount of hydraulic flow is related to the magnitude of the electroosmotic flow in the CE separation, the dimension of the separation channel and in case an LC electro-spray needle is used

the dimension of the spray capillary. In a practical situation, the volumetric flow rate generate through EOF is on the order of 1-100 nL/min. An LC electro-spray needle requires though some µL/min. On the other hand, as discussed in chapter 2, under some circumstances EOF may be absent. An ancillary flow is then mandatory to establish a spray.

Following general approaches that meet the hydraulic and contact requirements for interface CE and MS have been developed and in part commercialized:

A. sheath flow interface
B. sheathless interface

3.6.3.1. Sheath flow interface for CE-MS

Smith *et al.* have come up with a robust concept for CE-MS interfacing that meet above electrical and hydraulic requirements.[68] This approach has become known as the tri-axial capillary sprayer and has been commercialized by Agilent Technologies. A pictorial representation is given in figure 3.40.

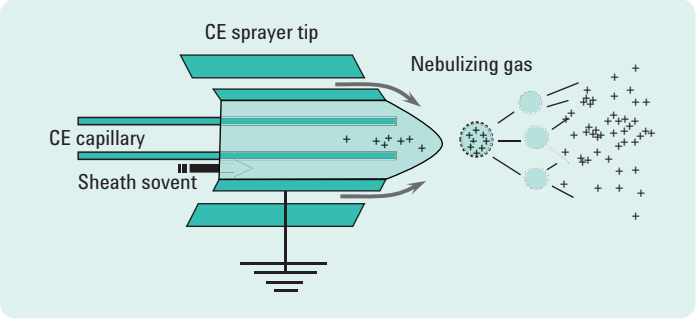

Figure 3.40
Tri-axial sheath flow CE-MS sprayer.

The CE separation capillary is the inner tube of the assembly and forms the spraytip. The sheath solvent is flowing outside the CE capillary and makes a liquid contact with the BGE of the CE separation. The capillary delivering the sheath solvent is grounded. The third tube delivers a nebulizing gas, for example nitrogen that assists in establishing the spray.

In this way it is secured that independent of the EOF, there always is enough hydraulic flow to establish an electrospray. In addition, a robust electrical contact exists. In addition sheath flow has been shown to be advantageous to drive the ionization towards the formation of cations or anions independent of the pH of the background electrolyte. Typical the composition of sheath liquids is aqueous mixtures of methanol, acetonitrile, isopropanol with an additive like acetic acid, formic acid or for anions ammonia. Flow rates are 1-10 µL/min.

On the downside, one may be concerned about dilution of the solutes when they are leaving the CE capillary. Especially, in case the EOF is low. This is particularly disadvantageous since an ESI interfaces behaves like a concentration sensitive detector, that is response decreases in case the (sheath) flow increases. Also, the sheath flow needs to be delivered requiring additional pumping capabilities.

In a practical situation therefore quite a number of parameters, sheath liquid flow rate and composition, nebulizing gas, ESI voltage, temperature etc. need to be set at optimal value. So finding the best settings of all these parameter needs to be done by a multiparameter optimization experiment.

In practice, ESI has proven to be particularly useful for the ionization of high molecular weight substances since the solute molecules become gaseous ions directly from the liquid. An additional advantage is that the solute molecules can carry multiple charges which decrease the mass to charge ratio allowing their analysis within the practically limited mass range of the mass analyzers. These advantages of ESI are also very effective when CE is the separation mode.

The sheath flow interface has proven itself as the most robust CE-MS interface that is commercially available. In the next section, ways to do a sheath less flow CE-MS will be described. To the authors knowledge though, none of these are commercially available and need to be home-built.

3.6.3.2. Sheathless interface for CE-MS

The perceived advantage of interfacing CE with MS without using a sheath solvent is the absence of dilution in the interface and therefore higher sensitivity. In practice though, this advantage is difficult to achieve.

In a recent review paper Chen has given a comprehensive overview of approaches to interface CE with MS without a sheath solvent flow.[69] In all cases, more or less ingenious approaches have been described, and are depicted in figure 3.41. So far, none of these approaches have been made commercially available. High practical skills are required to prepare such interfaces which still are not very robust.

One essential problem is not well solved in these interfaces. As mentioned before, there needs to be a return path for the CE current. At the interface between BGE and electrode there will be electrochemical processes that carry the current. On the anode, oxygen is generated and on the cathode hydrogen. Independent on whether the outlet of the CE capillary acts as an anode or cathode gas bubbles are formed which will have a large impact on resistance and so forth. In contrast to the triple tube coaxial interface where such gas bubbles are flushed out, in a sheath less flow interface this may represent a major problem.

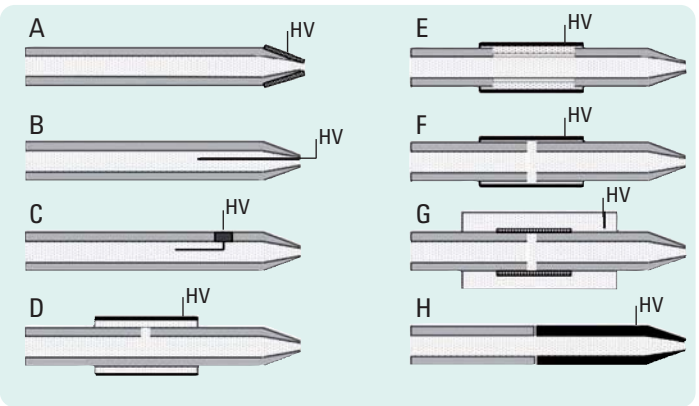

Figure 3.41
Methods for creating electrical contact in sheathless interfaces. A) Conductive coating applied to the emitter tip, B) wire inserted at tip, C) wire inserted through hole, D) split-flow interface with a metal sheath, E) porous, etched capillary walls in metal sleeve, F) junction with metal sleeve, G) microdialysis junction, and H) junction with conductive emitter tip.[69]

Very recently, Moini published an original new approach for interfacing CE with MS which avoids the problems related to electrochemical processes but which also does not need a sheath solvent flow.[70] The design of this interface is given in figure 3.42.

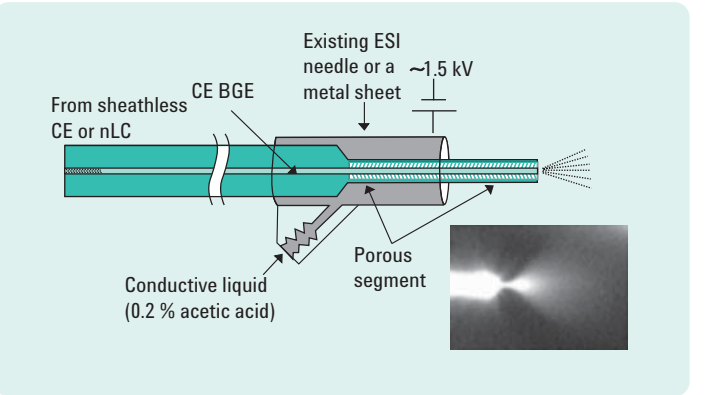

Figure 3.42
Sheathless flow CE-MS interface (from Moini).[70]

The polyimide coating is removed from the fused silica CE capillary and the glass etched down with hydrogen fluoride to an OD approximatly 80-90 µm. By this etching the end of the capillary becomes porous so that a liquid and electrical contact is established with a liquid outside of the capillary. This liquid is contained in a concentric electrode tube around the etched fused silica capillary. This tube is grounded or put at ESI voltage. The liquid between the electrode tube and CE capillary is stagnant. Electrode processes take place outside of the CE capillary and therefore do not disturb the CE field and current.

At the moment of writing this primer, this interface has become available for evaluation through Beckman-Coulter.

3.6.4. Other ionization methods

Electrospray ionization has proven to be a versatile ionization mode for highly polar or charged molecules. Less polar molecules are not as well charged in the electrospray process. Since CE deals largely with charged molecules it has become the preferred ionization mode. Nevertheless in many instances the ionization yield is low and consequently sensitivity is poor.
Moreover, electrospray ionization mandates the usage of volatile buffers which in many cases compromises CE separation performance. In addition, since electrospray ionization renders the mass spectrometer largely to a concentration sensitive detector, solute response will depend on the overall flow rate thus largely depending on the sheath solvent flow rate.

Besides ESI in for HPLC/MS, ionization techniques as atmospheric pressure chemical ionization (APCI) and atmospheric pressure photo ionization (APPI) have become popular. Both techniques are pictured in figure 3.43.

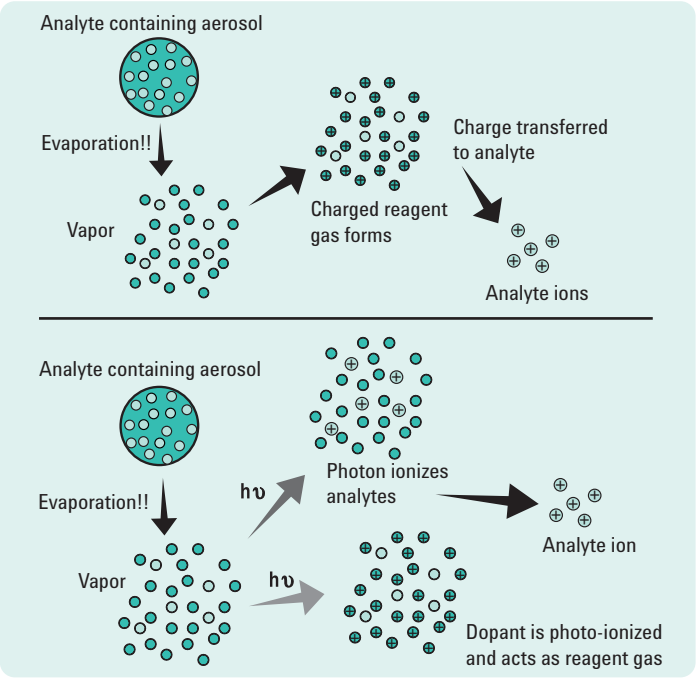

Figure 3.43
Pictorial representation of the APCI process (top) and the APPI process (bottom).

It is essential to realize that these ionization processes mandate the transfer of the solute molecules into the gas phase. So the interface contains a heated zone in which the solute molecules can evaporate from the eluate spray. Subsequently the solute molecules enter the zone in which by a corona discharge or high energy light an electron is transferred to the solute molecules allowing them to enter the MS. This is illustrated in figure 3.44.

In coupling with CE, the HPLC-double tube axial sprayer (nebulizer in figure 3.44) is replaced by the same triple tube axial sprayer used for ESI (a slight height adaption is necessary). The vaporizer is typically heated at 200-300 °C. Therefore in practice, both APPI and APCI interfacing for CE-MS is limited to low molecular weight substances (< 1000 Dalton) that have sufficient volatility. High molecular weightsubstances like peptides and proteins cannot be ionized by these techniques.

Matrix assisted laser desorption ionization (MALDI) is a quite popular interfacing method for liquid phase separations. In practice a solute is isolated in solution and deposited on a MALDI target. Effectively though this is not an on-line interfacing mode. For example in HPLC separation, the eluate from separation is "spotted"on the target. For CE the similar process applies. The fraction collection method, described in section 3.5, is an ideal preparation step for CE-MALDI-MS.

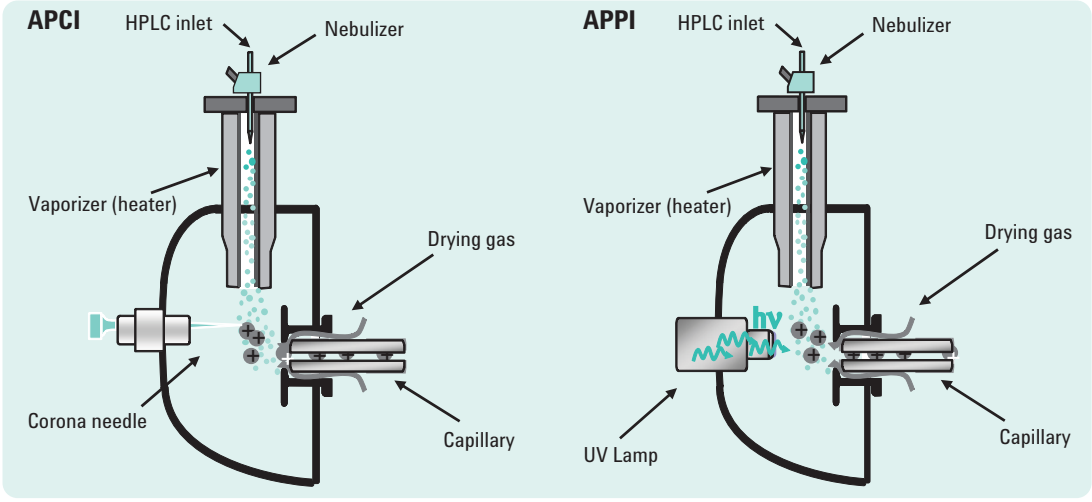

Figure 3.44
Illustration of typical APCI and APPI interfaces for HPLC.

Chapter 4

Practical Operation and Method Development

Practical operation and method development

4.1. Separation capillary

Ideal properties of the capillary material for electrophoresis include being chemically and electrically inert, transparent for light in the UV-visible wavelength range, flexible and robust, and inexpensive. Meeting most of these requirements, fused silica tubing is the primary capillary material employed today. Fused silica (FS) tubing has been used as flow cells for optical detection and for gas chromatography (GC) columns. Analogous to GC columns, FS capillaries are coated with a protective layer of polyimide to make them robust and easy to handle. For optical detection, a window is easily made by removal of a small section of the protective polyimide layer. This is accomplished by burning off a few millimeters of polyimide using an electrical arc or electrically heated wire, or with a drop of sulfuric acid. Ready toolkits are commercially available for this purpose. Care must be exercised when handling a capillary with a window, since the window zone is much less robust after the polyimide has been removed.

Fused silica capillaries with internal diameters (id) ranging from 10 to 200 µm with a range of outer diameters are commercially available. Typically capillaries with 25- to 100-µm id and 350- to 400-µm od are used. In order to shorten analysis time capillaries as short as possible should be used. Effective lengths range from 10 cm for gel-filled capillaries to 80 to 100 cm for complex-sample CZE separations. Most commonly, 25 to 75 cm effective lengths are employed. Ideally the effective length should be as large a percentage of the total length as possible in order to effectively use the separation capacity with applied electric field and to properly determine the run cycle time and time necessary for fraction collection. The total length typically is 5 to 15 cm longer, depending on the configuration of the instrument (that is, the distance from the detection point to the exit reservoir or outlet vial).

4.1.1. Bare fused silica

In practical CE, usage of uncoated (bare) fused silica capillary is the first choice. However, the bare fused silica inner surface is not chemically inert which has readily become clear in the early days of CE practice. For example when the separation of proteins by CE was initiated, solute surface interactions and lack of control of EOF were obvious. Ways to overcome these problems have already been discussed in depth in sections 1.3.2, 1.3.4.4 and 2.1. For the sake of clarity, this general problem is once more depicted

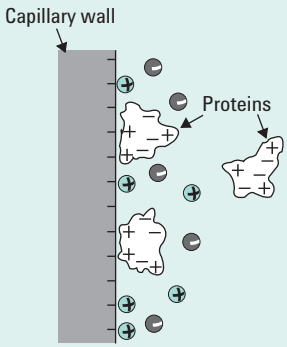

Figure 4.1
Possible interaction of proteins with capillary surface at pH = pI of protein.

in figure 4.1, which shows that "neutral" (or charge balanced) proteins are able to interact with the fused silica capillary wall.

Some simple and general remedies to diminish solute-surface interactions have been described as:
- Work at pH extremes (low or high pH)
- Use buffers with high ionic strengths.

In most cases these guidelines are not sufficient and also introduce other limitations such as, alteration of protein structure at non-biological pH values and the onset of appreciable Joule heating with high ion strength BGE. While narrow-bore capillaries can be used to reduce Joule heating, protein-surface interactions are usually exacerbated by the higher surface-to-volume ratios of small id capillaries compared with larger id capillaries.

Capillary wall modification is an alternative to limit solute-surface interactions and two fundamental approaches have been followed:
- Permanent modification of the wall by covalently bonded or physically adsorbed phases
- Dynamic deactivation using running buffer additives.

Both approaches will be discussed in sections 4.1.2. and 4.1.3., respectively.

Besides wall modifications, well defined solvent pre-treatment of new and used capillaries and their storage as a strict protocol is of great importance to attain reproducible separation methods (see section 4.2.).

Two other factors that are easily overseen when using uncoated or coated capillaries are:
- Capillary end effects
- Capillary batch-to-batch variability.

The capillary ends have to be flat and undamaged to prevent peak tailing and sample carryover. An example of peak tailing during injecting on a damaged capillary is given in figure 4.2. The reason for the strong asymmetrical peak formed in the left picture is the strong deformation of the electrical field lines in case the capillary end is not flat. As a consequence, local EOF and/or electrophoretic velocity will be variable at the capillary inlet.

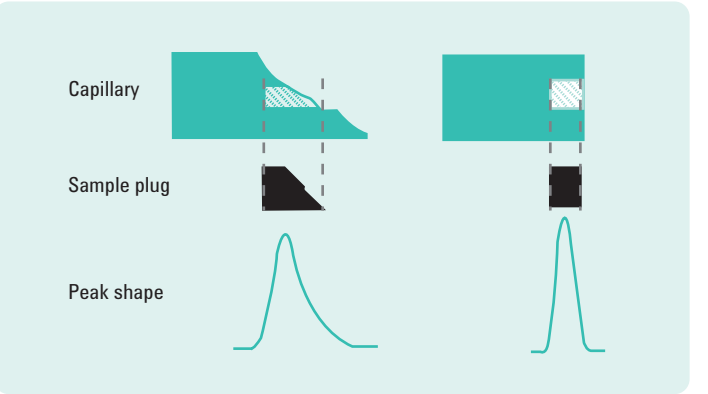

Figure 4.2
Effect of capillary injection-end deformation on peak shape.

It is discouraged using a ceramic blade to score the FS surface and break one side away. In most case a cut like in figure 4.2 is obtained or vice-versa an edge remains.

Organic solvents such as acetonitrile are sometimes used in CE for example in non-aqueous mode (NACE). These can swell the polyimide coating so that it separates from the capillary and blocks the inlet. Therefore it is recommended to remove 1-2 cm of the polyimide on the inlet (and outlet) side in case organic solvents, in particular if acetonitrile is used in the CE separation.

Fused silica tubing is drawn from larger silica preforms at a temperature around 2000 °C under inert atmosphere. Under these conditions, silanol groups present at the capillary surface condense completely to form siloxane bonds. In the drawing process, on the outside of the capillary polyimide is deposited which gives fused silica it extreme robustness and pressure stability while remaining flexible. The inner surface of a pristine capillary therefore is very hydrophobic. With time though, the inner surface becomes slowly rehydroxylated by humidity and eventually in CE by the BGE.

Batch-to-batch variability therefore is strongly dependent on the residual surface silanol concentration and to some extent also on amount of (metal) impurities in the silica. Therefore, as already indicated above,

rigorous pretreatment and preconditioning procedures should be applied in order to render the capillary in a well defined, reproducible state of surface hydroxylation. Washing procedures in between runs and brief reconditioning with the BGE should be part of a routine method.

4.1.2. Wall-coated capillaries

Like in capillary gas chromatography, deactivation of the capillary inner wall can be achieved by applying a permanent coating to the surface. For GC capillary columns this is achieved in practice by first full rehydroxylation of the surface, followed by applying a surface deactivation coating and a retentive coating. In GC these functions are always combined rending a GC column deactivated and with particular retentive selectivity.

In CE, these functions, rehydroxylation (see previous paragraph), deactivation and surface property change are well separated. So for example it may be adequate for the CE separation of anionic substances to run at high pH on a fully hydroxylated and therefore negative surface with polarity field (cathode at detector side). Under these conditions, anions will not interact with the surface, the EOF is large and in the direction of the detector while analyte anions move opposite the EOF in the direction of the anode but will be swept by the large EOF to the detector!

In CE surface modification is intended to:

a. Suppress interaction of the solutes with the surface, which adds a chromatographic retention term to the zone broadening process or peak tailing by slow adsorption/desorption.
b. Control magnitude and direction of the electroosmotic flow.

Such surface modifications are achieved by:

- Chemical bonding or physical adherence; permanent coating
- Dynamic coating; the surface modifier is part of the BGE or of the preconditioning electrolyte. Equilibrium driven.

More details are given in the next paragraphs.

4.1.2.1. Permanent coating capillaries

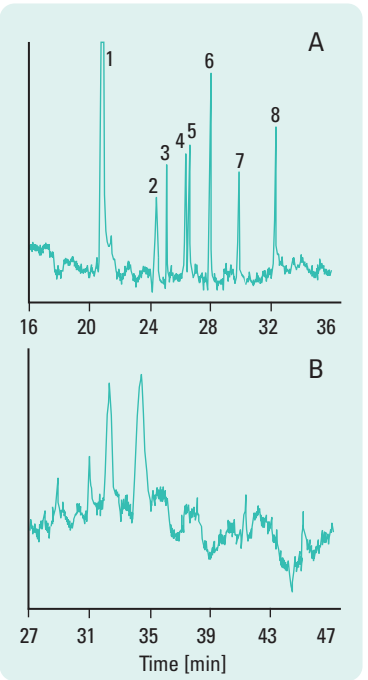

Figure 4.3
Aryl pentafluoro-coated capillary to improve protein separations. Coated capillary top, bare fused silica bottom.[72]
Peaks: 1, hen egg white lysozyme; 2, DMSO (EOF marker); 3, bovine ribonuclease A; 4, bovine pancreatic trypsinogen; 5, whale myoglobin; 6, horse myoglobin; 7, human carbonic anhydrase; 8, bovine carbonic anhydrase.
Conditions: Buffer: 200 mM phosphate pH 7.0 + 100 mM KCl; effective length: 100 cm; id: 20 µm; electric field: 250 V/cm; detection: 219 nm.

Several methods for permanent surface modifications have been described in the literature. Notably, reaction with a simple silane containing a functional group (for example vinyl or epoxy group) for further reaction is followed by a polymerization reaction with a suitable monomer or bonding with an appropriate molecule. A mixture of (meth)acrylamide and bis-acrylamide results in a very stable, low EOF, deactivated capillary very well suited for protein separations.

Direct binding of silanes to surface silanols has been successfully applied. Deactivation is accomplished with such varied species as, aryl pentafluoryl groups, or polysaccharides. The electropherograms in figure 4.3 show the type of improvement that can be expected for the separation of proteins using coated capillaries. Unfortunately, the siloxane bond (Si-O-Si) is stable only between pH ≈ 4 and 7 and hydrolysis usually limits long term stability.

Physical adherence is achieved by depositing a polymer (for example PEG) on the inner surface followed by reaction with a cross-linking reagent. Alternatively polyvinyl alcohol has been deposited on the inner wall followed by heating the polymer at 150 °C. Both approaches render the polymer insoluble in common BGE and suppress EOF effectively.

Depending on the deactivation, the EOF is eliminated, controlled or reversed. Neutral deactivation with polyacrylamide or polyethylene glycol, for example, eliminates EOF. This results from both decreased effective wall charge and increased viscosity at the wall. Deactivation with cationic groups reverses the EOF. Deactivation with amphoteric species, such as proteins or amino acids, yields reversible EOF depending on the pI of the coating and pH of the buffer.

These modifications are intended to be permanent and to require little or no maintenance. Since the capillaries are usually washed after use (adsorption may occur even with the coating), they must be stable to washing solutions and to hydrodynamic flow.

Permanently coated capillaries are available from CE instrument and consumables supplier. The added cost for making a permanent coating causes them to be significantly more expensive.

4.1.2.2. Dynamically coated capillaries

Addition of modifiers to the running buffer is nowadays the preferred alternative to deactivate/modify the capillary inner wall surface properties to bonded or adhered phases. Since the modifier is in the buffer, the coating is continuously regenerated and permanent stability is not required. Dynamic coatings have following advantages:[73]

- Easy to generate
- Use standard, cheap fused silica tubing
- In most cases inexpensive
- Applicable over a wide range of buffer concentrations.

The modifier though should not interfere with detection, it should be compatible with both optical and mass spectral detection.

Additives can interact with the wall and alter surface charge and hydrophobicity. Such modifiers are both easier to implement and optimize since they are prepared by simple dissolution of the modifier in the buffer.

Surfactants at concentrations below the critical micelle concentration (CMC) are among the most widely used buffer additives in CE. Numerous types of surfactants can be used in CZE (that is, anionic, cationic, zwitterionic, or non-ionic). Monomer ionic surfactant molecules can act as solubilizing agents for hydrophobic solutes, as ion-pairing reagents, and/or as inner wall surface modifiers. The interaction of the monomer surfactant with the solute can occur via two mechanisms:

1) ionic with the charged end of the surfactant and/or
2) hydrophobic between the alkyl chain and hydrophobic moieties of the solute.

In addition to interacting with the solute, many surfactants adsorb to the capillary wall thereby changing the charge state of the surface which modifies EOF and reduces solute adsorption simultaneously. Depending on surfactant charge, EOF can be increased, reduced, or reversed. EOF reversal, for example, can be obtained by addition of cationic surfactants such as cetyltrimethylammonium bromide (CTAB) to the buffer. As depicted in figure 4.4, CTAB monomers adhere to the wall through ionic interactions. The positive charge results from hydrophobic interaction of free CTAB molecules with those bound to the wall.

Surfactant concentrations above the CMC significantly alter the mechanism of separation. This leads to another mode of CE, micellar electrokinetic chromatography (MEKC), which was discussed in section 2.2. Several dynamic deactivation methods are listed in table 4.1.

Type	Result	Comment
Low or high BGE pH	Reduces coulombic interactions by eliminating wall and solute charge differences.	pH range from 2 to 12. EOF nearly eliminated at low pH. EOF very fast at high pH. May denature protein. Can decrease peak capacity by decreasing charge differences.
High BGE ionic strength/ concentration	Reduces coulombic interactions.	Decreases EOF. Often limited by Joule heating.
Neutral hydrophilic polymers (Alkyl celluloses, PEO, polyvinyl alcohol, dextrans, polyacrylamide)	Mask wall charge and reduce EOF.	Increases viscosity. Can separate by size if used at high concentrations (CGE).
Cationic polymers* (PEI, Polybrene, PDADMAC, PolyE-323, Poly-LA 313, Chitosan) Successive multiple ionic-polymer layer (SMIL)*coatings (PB-DS, PB-DS-PB, PB-PVS, PDADMAC-PSS, Ceofix)	Deactivate capillary surface through ionic interaction.	Semi-permanent coatings. Reverse EOF.
Single chain surfactants Anionic (SDS) Cationic (CTAB) Non-ionic (BRIJ & TWEEN series) Zwitterionic (CHAPS) Double chain surfactants* Cationic (DDAB, $2C_{14}$DAB, DLPC) Zwitterionic (DLPC2C_{12}, DMPC2C_{14})	Deactivate capillary surface through hydrophobic and/ or ionic interaction.	Wide variety of surfactants. Easy to use. MEKC above CMC. Can decrease or reverse EOF. May irreversibly denature protein. Can be used in conjunction with reversed phase: - LC surface. - Double chain surfactants: semi-permanent.
(Amines)/Quaternary amines (Spermine, TEA, DETA, diaminopropane)	Decrease or reverse of EOF.	Also act as ion-pairing reagents.

* These surfactants are semi-permanent. It is therefore not necessary to maintain these surfactants in the BGE during separations. PEI = poly(ethylene imine); PB = polybrene; PEO = poly(ethylene oxide); PDADMAC = poly(diallyldimethyl ammonium chloride; DS = dextran sulfate; PVS = poly(vinyl sulfonate); PSS = poly(styrene sulfonate); SDS = sodium dodecyl sulfate; CTAB = cetyltrimethylamonium bromide; CHAPS = 3-[(3-cholamidopropyl)-dimethylammonium]-1-propane sulfonate; DDAB = didodecyldimethylammonium bromide; DLPC = 1,2-dilauroyl-sn-phosphatidylcholine; DMPC = 1,2-dimyristoyl-sn-glycero-3-phosphocholine; Spermine = diamino-propyl-tetramethylene-diamine; TEA = triethanolamine; DETA = diethylenetriamine (see reference 74 for proper naming of all polymers and surfactants).

Table 4.1
Dynamic deactivation and coating methods.[74]

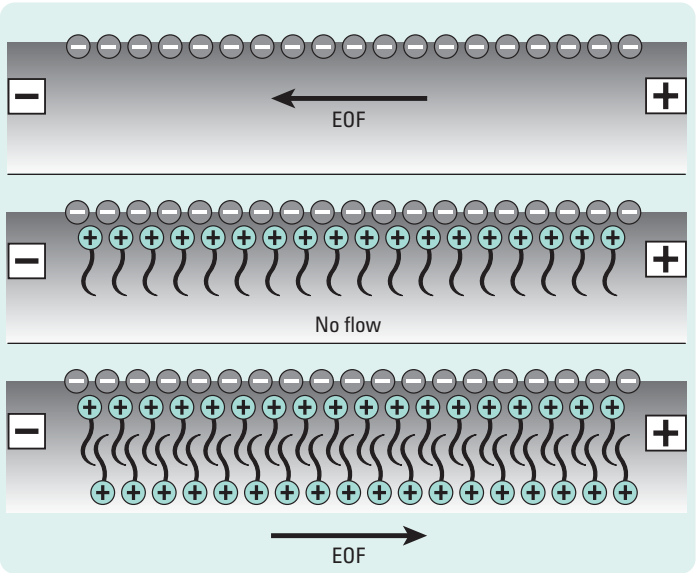

Figure 4.4
Elimination and reversal of electroosmotic flow using a cationic surfactant.

A potential disadvantage of the dynamic modification approach is that solutes as well as the capillary surface are affected. Biological-type conditions will be sacrificed by the use of pH extremes and addition of surfactants. Another limitation can be the equilibration time needed to obtain a reproducible surface and constant EOF. Furthermore, postcolumn analyses such as mass spectrometry and enzymatic assays are sensitive to additives, especially those in high concentrations.

There is, however, a strong trend from dynamic additive coatings such as spermine and CTAB to semi-permanent or static non-covalent coatings where the coating agent is not present in the BGE. This trend is reflected by the use of double chain surfactants, polymerizable phospholipid surfactants and by physically adsorbed polymer coatings (see table 4.1).

An example of using a single and double chain surfactant for the separation of basic proteins (pI > 7) is depicted in figure 4.5.

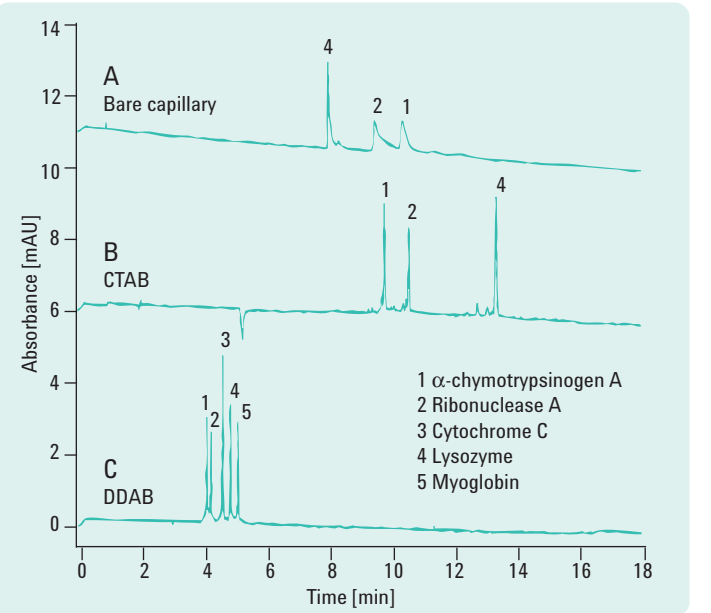

Figure 4.5
Separation of five basic proteins at pH 3.0, using (A) bare fused silica capillary; (B) CTAB-coated capillary; (C) DDAB-coated capillary.[75]
Conditions: 50 cm x 50 µm id capillary (40 cm to detector); UV detection at 214 nm; +15 kV applied voltage (A), -1 5 kV applied voltage (B, C); BGE, 25 mM phosphate at pH 3.0 containing (A) no surfactant; (B) 0.5 mM CTAB, or (C) 0.1 mM DDAB**.**
Note *that the myoglobin peak was not observed after a 40-min run time in (B).*

This figure clearly shows that addition of either CTAB or DDAB to the BGE reverses the direction of the EOF. Single chain surfactants such as CTAB generally must be maintained in the BGE to be effective and are therefore typically only used as dynamic coatings. Double chain surfactants such as DDAB can form semi-permanent coatings and thus need not be maintained in the BGE to be effective.

By using the CTAB-coated capillary three of the five model proteins were separated in less than 15 minutes with efficiencies of 500 000 plates/m. The other two proteins never eluted from the capillary. Furthermore, for the three detected proteins the recoveries were only ~ 80 %. In contrast

with the DDAB-coated capillary all five proteins are separated in less than 6 minutes with efficiencies of 500 000 plates/m, and recoveries from 85-100 %. This indicates that the two-chain surfactant DDAB has an increased surface coverage and is more effective in preventing protein adsorption than the single chain surfactant CTAB.

In figure 4.6, a schematic coating procedure for a polycationic coating with a successive multiple ionic-polymer layer coating (SMIL)[76] is illustrated.

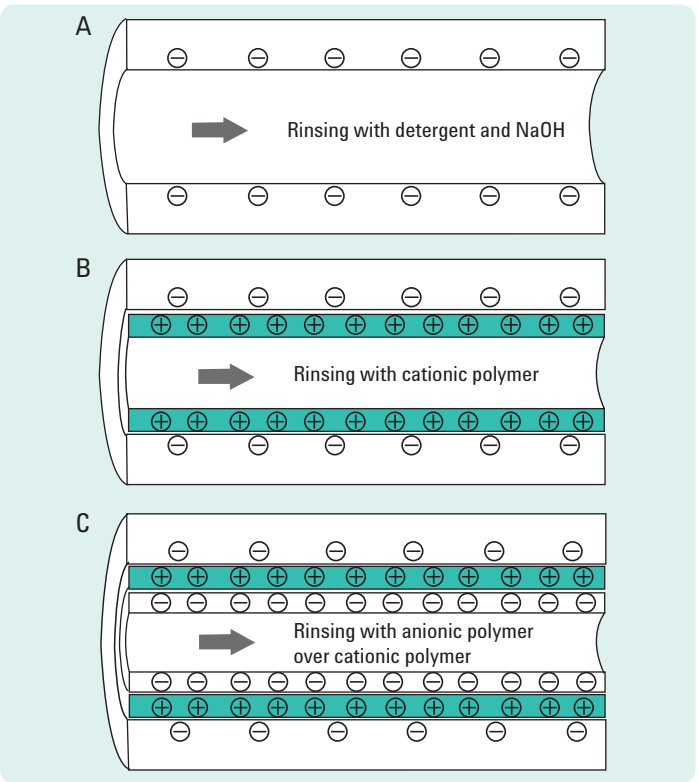

Figure 4.6
Coating procedure for polycationic polymer coatings (steps A-B) and successive multiple ionic-polymer layer (SMIL) coatings (steps A-C). A) Activation of the silanol groups; B) adsorption of polycationic polymer layer; C) adsorption of a polyanionic polymer as a second ionic-polymer layer.

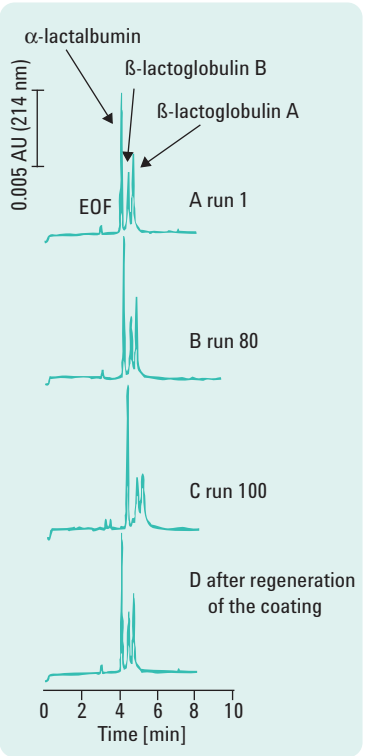

Figure 4.7
Separation of acidic proteins on a SMIL-DS coated capillary.[76]
Conditions: 27 cm x 75 µm id capillary (20 cm to detector); buffer: phosphate pH 7.0 (I = 0.05); +7 kV; temperature: 25 °C; sample: 0.1 mg/mL protein; injection: 140 mbar x s; regeneration solution: 0.1 M HCl.

The first example of a SMIL was a SMIL-DS [=PB-DS, a first layer of polybrene followed by a second layer of dextran sulfate]. The EOF generated by the SMIL-DS was strongly cathodic and was constant throughout the pH 2-11 range, in keeping with the strong acid character of the sulfonic groups in DS. SMIL-DS coated capillaries gave moderate efficiencies (300-500 x 10^3 plates/m) for three model acidic proteins. The capillary-to-capillary RSD for the EOF was 0.6 % (n=3), while the migration time reproducibility for the acidic model proteins was 0.5-0.8 % (n=3). The SMIL-DS capillaries were stable for 100 consecutive runs and the authors stated that the multiple layers of the SMIL coatings increase the coating stability relative to that of a single polymer layer coated capillary. The SMIL-DS coating was stable (based on constancy of EOF) to exposure of 1 M NaOH, methanol, acetonitrile and 5 M urea, and was degraded by 0.1 M HCl. Based on this result, the SMIL-DS coated capillaries were regenerated by flushing with 0.1 M HCl and then repeating the the SMIL-DS coating procedure. This returned the separation to its original efficiency as is depicted in figure 4.7.

A, PDADMAC-PSS[77] coating produced even better results. The reproducibilities of the EOF with a negative mobility marker were < 0.5 % for replicate runs and < 1.5 % for replicates over a 2-week period with other samples interspersed. High efficiencies (437-803 x 10^3 plates/m) were obtained for a separation of model proteins (as used in figure 4.5, but performed with 20 mM phosphate buffer) at pH 4.0. These efficiencies are up to 90 % better than on a PDADMAC only coated capillary.

Usage of dynamic coatings for CE has been recently reviewed by Lucy *et al.*[74]

4.2. Electrolyte replenishment & capillary conditioning

4.2.1. Buffer replenishment

Buffer replenishment is an integral part of maintaining high migration time reproducibility. Electrolysis of solution can alter running buffer pH and subsequently change EOF. In aqueous solution, electrolysis of water produces hydrogen (H_2) from hydronium ions (H_3O^+) at the cathode ($2H_3O^+ + 2e \rightarrow H_2 + 2H_2O$) and oxygen ($O_2$) from hydroxide ions ($OH^-$) at the anode ($4OH^- \rightarrow O_2 + 2H_2O + 4e$). These electrochemical processes result in buffer depletion. The extent of electrolysis is dependent on the current generated and total run time. The extent of the pH change is dependent on the *buffering capacity* of the buffer system, the volume of the reservoirs, and whether the *capillary conditioning washes* are flushed into the exit reservoir (not recommended!). For these reasons, frequent replacement of buffer is recommended. In order to get an impression about the frequency of buffer replenishment, it should be investigated at which run number the buffer electrolyte starts being depleted (that is when migration time shifts are observed). An example of the benefit of frequent buffer replenishment is shown in figure 4.8.

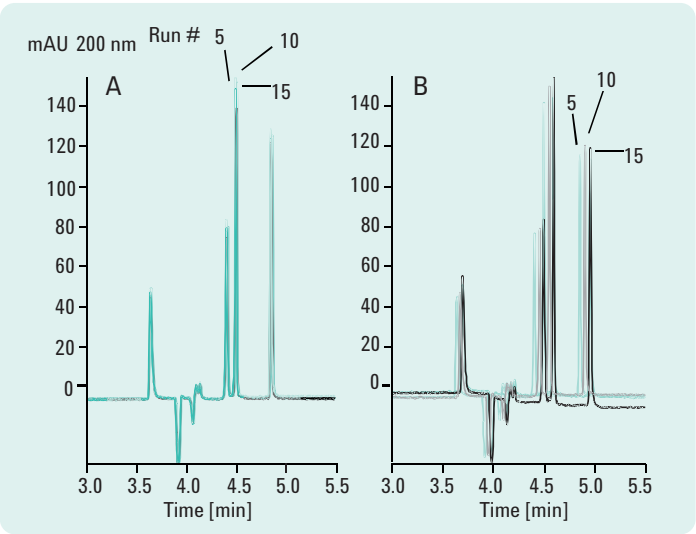

Figure 4.8
Improved migration time reproducibility using buffer replenishment. Overlay of runs 5, 10 and 15. A) replenish after every 5 runs. B) no replenishment.
Conditions: Buffer: 89 mM tris-borate pH 8.2; effective length: 56 cm; id, 50 µm; applied voltage: 25 kV; current: 13 µA; injection: 100 mbar x s; detection: 200 nm.

The RSDs for the migration times of the peaks, depicted in figure 4.8, are tabulated in table 4.2, which clearly shows that buffer replenishments with voltage conditioning attain highly reproducible migration times.

Compound	% RSD (migration time. n=10)		
	No replenishment	Replenishment	Replenishment +volts
1. Acetaminophen	1.62	0.70	0.15
2. Nicotinic acid	2.50	1.11	0.21
3. Salicyclic acid	3.00	1.21	0.25
4. Dihyroxybenzoic acid	3.53	1.47	0.25

Table 4.2
Comparison of migration time RSDs without and with replenishment or voltage conditioning (from figure 4.8).

The replenishment system operates by emptying the contents of the reservoirs into a waste bottle and then refilling them with fresh buffer. With an external, large buffer replenishment system only two vial locations in the autosampler are needed for buffer, leaving more locations for samples. In addition, a large reservoir affords the capability to run automated analysis for a long period of time.

A satellite station for filling and refilling of vials, with random access and automated buffer leveling is depicted in figure 4.9.

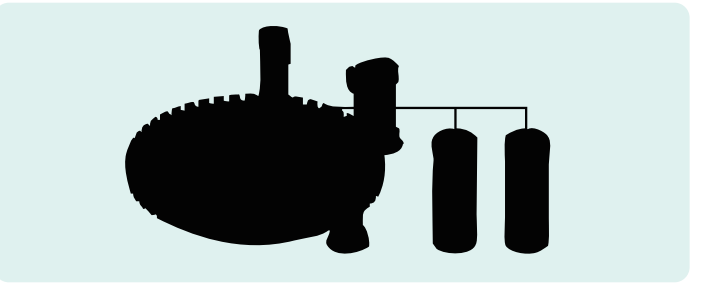

Figure 4.9
Satellite station for filling and refilling of electrolyte vials.

4.2.2. Capillary conditioning

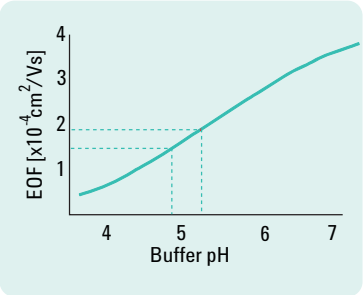

Figure 4.10
Influence of buffer pH on EOF.

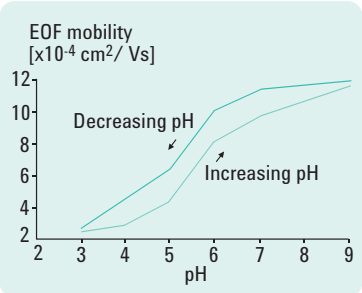

Figure 4.11
pH hysteresis of EOF in a bare fused silica capillary.

Capillary conditioning is a prerequisite for the development of robust CE methods. For bare fused silica, buffer pH is critical for controlling EOF, especially in the range pH 4-7 where small pH changes can cause large changes in EOF, as shown in figure 4.10 where pH 5 ± 0.18 produces a change in EOF mobility (mEOF) of about 25 %. As discussed above, buffer electrolysis can easily produce such a change if the buffer capacity is insufficient. A good buffer capacity is thus mandatory and as a rule buffers should be used at a pH = analyte pK_a ± 1.

Another phenomenon that affects EOF is when one wants to condition a bare fused silica capillary from a high pH application to one at a lower pH and vice versa. It appears that the capillary wall shows a hysteresis (path dependent memory effect) when going through a pH cycle (low pH-to-high pH-to-low pH) as depicted in figure 4.11. This behavior can only be "circumvented" if sufficient conditioning washes are performed to obtain a wall surface that is in equilibrium with the pH of the BGE to be used for a particular application. It is therefore good practice to track the history of a capillary. However, it is generally recommended to dedicate the capillary to one particular method or BGE.

General approaches for capillary conditioning have been described in the literature[78-80] and are given below.

Conditioning of a new capillary (coated or uncoated)
Flush with MeOH (5-10 min), 1 M NaOH, water (5-10 min each), run buffer (20 min), or flush with 1 M NaOH (5 min), wait 5 min, water (5 min), run buffer (20-30 min). For a new coated capillary a flush with NaOH is, in general, not recommended, check therefore instructions of the manufacturer. Flushing with water is not recommended for non-aqueous CE (NACE) applications.

Daily conditioning prior to analysis
Flush with 0.1 M NaOH or 10 % (v/v) phosphoric acid (10 min each) depending on the pH of the BGE (see pH hysteresis) followed by water (10 min) and conditioning with BGE (10 min). Application of voltage (20 kV, 2 min during BGE flush) will usually shorten conditioning time. When the capillary is used on a day-to-day basis, cleaning (acid or base, water) and storing in BGE overnight (capillary ends should be immersed in BGE) so that a short conditioning with BGE suffices for restarting analysis.

Conditioning between analyses

First try flushing with buffer only. This does not disturb your surface equilibrium (which occurs when flushing with other liquids) as some BGE components, such as phosphate, are known to adsorb to the surface thereby affecting the equilibrium time that is needed. When using a neutral or basic buffer, flush with 0.1 M NaOH (2 min) and then buffer between runs (2 min). ***Note:*** *A high pH wash is not compatible with all coatings!*

When using an acidic buffer, flush with 10 % (v/v) phosphoric acid (H_3PO_4, 2 min) and then buffer between runs (2 min).
Note: *A low pH wash is not compatible with all coatings!*

For complex sample matrices (for example biological samples) conditioning with SDS in the BGE could be preferred to basic or acid cleaning. A small amount of SDS in the running buffer can also improve precision.[81]
Note: *Be aware that for coated capillaries, some SDS can stick to the surface causing a permanent change.*

Capillary long term storage

A bare fused silica capillary should be cleaned properly with NaOH followed by an extensive water flush and then blown dry (with air from an empty vial).

4.2.3. Common buffer systems

Table 4.3 gives an overview of commonly used CE buffers, their optimal pH range and transparency for UV-vis absorbance detection.

Buffer	Useful pH range	UV-vis transparent above (nm)
Phosphate	1.1 – 3.1	195
Formate	2.7 – 4.8	200
Acetate	3.8 – 5.8	200
Citrate	3.8 – 4.8	200
2-(N-)morpholino-ethanesulfonic acid[1]	5.1 – 7.1	230
Citrate	5.4 – 7.4	200
Piperazine-N,N-bis(2-ethanesulfonic acid)[2]	5.8 – 7.8	215
Phosphate	6.2 – 8.2	195
4-(2-hydroxyethyl)-1-piperazineethanesulfonic acid[3]	6.5 – 8.5	230
N-trihydroxymethylglycine (TRICINE)	7.1 – 9.1	230
Trihydroxymethylaminomethane (Tris)	7.3 – 9.3	220
Borate	8.1 – 10.1	180
N-cyclohexyl-3-aminopropanesulfonic acid[4]	9.7 – 11.1	220

Table 4.3
Common buffers for CE.
Abbreviations: [1]MES, [2]PIPES, [3]HEPES, [4]CAPS.
In green: zwitterionic buffers.

4.3. Troubleshooting

Table 4.4 summarizes symptoms commonly encountered in CE experiments, indicates their possible causes and points at conceivable solutions and/or comments.

Table 4.4
Troubleshooting CE symptoms.

Sympton	Possible cause(s)	Solution(s)/comment(s)
Unstable current		
No current	Empty capillary/wrong solutions in buffer vials.	Fill/change buffer vials.
	Broken capillary.	Apply gas pressure and check for bubbles at outlet. No bubbles: replace capillary.
	Clogged capillary.	Flush capillary with absorbing solution, a base line jump should be observed.
		If still plugged, flush with high pressure or "off-line" with syringe.
		If unsuccessful: replace capillary.
	Safety interlock not closed.	Close interlock.
	Large injection volume with different sample matrix (stacking).	Normal condition – current should stabilize during analysis.
	Different cathode/anode buffers.	Check buffer identity.
	Temperature/Voltage change.	Check oven temperature and voltage with a buffer of known conductivity.
Current fluctuations or loss	Air bubbles in capillary.	Flush capillary.
		Ramp voltage to limit initial heating.
		Degas buffer.
	Broken or cracked capillary.	If the current breaks down repeatedly after flushing with buffer, the capillary is probably cracked (see also no current).
	System short-cut (buffer on vial cap).	Clean and dry cap or replace.
Unstable baseline		
Spikes on baseline	Precipitates/contaminants in buffer.	Filter buffer through 0.2-0.45 mm filter.
	Microscopic bubbles in buffer.	Degas buffer.
	Precipitation of sample.	Verify that sample components are soluble in buffer.

Table 4.4
Troubleshooting CE symptoms.

Sympton	Possible cause(s)	Solution(s)/comment(s)
Unstable baseline		
Noisy baseline	Optical slit on capillary interface occluded.	Clean with methanol or water, check with magnifying glass.
	Ageing deuterium lamp.	Use DAD test feature to measure lamp output and time on – replace.
	High data acquisition rate.	Determine peak widths and decrease rate if appropriate.
	Buffer absorbs at detection wavelength.	Use minimally absorbing buffer or clean buffer through C18 column.
Flat baseline (often too stable!)	Improper capillary alignment.	Reseat capillary cassette in detector block.
	No voltage.	Check voltage setting and current.
	No sample injected.	Ensure capillary ends immersed in buffer.
		Check sample level in vial and vial leakage.
		Check capillary extends in sample.
	Incorrect detection wavelength.	Check injection time.
		Check wavelength setting and accuracy.
	Detector lamp not on or out of order	Ignite lamp or replace.
	Data system of the hook.	Check functioning of data system.
Drifting baseline	Improper capillary alignment.	Reseat capillary cassette in detector block.
	Temperature not stable.	Allow 10-20 min to equilibrate after opening top cover.
	Detector lamp not yet warmed up.	Allow 15-30 min to equilibrate after ignition.
Irregular peak shapes		
Broad and/or flattened peaks	Sample overload.	Decrease sample injection or concentration.
	Excessive Joule heating.	Reduce voltage, buffer concentration or capillary id.
Skewed peaks	Mismatch of sample and buffer ion mobilities.	Match mobilities or maximize difference between sample and buffer conductivity.
	Sample overload.	Decrease sample injection or concentration.

Table 4.4
Troubleshooting CE symptoms.

Sympton	Possible cause(s)	Solution(s)/comment(s)
Irregular peak shapes		
Tailing peaks	Adsorption to capillary wall.	Use pH extremes, higher buffer concentration, buffer additives (diamino propane, triethanol amine, 0.05 % CTAB), polymer additives (0.05 % cellulose) or coated capillary.
	Capillary end(s) damaged or resting on vial surface.	Check if capillary ends are properly cut.
		Check capillary distance from vial surface.
Low signal		
	Insufficient injection.	Check microvial for content or bubbles.
		Check proper seal of vial cap.
	Sample concentration too low.	Increase sample concentration and check with pressure flush.
	Detection wavelength not optimized.	Acquire UV spectra and use maximum plus appropriate band width.
	Insufficient sample stacking.	Maximize difference between sample and buffer conductivity.
	Capillary id too small.	Use extended light path capillary.
Shifting migration times		
	Changes of capillary surface (due to pH changes or adsorption).	Conditioning of capillary to achieve surface equilibrium and/or to avoid batch-to-batch capillary differences. Do not cycle pH (surface charge hysteresis!).
	Changes in buffer composition (due to electrolysis, buffer evaporation, conditioning waste flushed into outlet vial).	Increase buffer concentration (capacity) or replenish regularly to limit buffer depletion, to avoid evaporation check seal on vial cap, check destination of conditioning waste.
	Siphoning due to unleveled buffer vials.	Use replenishment for automated leveling [important for short, wide id capillaries (75-100 mm)].
	Sample overload.	Decrease sample injection or concentration.
		Particularly evident with indirect UV- detection of small ions.
	Temperature changes.	Thermostat capillary.

Table 4.4
Troubleshooting CE symptoms.

Sympton	Possible cause(s)	Solution(s)/comment(s)
Non-reproducible peak areas		
	Sample shortage in sample vial or injection time too short compared to system rise time.	Check sample availability in vial. Increase injection time.
	Sample expulsion.	Inject buffer plug after sample or use voltage ramping.
	Sample carry-over.	Check if capillary ends are properly cut. Remove polyimide coating from capillary ends. Perform intervial change for buffer dipping of both capillary ends.
	Sample depletion after electrokinetic injection.	One injection per sample.
	Sample evaporation (in particular for small sample volumes < 20 mL).	Tightly cap sample vial. Thermostat sample tray (cool).
	Sample adsorption to capillary surface (peak tailing, non-eluting components).	Use pH extremes, higher buffer concentrations, buffer additives (diamino propane, triethanol amine, 0.05 % CTAB), polymer additives (0.05 % cellulose) or coated capillary.
	Zero-injection thru capillary dip in sample.	Cannot be eliminated! Increase injection amount.
	Migration time shifts.	Use corrected peak areas (A/t).
	Improper peak integration due to low signal-to-noise ratios.	Monitor integration parameters closely.
	Temperature changes.	Thermostat capillary.
Peak problems		
No peaks	Separation time too short.	Increase analysis time. Increase capillary length.
	Other causes: see no current and flat base line.	
Too many peaks/spikes	Residue from previous analysis.	Flush capillary.
	Sample degradation.	Renew sample; check temperature sample vial.
	Bubbles.	Warm buffer to running temperature. Reduce voltage.
	Solid contaminants in sample/buffer.	Filter sample/buffer (0.20-0.45 mm filter).

Table 4.4
Troubleshooting CE symptoms.

Sympton	Possible cause(s)	Solution(s)/comment(s)
Peak problems		
Too few peaks	Improper wavelength.	Check wavelength setting and accuracy.
	Separation time too short.	Increase analysis time. Increase capillary length.
	Sample depletion after electro-kinetic injection.	One injection per sample; renew sample.
	Analyte wall interaction.	Flush with buffer and/or recondition. Check run conditions.
	Hampered EOF due to wall adsorption or buffer depletion.	Flush with buffer and/or recondition. Use buffer replenishment.

4.4. Method development

Before attempting to develop a CE method, it is very useful to gather information about the particular compounds one wants to analyze and capture in a robust application method.

1. The fastest and most secure way is to research detailed applications and technical notes from CE instrument manufacturers that have been transformed into compound and method related application kits. The availability of such kits ensures that the applied method is robust, reliable and easy to transfer to other labs. When this search is unsuccessful, the next step is:

2. Search the scientific literature for compound specific application methods. Alternatively many free internet services are available to screen the scientific literature for specified application. **http://scholar.google.com** is a particular versatile internet browser program to look for relevant information. When these are found, the job has not yet been finished as one has to investigate whether these applications are reliable and robust (that is will the method hold up to serious variations in the most important experimental parameters). If the literature search does not bring any information one has to:

3. Use available expertise within the user's organization. Development of robust and transferable CE methods is of great importance in the pharmaceutical industry as such methods have a considerable impact on product development time limits. Therefore, reliable information on how to develop a method comes from experienced CE scientists working in pharmaceutical companies.[80, 82] If this does not work, one has to:

4. Start developing a method from scratch.

When a method is developed, the purpose of the method should be clear. For example is it to be transferred to a quality control (QC) lab or is used in product development (biopharmaceuticals), resolving acute issues like contamination, pollution, process problems?

When the purpose of the method is clear, one has to define method performance requirements for the target compounds such as: resolution, reproducibility of migration times, quantitation etc. In general, a CE method should be very robust for example by using simple BGE with sufficient buffering capacity. It has been shown that robust methods were successfully transferred to relatively inexperienced QC labs.[80] To enhance the performance of a CE method one has to carefully consider important experimental parameters such as instrument settings, injection procedures, composition and preparation of the BGE, including sample and standards.

In chapter 2, six essential modes of CE have been introduced. The choice of a CE mode highly depends on the type of compounds one wants to analyze. In table 4.5 suggestions for application of these modes are given.

Mode	Analytes	Application
Capillary zone electrophoresis (CZE)	Small, ionizable organic compounds. Inorganic ions.	Quantitation; e.g. impurity determination, drug stability testing, QC, process control, corrosion.
Micellar electro-kinetic chromatography (MEKC)	Small, ionizable and neutral organic compounds.	Quantitation; e.g. impurity determination, drug stability testing, QC.
Capillary electro-chromatography (CEC)	Small, ionizable and neutral organic compounds.	Not very widespread. Preconcentration by solid phase extraction.
Capillary gel electrophoresis (CGE)	Proteins, peptides, oligo-nucleotides, DNA, RNA.	Biopharmaceuticals; size determination, purity check (PCR products), composition analysis (charge heterogeneity, posttranslational modifications, carbohydrate analysis). QC and process (fermentation) control.

Mode	Analytes	Application
Capillary isoelectric Focussing (CIEF)	Proteins, peptides.	Biopharmaceutical pI determination, identity.
Capillary isotacho-phoresis (CITF)	Small ions.	Preconcentration technique.

Table 4.5
CE modes, analytes and applications.

4.4.1. How to start?

Is the analyte soluble in water and generic BGEs at concentrations up to 1 mg/mL and at all pHs? If aqueous solubility is problematic, will small amounts (up to 25 % v/v) of methanol or acetonitrile solubilize it? Will small, neutral molecules solubilize using 100 mM SDS? For a protein sample, will 7 M urea or a dispersant such as ethylene glycol help?
Is the analyte thermally labile and/or unstable at certain pHs? Is the solute ionizable (pK_a)? Does it have a chromophore? In what matrix, if any, is it contained and how many components are expected at what concentration?

These considerations can be put into fact finding diagrams that help to determine the route of method development. One such diagram, that answers some of the above questions, is depicted in figure 4.12.

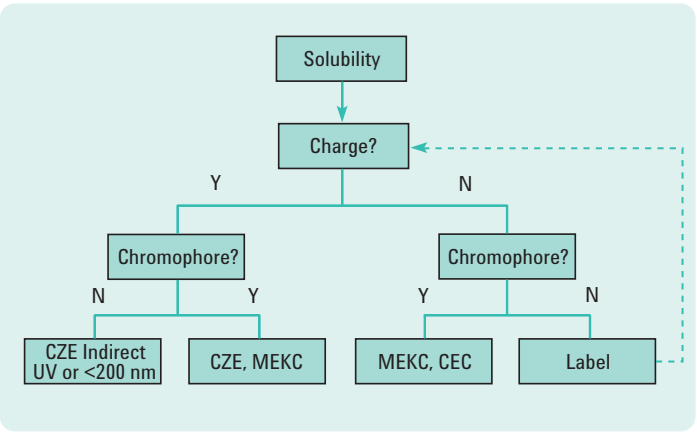

Figure 4.12
Fact finding diagram to fine-tune the choice of a CE method.

It is clear that molecular properties are important attributes of a sample compound that can affect analysis. Poor solubility produces erroneous quantification/calibration and may cause sample precipitation leading to capillary clogging and unstable current. Poor compound stability will produce too many unwanted peaks that are hard to identify. When these properties cannot be gathered from any data base, some real life experiments (visual check of solubility in various solvents, checking sample decay by flushing through DAD and check spectral change of signal during different time intervals at 200 nm, etc.) may be called for.

The sample matrix is another problem to tackle. Low analyte concentrations in a high salt concentration matrix will always cause zone broadening through electro-dispersion (section 1.3.4.5.) and poor detection, which will even worsen if electrokinetic injection has to be applied (due to high sample conductivity a very low amount of analyte will be introduced). One therefore has to remove excess of salt. Techniques to eliminate salts in samples are:

- Float dialysis* to remove ions which interfere in electrokinetic injection (in float dialysis salts diffuse through the pores of a membrane into a dish of water while the analyte [e.g. DNA] remains behind).
- Desalting with a C 18 cartridge* (e.g. for tryptic digests of proteins to allow neat peptide mapping).
- Dilution (10 to 50-fold) of sample with deionized water so that sample stacking techniques can be applied (section 3.2.3.).
- Water plug prior to injection to deplete injection zone of ions.
- Buffer plug before (with high conductivity: forms leading electrolyte for ITP concentration of analyte) or after (with low conductivity: forms terminating electrolyte for ITP concentration of analyte) sample injection.
- Sandwich sample between leading and terminating electrolytes (for ITP concentration of analyte).

(* These techniques really remove salt content from the matrix).

A flow chart indicating possible procedures to handle salty sample matrices is shown in figure 4.13.

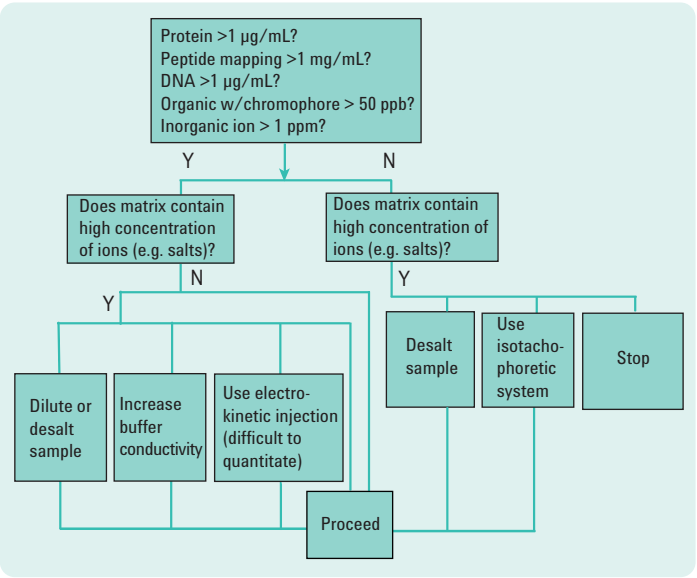

Figure 4.13
Flow chart indicating solutions for salty sample matrices.

4.4.2. Capillary zone electrophoresis (CZE)

This CE method has been applied to a large size range of ionizable molecules (see table 4.5). The development of a robust CZE method (and in fact all other CE modes!) largely depends on a simple and robust BGE that anticipates the principal requirements of a method. A good start is to work with a series of simple (or generic) buffers which cover a pH range of 2-9. In order to reduce the effect of buffer depletion, it is good practice to choose a buffer pH close to its pK_a. Extensive capillary conditioning (section 4.2) and establishment of a stable EOF (section 1.3.2.) will ensure that the first initiating steps to a good result can be taken as shown in the flow chart depicted in figure 4.14.

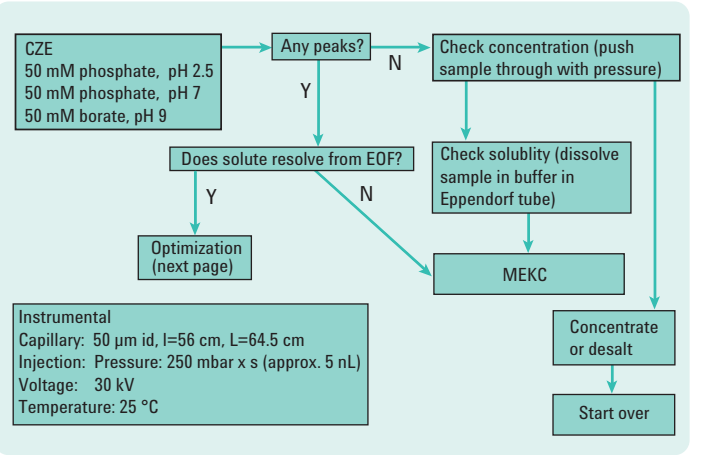

Figure 4.14
Flow chart for initial steps to proper development of a CZE method.

In CZE the separation of analytes is primarily based on mobility differences, caused by all factors that affect the charge to mass ratios (sections 1.3.3 and 1.3.5). In order to change the effective mobility (μ_{eff}) of a compound, its degree of ionization (α_i ; section 1.3.1) and thus its net charge (q) has to be altered. The latter can be manipulated by:

- Buffer pH
- Buffer ionic strenght (I)
- Complex formation
- Surfactants (ion pairing) and,
- Specific dye labels (FITC, APTS; section 3.4.2)

The mass of a component cannot be manipulated, but its hydrodynamic (or ionic) volume is definitely affected by:

- Solvation with buffer ions (I) and/or different buffer co-ions
- Denaturation (e.g. proteins by temperature and a surfactant, like SDS) and,
- Other factors mentioned under charge manipulation

In the case of fully ionized species [for example anions (F^-, Cl^-, Br^-) and cations (Li^+, Na^+, K^+)] the net charges of these ions are equal, but as they have increasing crystal radii their charge densities are in the order:

F > Cl > Br; Li > Na > K. When these ions are in solution their solvated (ionic) volumes follow the same order, which causes a reversed order of elution in CZE.

The separation of small weak acids and bases by CZE is, however, hardly feasible when these components are brought into their fully ionized state ($\alpha_i = 1$). In this case their charges are equal but their ionic volumes may be still too close. Fortunately, these compounds usually have different pK_a`s (see figure 1.3), and a well chosen buffer pH [for example with $pH = \Sigma(pK_a`s)/2$] may then help out. This effect of buffer pH in conjunction with a charge calculation for this type of components is made possible through the well-known Henderson-Hasselbach equation:

4.1
$$pK_a = pH - \log\left(\frac{\alpha_i}{1-\alpha_i}\right)$$

in which α_i is derived from equation (4.1) as:

4.2
$$\alpha_i = \frac{10^{(pH-pK_a)}}{1+10^{(pH-pK_a)}}$$

For a monoprotic acid or base, the charge (q) can then be calculated:

q = $-\alpha$ (for weak acids)
= $(1-\alpha)$ (for weak bases)

For polypeptides and proteins, the net charge and isoelectric point (pI) can also be calculated if the constituting amino acids (AA) are considered to be independent from each other.[83,84]

In CZE, the elution order of the compounds of interest can therefore be predicted if buffer pH and compound net charge are known. Experimental verification of this prediction together with a check on peak shape, resolution and reasonable migration times can be best performed by following a flow chart as shown in figure 4.15.

A further optimization of parameters, indicated in the chart, will usually lead to the desired method which can then be tested for robustness.

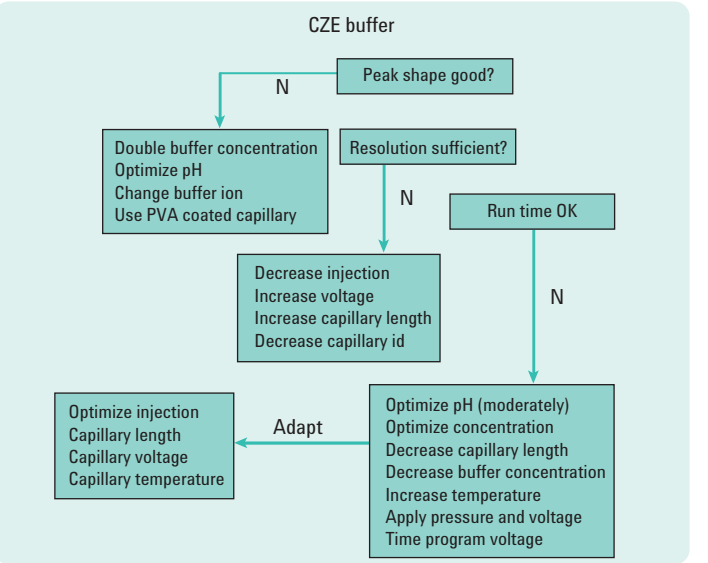

Figure 4.15
Flow chart that may lead to a final CZE method.

Two of the method performance requirements: the run time of a compound and its quantification, have not been discussed in detail. It is not enough to consider if a run time fits an allocated analysis time frame. Compound migration time (t_m) should, in principle, be reproducible as shifting migration times lead to quantification errors. To tackle shifting migration, proper capillary conditioning (section 4.2) is mandatory. A closer look at possible solutions to migration time shifts can be found in the troubleshooting section (table 4.4). When small changes in EOF cannot be solved, it might be advisable to use relative migration times or relative mobilities instead of absolute ones.

Proper quantification of the target compounds is of major importance in any CE method. To separate analytes by CZE they should have different electrophoretic mobilities (section 1.3.3). However, this will cause that they also spend different times in the allocated detector, which will report different peak areas even when injected amounts (mols) and molar detector responses are the same. A simple normalization of

reported areas (that is A/t_m) will eradicate this inconvenience. Other phenomena that should be considered when quantification is at hand are:

- Non-reproducible peak areas
- Low detector signal
- Unstable (e.g., noisy) baseline
- Irregular peak shape.

These phenomena with probable cause(s) and possible solution(s) are indicated in sections 4.3 (troubleshooting) and 3.4 (detection).

Note on quantification: *The use of an internal standard (IS) is highly recommended as it compensates for variations in the injected amount even when the injection is faulty.*

4.4.2.1. Simulations with PeakMaster

A very elegant tool, directing the way to an insightful and reliable CZE method, has been developed by Gas and co-workers[85] in the form of a simulator called: PeakMaster. This program is able to predict the behavior of BGEs and analytes in CZE.

PeakMaster (PM) can calculate:

- Important parameters of the BGE, such as pH, ionic strength (I) and buffer capacity.
- Important parameters of analytes, such as the signal response of direct UV or fluorescence detection, the transfer ratio (TR = sensitivity; see section 3.4.1.4) of indirect photometric detection and the molar conductivity response (= sensitivity) of contactless conductivity detection (CCD).
- The tendency of an analyte to cause peak deformation (= electrodispersion; section 1.3.4.5).
- Position of system ghost peaks (= eigenpeaks).
- Amplitudes of system eigenpeaks.

PM simulates:
The electropherogram of sample constituents in a given electrolyte.
A comparison between a simulated and an experimentally obtained electropherogram is depicted in figures 4.16 (simulation) and (experiment).

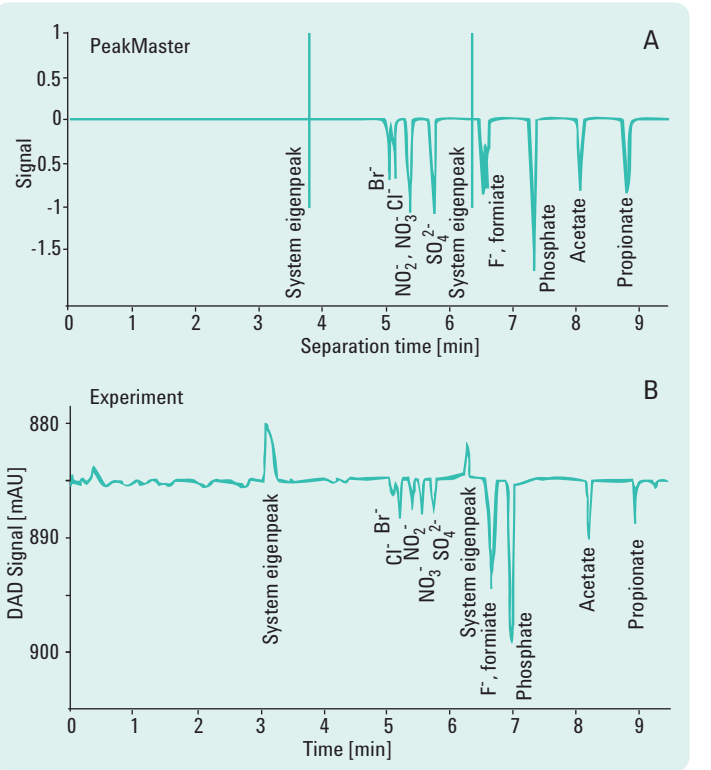

Figure 4.16
Simulation of response, peak shape and eigenpeaks of anion mixture in a buffer at pH 12.1. B) Experimental electropherogram of anion mixture in a buffer at pH 12.1.

In these experiments, an anionic mixture in a commercially available buffer [20 mM PDC (pyridine 2,6 dicarboxylic acid) with addition of 0.5 mM tetradecyltrimethylammonium hydroxide (TTAOH) for the reversal of the electroosmotic flow and about 55 mM NaOH to reach pH = 12.1] is used and the anions detected with indirect UV.

Both figures show that positions and shapes of the analytes together with the eigenpeaks are in good agreement between simulation and experiment. There are, however, some more things PM has to offer:

PM predicts:
- The existence of system eigenpeaks or resonance phenomena causing anomalous dispersion of analyte peaks.

PM allows:
- Optimization of the BGE composition resulting in enhanced detector sensitivity while maintaining acceptable zone broadening phenomena.
- PM is a user-friendly program (including explaining tutorials) that can be freely downloaded from reference 85.

4.4.3. Micellar electrokinetic chromatography (MEKC)

This mode of operation was discussed in section 2.2 and is called for when the bulk of analytes in a sample carry no or fractional charge. A pseudo stationary phase, formed by surfactants above their critical micellar concentration (CMC), ensures that partitioning of solutes between micelles and bulk solvent (BGE) takes place. Therefore, like in RP-HPLC, different selectivities (e.g., $\alpha_{1,2} = k_2'/k_1'$ etc., see equation 2.2), based on differences in hydrophobicity of the analytes and their interaction with the micelles, are responsible for the separation of the analytes. In most MEKC applications the optimization of a separation and, more or less, the development of a MEKC method is quite similar to RP-HPLC. However, the comments on *compound solubility, stability* and its initial environment (*sample matrix*) together with mandatory *conditioning steps*, as mentioned in CZE method development, should also be considered in MEKC method development. These factors all determine the choice of a proper BGE (buffer) and the availability of a sufficient elution time window from a moderate EOF and micelles exhibiting high mobilities (see also section 3.2.3 on sample stacking in MEKC). Once the *proper buffer* has been chosen (for example from initial CZE experiments), the essential method performance requirements (*resolution, reproducible migration and proper quantification*) have to be established like before.

Not surprising (if one is familiar with HPLC), resolution in MEKC is dependent on:
- Surfactant concentration or type (e.g., k' increases with SDS concentration).
- Temperature (in general: k' decreases with temperature).

- Content of organic modifier (methanol, propanol, acetonitrile, usually < 40 % v/v), will decrease retention when its amount is increased and at the same time will open up the available time window.
- pH (usually pH > 6 to generate sufficient EOF; lower pH may decrease EOF: increasing migration time and/or alter the analyte's charge).

Fine-tuning of these parameters has been laid out in the flow chart, indicated in figure 4.17, which usually leads to a proper optimized MEKC method.

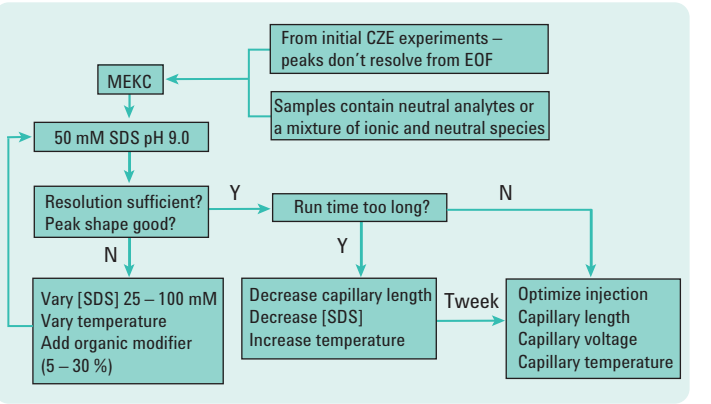

Figure 4.17
Flow chart optimizing resolution and migration times in MEKC.

Note: *Changes in resolution due to the above indicated parameter variations (that is [SDS], T, % organic and pH) can cause a dramatic change in the elution order of analytes. In order to keep track of component identity, use of spectral recognition with a self created or pre-installed spectral data base is highly recommended.*

4.4.3.1. Separation of enantiomers

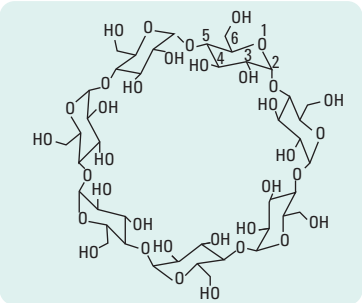

Figure 4.18
Topview of chiral selector (ß-cyclodextrin).

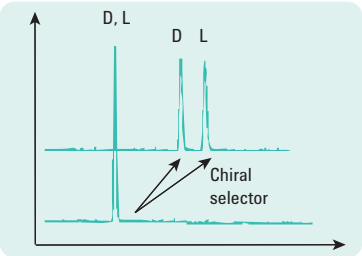

Figure 4.19
Chiral selector causing separation.

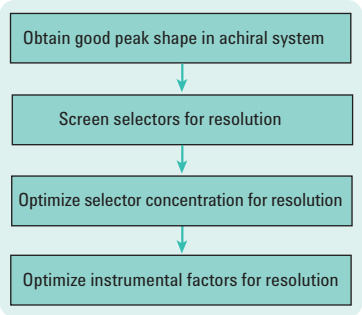

Figure 4.20
Flow chart indicating initial and forthcoming steps leading to chiral method development.

This is a hybrid method of MEKC and CZE as not only chiral micelles but also non-micellar chiral selectors such as, cyclodextrins and cholates can be added to the BGE. Analysis of enantiomeric compounds by CE has been applied extensively in the pharmaceutical industry as this technique, due to its versatility and cost effectiveness, is preferred over HPLC. Method development and robustness testing of chiral separations by CE has therefore been well documented by pharmaceutical analysts.[80, 82]

Enantiomers are molecules containing one or more asymmetric carbon centers. They are molecular mirror images identical from a physicochemical point of view, which makes it extremely difficult to separate them by common LC or CE techniques. Upon interaction with other enantiomeric pure compounds (chiral selectors) which are bonded to a stationary phase (LC) or added to a BGE diastereomers are formed which can be separated. An example of a chiral selector and its effect on the separation of a pair of enantiomers is shown in figures 4.18 and 4.19.

Cyclodextrins (CDs) are the most commonly used chiral selectors. They are made up of glucose units and have a conical molecular shape (like a bukket without a bottom). The glucose units can be modified with different functional groups (charged or uncharged). CDs with 6, 7 or 8 glucose units are called: α-, β- or γ-CDs. The separation (chiral recognition) of an enantiomeric pair of molecules is based on the fact that one of these molecules has a better access (resulting in: hydrophobic inclusion and/or hydrogen bonding) into the CD molecular bucket than the other (steric repulsion). In CE, charged CDs are used to separate neutral enantiomers, while uncharged CDs can be used to separate charged enantiomers.

The development of a chiral analysis method usually starts with a good CZE buffer in which the chiral selectors (CDs) are not yet added and a well developed single peak of the substance racemate is obtained. A sequence of development steps for a successful chiral separation method is, hereafter, depicted in several flow charts. The first one is shown in figure 4.20.

The next chart (figure 4.21) is indicating decisions one can make when charged or neutral enantiomers are the sample components.

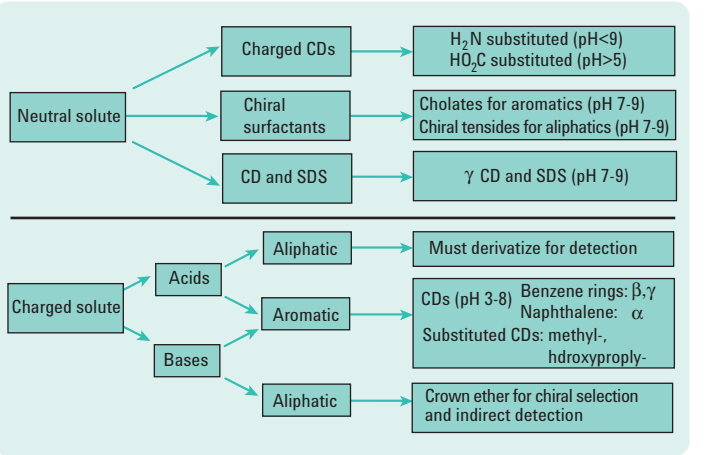

Figure 4.21
Flow chart for making decisions on how to handle neutral and charged enantiomers. (Note: the types of different CDs, chiral surfactants etc. are clarified in proper chemical catalogues.)

For neutral enantiomers a charged CD provides differential interaction and due to its charge a discrimination by the electric field. Chiral surfactants are also charged and a MEKC separation is the result. In a CD plus SDS case: CD provides enantiomeric discrimination while the SDS micelles are responsible for transport.

Charged (or chargeable) enantiomers are a bit more difficult to handle as they need a more careful buffer selection to induce charge. This approach is laid out in the following chart (figure 4.22).

When the peakshape of the enantiomer pair (no chiral selector added) looks good, a screening of chiral selectors has to be initiated and when finished with some result, further optimization takes place as shown in the chart (figure 4.23)

This continued optimization is thus on CD concentration and additional buffer and instrument parameters. An important instrumental parameter to optimize chiral separations is temperature (also indicated in figure 4.23). It controls chemical equilibria such as pK_a (section 4.4.2), enantiomer –

chiral selector complexation and may induce structural changes in molecules (for example proteins). For chiral separations, a lower temperature usually results in a better enantio-separation[86], but even the opposite has been observed.[87]

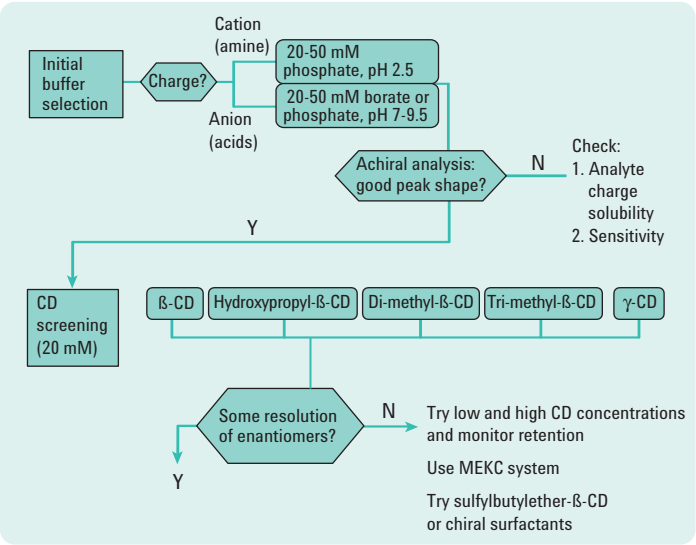

Figure 4.22
Flow chart indicating decisions on treatment of charged enantiomers. (Modifications on CDs are: HP = hydroxypropyl; DM = dimethyl; TM = trimethyl).

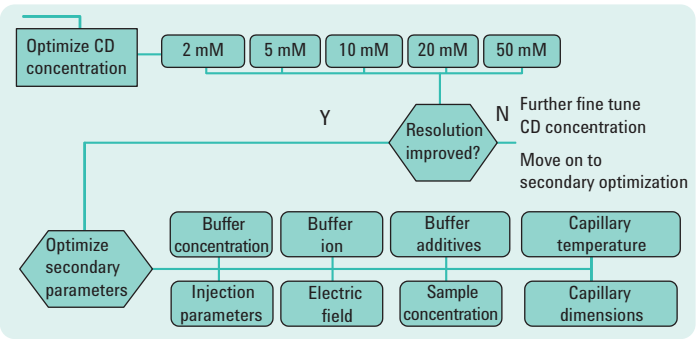

Figure 4.23
Flow chart, with charged enantiomers, further optimizing chemical and instrument parameters.

4.4.4. Capillary electrochromatography (CEC)

Similar to HPLC, a wide range of mobile phases can be employed in CEC to obtain separation of the sample compounds. If neutral solutes are to be separated, the same optimization strategies (variation of type and concentration of organic modifier) as in HPLC can be used. The major difference between CEC and HPLC lies in the fact that in CEC the stationary phase not only influences retention and selectivity but also the EOF and thus the linear velocity of the solvent. As has been shown in section 2.3, the velocity of the electroosmotic flow depends on the surface charge density of the surface on which the EOF is generated. In the case of silica based packing particles, the degree of dissociation of the surface silanol groups and therefore the charge density depends strongly on pH of the eluent. EOF-velocity changes with pH on different RP stationary phases together with other influential chemical parameters such as, % organic modifier and buffer ionic strength (I) have been published.[88,89] During CEC method development the effects of changing these parameters on selectivity (α), efficiency (N) and therefore resolution (R) can be estimated. In summary:

The eluting solvent can be best prepared with 80 % acetonitrile mixed with 20 % buffer. Acetonitrile appears to generate a 2x higher EOF than methanol while thiourea is used as the non-retained solute to measure t_0 for calculating EOF mobility (μ_{EOF}).

Preferred buffers, properly adjusted before mixing with acetonitrile, that cover a suitable pH and neither affect selectivity nor efficiency are: Tris (pH 8), MES (pH 6), sodium acetate (pH 4) and phosphate (pH 2). Decreasing buffer ionic strength will increase EOF. It is advisable to work at low buffer concentrations (for example 20-50 mM) and at temperatures above ambient. Most RP-HPLC phases behave similar in HPLC and CEC. In transferring methods from HPLC to CEC, gradient LC methods can often be replaced by isocratic CEC methods when acetonitrile is used as modifier.

Not surprising, the *sample matrix* also plays an important role and one has to ensure that it is suited for CEC. An excellent example of this was given by Taylor *et al.*[90] in which steroids in urine destroyed a column after a few injections. However, after a cleanup of the urine with C8 followed by SAX extraction (SAX = strong anion exchange) column longevity was enhanced to over 200 runs.

Finally, Euerby *et al.* concluded that in the separation of neutral species established theories, used in HPLC method development, are directly applicable to CEC.[91]

4.4.5. CE-MS

As was explained in paragraph 3.6, mass spectrometric detection adds a powerful dimension to CE separations. MS allows unambiguous identification of the solutes through exact determination of molecular weight (at ppm level), through substance specific fragmentations (multiple reaction monitoring), through dedicated gas phase molecular reactions (electron transfer dissociation) or library search.

However in coupling, important practical aspects have to be dealt with and their settings optimized. This will be discussed here for the triaxial tube CE-MS interface specifically.

4.4.5.1. Hydraulic interfacing and electrical connections

As described in paragraph 3.6 the outlet of the CE separation capillary needs to be connected to ground via liquid contact as well be sprayed in front of the MS inlet. The CE separation capillary is fed through the triple tube until it protrudes about 1 mm from the inner SST tube. Precise and in particular reproducible adjustment of the CE capillary end is achieved with the adjustment ring on the sprayer. The importance of this adjustment for good electrical contact is illustrated in figure 4.24.

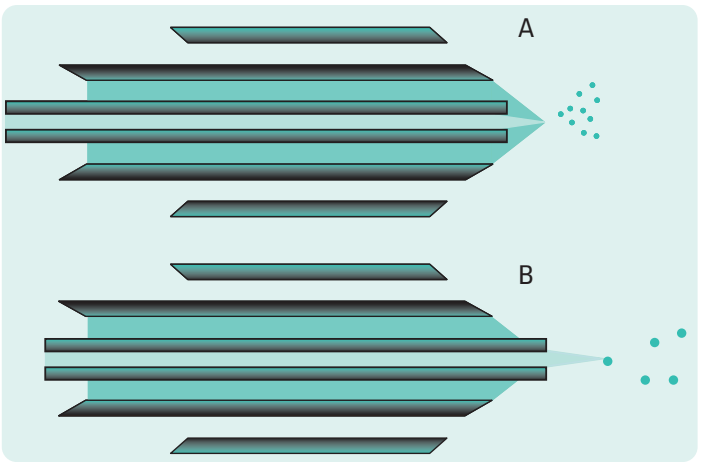

Figure 4.24
A) Optimal positioned CE capillary with good electrical contact; B) CE capillary protrudes too far resulting in unstable CE and ESI current.

Mandated by the bulkiness of the CE instrument and the MS interface, a minimal capillary length ca 50-60 cm will be required to connect from the CE inlet vial to the MS interface. By using UV-vis detection in the CE instrument, which is advised for diagnostic and optimization work, another 20 cm will be added.

Since the end of the capillary is open, the height position of the inlet capillary should be level with outlet capillary. Else siphoning will occur in either direction which may empty the inlet vial or draws the solvent in the separation capillary. Figure 4.25 illustrates this important point.

As explained in paragraph 3.6, both the CE and ESI voltage are at ground with Agilent Technologies and Bruker MS. The ground contact is provided by a simple cable which connects the sprayer with metal contact on the CE respectively the MS.

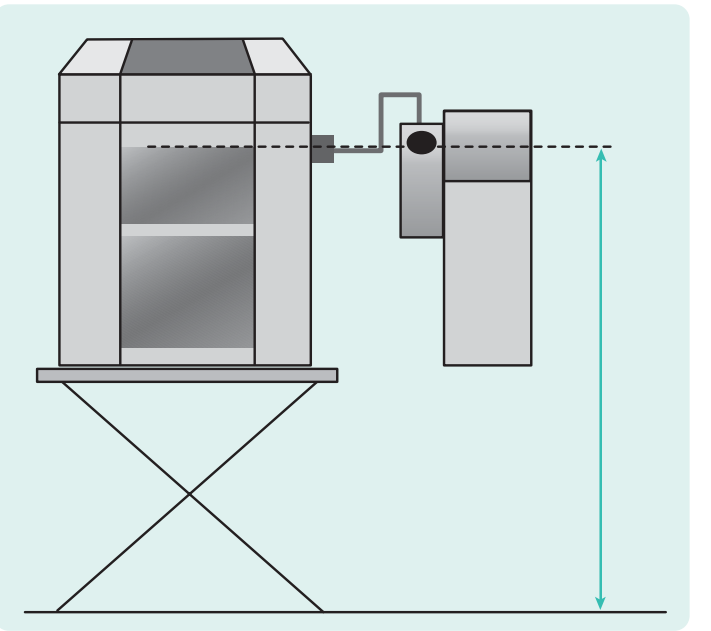

Figure 4.25
Secure height inlet vial liquid equals height outlet (sprayer tip).

4.4.5.2. Setting nebulizing gas pressure

In this kind of sprayers, a nebulizing gas is required to assist in spray formation. Typically dry nitrogen gas suffices. Gas flow rate will be determined by setting the gas pressure at typical values around 10-20 psi.

The practitioner needs to be aware that the nebulizing gas imposes an additional hydraulic flow component to the movement of the solutes in the capillary. The pressure of the nebulizing gas can create a suction effect that pulls the BGE through the capillary. Since this flow is pressure driven zone broadening increases. In addition, when this suction effect occurs during injection a gas bubble may be drawn into the capillary causing current breakdown. The first effect can be counteracted by balancing with a negative pressure on the inlet vial. The second effect is easily off set by switching of the nebulizing gas during the time the sample is injected.

4.4.5.3. Delivering sheath solvent, composition of sheath solvent

Since the sheath solvent is intended to provide an electrical contact between the BGE and the capillary delivering the sheath solvent, it needs to be conductive itself. This is achieved by simply adding a volatile organic acid or base (ammonia) to the sheath solvent in low concentration. Since the sheath solvent may have a pH different from the BGE and delivered in excess over the BGE, its pH will determine the ionization state of the solutes. For example while the CE separation may be at pH 7 with a low sheath solvent pH basic solutes will be cationic. Vice-versa, ammonia adjusts the pH at high value for negative ion mode MS.

The sheath solvent consists mostly of hydro-organics such as acetonitrile, methanol or isopropanol. Water makes up about 1- 20 % of the mixture. The sheath flow solvent composition is optimized experimentally in most cases.

Sheath solvent is delivered at flow rate 5-25 µL/min. So a motorized infusion pump may do the job. However, such devices typically do not show a constant delivery while emptying the syringe barrel. Consequently the MS baseline signal becomes noisy and may be jumping (figure 4.26).

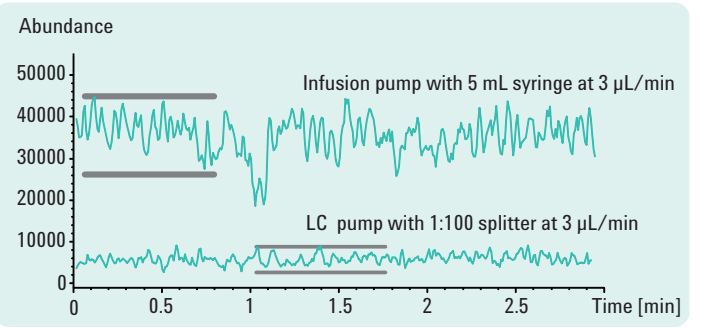

Figure 4.26
Baseline signal in CE-MS with sheath flow delivery. Lower trace, isocratic HPLC pump at 300 µL/min with 100:1 split. Upper trace motorized infusion pump with 5 mL reservoir set at 3 µL/min. The stick-slip effect occurs when the plunger briefly sticks to the barrel wall.

4.4.5.4. Buffer choice for CE-MS

Buffers used in a CE separation coupled to a mass spectrometer should be volatile and not interfere with the ion formation process. Figure 4.27 compares the separation of a standard mixture of 10 peptides using a BGE of either 10 mM acetic acid or 20 mM phosphate buffer.

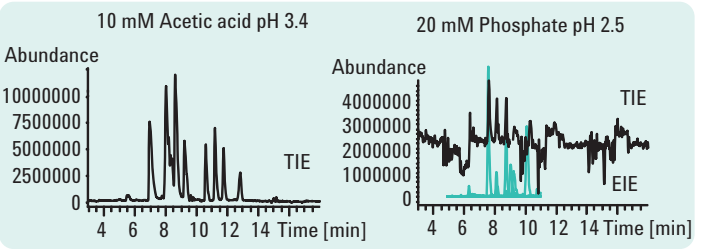

Figure 4.27
Black trace: total ion electropherogram. Green trace, extracted ion electropherogram. Conditions: Capillary: 75 cm (22 cm) x 50 µm; injection: 150 mbar x s; voltage: 27 kV; temperature: 25 °C; detection: 206/10 nm, ref 450/80 nm; sheath solvent: 0.5 % HAc in 50 % MeOH 4 µL/min; nebulizer gas: 10 psi; drying gas: 10 L/min, 150 °C; ES volt: - 4 kV; MS detection: m/z 350-650; sample: 0.16 mg/mL 10 peptide mix.

It is easily seen that with acetic acid in BGE, the abundance is a factor 3-5 higher. However, with phosphate the total ion electropherogram is very noisy and the peptide signals faint. Nevertheless the peptides can be observed well

in the extracted ion electropherogram (lower trace on the right). It also shows that peaks are narrower with the phosphate buffer in the BGE. This is an unevitable compromise one has to face in CE-MS. Usage of volatile buffer in relatively high concentration compromising zone width versus using non-volatile buffers in very low concentration (low buffering capacity) with narrow peaks.

Typically buffers like acetic acid, formic acid and their acetates are used in practice.

4.4.6. Capillary gel electrophoresis (CGE)

This type of zonal electrophoresis was discussed before (see section 2.4) and is particularly used for size-based separations of biological macromolecules such as nucleic acids and proteins.

For *nucleic acids*, practically all existing methods are already developed and can be considered as a spin-off from the road to completion of the human genome project (HUGO). It is therefore not surprising that many CE-instrument manufacturers offer instrument-independent, pre-made chemistries and kits for specific applications. These applications may include:

- Synthetic oligonucleotides* (primers, standard DNA ladders etc.)
- Antisense therapeutics* (phosphothioates)
- DNA restriction fragment mapping
- Genetic desease identification (for example point mutations on genes)
- PCR product analysis*
- Forensics [variable number of tandem repeats (VNTRs), short tanden repeats (STRs)]
- DNA-protein interactions

The *marked applications are usually subjected to extensive QA/QC-protocols establishing size, purity and concentration of the products.

The separation kits generally contain: coated/uncoated capillary, separation matrix [replaceable polymers such as dextrans, celluloses or linear polyacrylamide dissolved in buffer (mostly, Tris-borate/EDTA/urea pH ~ 8)] and if necessary calibration markers, DNA ladders etc.

Common separation conditions: capillary, $L_{tot} \approx 50$ cm, $L_{eff} \approx 40$ cm; id = 75-100 µm; electrokinetic injection (-), 5-10 kV for 5-20 s; separation voltage (-), 10-25 kV; temperature: 25-30 ºC; detection: 260/8 nm.

Some general remarks with respect to the sieving matrix are in place:
- Can be viscosity adjusted to enable to sieve different fragment sizes
- Should be refilled after each run to improve:
  1) sample stability,
  2) migration time reproducibility;
  3) to prevent capillary fouling and sample carry-over and
  4) to increase coating longevity on a single capillary so that 150-200 runs are not unusual
- When bare fused silica is used the run number is not dependent on coating stability.

Note: *In real-life samples and PCR products the nucleic acid sample matrices can be quite salty. Techniques to overcome salty samples were discussed in the introduction of section 4.4.*

For protein size analysis, sodium dodecyl sulphate-poly acrylamide gel electrophoresis (SDS-PAGE) in the slab gel format has been the preferred method. To enable protein size analysis, proteins are treated with the anionic surfactant SDS forming complexes with a constant charge to mass ratio (1.4 g SDS/g protein). The gel forms a molecular sieve on which electrophoretic separation can be performed. With the arrival of recombinant techniques to produce therapeutic proteins and monoclonal antibodies (mABs), SDS-PAGE in capillary format is often preferred over the slab gel format. This is mainly due to the fact that CGE, in contrast to SDS-PAGE, is able to:
- Provide higher resolution of major and minor species
- Better quantitate results and therefore,
- Determine process related impurities of proteins and antibodies
- Automate and
- Document the separation result.

For CGE analysis kits are available with SDS sample buffers and gels (commonly proprietary), which are also used for sample preparation (see below). The method development of this technique entails the following steps to determine:
- Sample preparation conditions to ensure fully denatured and/or reduced proteins
- Linear detection range to optimize ability to quantitate major and minor protein species using internal standards (IS) and corrected peak areas (A/t_m)

- Optimization of separation parameters
- Best detection wavelength (in most cases at 280 nm to avoid high background absorbance) for obtaining maximum sensitivity and,
- Proper data processing method.

Sample preparation[92] follows the route: to 150 mg of protein or antibody, add 3 µL IS (10 kDa MW marker), 10 µL BME (for rCE-SDS or the same amount of 250 mM IAM for nrCE-SDS) and fill up to 150 µL with SDS sample buffer. Mix, briefly centrifuge, properly heat at 75 °C for 10 minutes, cool to room temperature, briefly centrifuge and mix again. The sample is now ready to inject.
(r = reduced; nr = non-reduced; BME =ß-mercapto ethanol; IAM = iodoacetamide).

Recommended separation conditions are: capillary (bare fused silica), $L_{tot} \approx 35$ cm, $L_{eff} \approx 25$ cm; id = 50-75 µm; electrokinetic injection (-), 10-15 kV for ~ 20 seconds; separation voltage (-), 10-15 kV; temperature: 20-30 °C; detection: 215/20 nm (or LIF depending on dye label).
In general, CLOD values (see section 3.4) for UV detection are: ~ 0.1 % (w/w) and for LIF: ~ 0.01-0.05 % (w/w).

Note: *It needs to be emphasized, that both DNA, RNA and protein size separation are a standard methodology in microfluidic capillary electrophoresis (MCE). The essential difference between these platforms is that in CGE, the user will be able to freely select and optimize buffers, polymers, voltage, capillary length etc. while in MCE these parameters where already optimized during the development of application-specific assays and kits and are therefore preset and fixed.*

4.4.7. Capillary isoelectric focussing (CIEF)

Classical IEF is an electrophoretic technique that is used to separate peptides and proteins on the basis of their isoelectric point ($pI = \Sigma(pK_a)/2$) on immobilized pH gradient (IPG) strips where the buffering groups (ampholytes) are directly attached to a polyacrylamide-matrix. This is usually the first step (1D) in 2D-electrophoresis as the proteins, resolved on the strip, are then treated with SDS and further separated in the second dimension by SDS-PAGE. 2D-electrophoresis is still a core technology for the separation of complex protein mixtures in the majority of proteome projects.

With the introduction of CIEF (see section 2.5) the same advantages, as outlined in CE-SDS (that is automation, high resolution, reproducibility and quantitation of proteins and antibodies with related impurities), are gained. Monitoring of the charge distribution of a protein and its possible isoforms (having different pI values) provides a fingerprint of the isoforms and a means to determine their identity. Therefore, CIEF is now commonly applied in mAB development and manufacturing (QA/QC) and in clinical chemistry for the determination of:

- Proteins in serum, urine and cerebro spinal fluid (CSF); (precursors of diseases)
- Hemoglobin variants (precursors of hemoglobinopathies)
- Isoenzyme patterns (e.g., lactate dehydrogenases: LDHs)
- Carbohydrate deficient transferrin (metabolic disorders)
- Lipoproteins (low and high density lipoproteins: LDL, HDL; cardio vascular risk)
- Protein modifications (deamidation and isomerization)
- Oligosaccharide structure analysis

Several accessories such as, ampholytes in polymer (MC, HPMC) solutions for different pH-ranges and/or polymer concentrations, and pI-markers are commercially available. (MC = methyl cellulose; HPMC = hydroxy-propyl-methyl cellulose).

Sample preparation[92] is, in general, as follows: an aliquot (~ 35 µg) of protein or antibody is thoroughly mixed with the chosen ampholytes in polymer solution (~ 0.2-0.4 % polymer) and added pI markers, to a final concentration of ~ 0.3 mg/mL (best concentration for sensitivity and resolution). The solution is then degassed and ready for injection.

Recommended separation conditions: capillary (coated with a neutral polymer), $L_{tot} \approx$ 35-80 cm, $L_{eff} \approx$ 25-70 cm; id = 50 µm; hydrodynamic flush of capillary with ampholyte in polymer solution; hydrodynamic injection of sample solution to a complete fill of the capillary; Focusing: (anode electrolyte, 100 mM phosphoric acid in 0.2-0.4 % polymer; cathode electrolyte, 20 mM NaOH in 0.2-0.4 % polymer) at 30 kV for 15 minutes mobilization: 50 mbar plus 30 kV with detection at 280 nm; temperature: ~ 20-25 °C.

Note: *For an identity assay test, quantitative parameters such as concentration limit of detection (CLOD) and concentration limit of quantification (CLOQ) are generally not required. It is important to minimize the amount of salt in the final sample solution to reduce possible sample interferences and precipitation.*

References

CHAPTER 1:
Principles of capillary electrophoresis

1. P.D. Grossman, J.C. Colburn eds., "Capillary Electrophoresis – Theory and Practice", *Academic Press Inc., San Diego, (out of print; excellent introduction to CE theory),* **1992.**
2. P.C. Hiemenz, R. Rajagopalan, "Principles of Colloid and Surface Chemistry", *Marcel Dekker Inc., 3rd edition,* **1997.**
3. R.B. Bird, W.E. Stewart, E.N. Lightfoot, "Transport Phenomena", *John Wiley & Sons Inc., 2nd edition,* **2001.**
4. J.P. Landers ed.,"Capillary and Microchip Electrophoresis and Associated Techniques", *CRC Press,* **2008.**
5. K.D. Lukacs, J.W. Jorgenson, "Capillary zone electrophoresis: Effect of physical parameters on separation efficiency and quantitation", *J. High Res. Chromatogr., 8, 407–411,* **1985.**
6. B.B. Van Orman, G.G. Liversidge, G.L. McIntyre, T.M. Olefirowicz, A.G. Ewing,"Effects of buffer composition on electroosmotic flow in capillary electrophoresis", *J. Microcolumn Sep. 1990, 2, 176–180,* **1990.**
7. A.S. Said, "Theory and mathematics of chromatography", *Hüthig Verlag, Heidelberg,* **1981.**
8. S. Hjertén, "Zone broadening in electrophoresis with special reference to high performance electrophoresis in capillaries: An interplay between theory and practice", *Electrophoresis, 11, 665–690,* **1990.**
9. X. Huang, W.F. Coleman, R.N. Zare, "Analysis of factors causing peak broadening in capillary zone electrophoresis", *J. Chromatogr., 480, 95–110,* **1989.**
10. W.Th. Kok, "Capillary electrophoresis: instrumentation and operation", *Chromatographia Supplement, 51, 1–89,* **2000.**
11. M.T. Ackermans, F.M. Everaerts, J.L. Beckers, "Quantitative analysis in capillary zone electrophoresis with conductivity and indirect UV detection", *J. Chromatogr., 549, 345–355,* **1991.**
12. F. Kohlrausch, "Über Koncentrations-Verschiebungen durch Elektrolyse im Inneren von Lösungen und Lösungsgemischen", *Annalen der Physik und Chemie, 62, 14,* **1897.**

CHAPTER 2:
Modes of operation

13. H.H. Lauer, D. McManigill, "Capillary zone electrophoresis of proteins in untreated fused silica tubing", *Anal. Chem., 58, 166–170,* **1986.**
14. S. Terabe, Koji Otsuka, Kunimichi Ichikawa, Akihiro Tsuchiya, Teiichi Ando, "Electrokinetic separations with micellar solutions and open-tubular capillaries", *Anal. Chem., 56, 111,* **1984.**
15. S. Terabe, "Electrokinetic chromatography: an interface between electrophoresis and chromatography", *Trends in Anal. Chem., 8, 129–134,* **1989.**
16. V. Pretorius, B.J. Hopkins, J.D. Schieke, "Electroosmosis: A new concept for high-speed liquid chromatography", *J. Chrom., 99, 23,* **1974.**
17. J.W. Jorgenson, K.D. Lukacs, "Zone electrophoresis in open-tubular glass capillaries", *Anal. Chem., 53, 1298*, **1981.**
18. J.H. Knox, I.H. Grant, "Miniaturisation in pressure and electroendosmotically driven liquid chromatography: Some theoretical considerations", *Chromatographia, 24, 135,* **1987.**
19. J.H. Knox, I.H. Grant, "Electrochromatography in packed tubes using 1.5 to 50 µm silica gels and ODS bonded silica gels", *Chromatographia, 32, 317,* **1991.**

20. M. Dittmann, K. Wienand, F. Bek, G. Rozing, *LC-GC Magazine, 13, 800*, **1995.**
21. M.M Dittmann, G.P. Rozing, "Capillary electrochromatography — a high-efficiency micro-separation technique", *J. Chromatogr. A, 744, 63,* **1996.**
22. N.W. Smith, M.B. Evans, "The analysis of pharmaceutical compounds using electrochromatography", *Chromatographia, 38, 649,* **1995.**
23. L.A. Colón, Glamarie Burgos, Todd D. Maloney, José M. Cintrón, Ramón L. Rodríguez., *"Recent progress in CEC", Electrophoresis, 21, 3965,* **2000.**
24. Nobuo Tanaka, Hisashi Nagayama, Hiroshi Kobayashi, Tohru Ikegami, Ken Hosoya, Norio Ishizuka, Hiroyoshi Minakuchi, Kazuki Nakanishi, Karin Cabrera, Dieter Lubda, "Monolithic silica columns for HPLC, micro-HPLC and CEC", *J. High Resol. Chromatogr., 23, 111,* **2000.**
25. F. Svec, T.B. Tennikova, Z. Deyl, "Monolithic materials: Preparation, properties and applications", *Anal. Bio. Chem., 379, 8,* **2004.**
26. Guttman, A.S. Cohen, D.N. Heiger, B.L. Karger, "Analytical and micropreparative ultrahigh resolution of oligonucleotides by polyacrylamide gel high performance capillary electrophoresis", *Anal. Chem., 62, 137–146,* **1990.**
27. F. Kilar, S. Hjertén, "Fast and high-resolution analysis of human serum transferrin by high-performance isoelectric focusing in capillaries", *Electrophoresis, 10, 23–29,* **1989.**
28. J. Wu, J. Pawliszyn, "Capillary isoelectric focusing with a universal concentration gradient imaging system using a charge-coupled photodiode array", *Anal. Chem., 64, 2934,* **1992.**
29. J. Wu, A. Watson, "Automated sample introduction for an imaged capillary isoelectric focusing instrument via high-performance liquid chromatography sampling devices", *J. Chromatogr. B, 714, 113–118*, **1998.**
30. F. Kohlrausch, "Über Konzentrationen – Verschiebungen durch Elektrolyse im Inneren von Lösungen und Lösungsgemischen", *Annalen der Physik und Chemie, 62, 14,* **1897.**
31. Th.P.E.M Verheggen, A.C. Schoots, F.M. Everaerts, "Feasibility of capillary zone electrophoresis with suppression of electroendosmotic flow in completely closed systems", *J. Chromatogr., 503, 245–255,* **1990.**

CHAPTER 3:
Instrumentation

32. X. Huang, M.J. Gordon, R.N. Zare, "Bias in quantitative capillary zone electrophoresis caused by electrokinetic sample injection", *Anal. Chem., 60, 375–377,* **1988.**
33. R.L. Chien, D.S. Burgi, "Field-amplified sample injection in high performance capillary electrophoresis", *J. Chromatogr., 559, 141–152*, **1991.**
34. P. Britz-McKibbin, D.D.Y. Chen, "Selective focusing of catecholamines and weakly acidic compounds by capillary electrophoresis using a dynamic pH junction", *Anal. Chem., 72, 1242*, **2000.**
35. A. Vinther, H. Soeberg, "Temperature deviations of the sample zone in free solution capillary electrophoresis under stacking conditions", *J. Chromatogr., 559, 27–42,* **1991.**
36. N.J. Reinhoud, U.R. Tjaden, J. van der Greef, J. Chromatogr., 1993, 641, 155, and N.J. Reinhoud, "Bioanalytical capillary electrophoresis", *thesis, Leiden (NL), 131–148,* **1995.**
37. J.P. Quirino, S. Terabe, "Sweeping of analyte zones in electrokinetic chromatography", *Anal. Chem., 71, 1638–1644,* **1999.**

38. D.S. Burgi, B.C. Giordano, "Online preconcentration for capillary electrophoresis", *Handbook of Capillary and Microchip Electrophoresis and Associated Microtechniques, Ed. J.P. Landers, CRC Press, 413–427,* **2008.**
39. A.G. Ewing, R.A. Wallingford, T.M. Olefirowicz, "Capillary electrophoresis", *Anal. Chem., 61, 292A–303A,* **1989.**
40. L. Huber, S.A. George Eds, "Diode Array Detection in HPLC", *Chromatographic Science Series, Volume 62, Marcel Dekker,* **1993.**
41. S. Hjertén, K. Ellenbring, F. Kilar, J.L. Liao, A.J.C. Chen, C.J. Siebert, M.D. Zhu, "Carrier-free zone electrophoresis, displacement electrophoresis and isoelectric focusing in a high-performance electrophoresis apparatus", *J. Chromatogr., 403, 47,* **1987.**
42. W. Th. Kok, "Capillary electrophoresis: instrumentation and operation", *Chromatographia, 51, 1–89,* **2000.**
43. E. Gassmann, J.E. Kuo, R.N. Zare, "Electrokinetic Separation of Chiral Compounds", *Science, 230, 813,* **1985.**
44. D.E. Burton, M.J. Sepaniak, M.P. Maskarinec, J. *Chromatogr. Sci., 24, 347,* **1986.**
45. B. Nickerson, J.W. Jorgenson, *HRC J.High Resolut. Chrom., 11, 533,* **1988.**
46. S.D. Gilman, A.G. Ewing, *Anal. Chem., 67, 58,* **1995.**
47. A. Gutman, F.T.A. Chen, R.A. Evangelista, N. Cooke, *Anal. Biochem., 233, 234,* **1996.**
48. F. Foret, M. Deml, Y. Kahle, P. Bocek, *Electrophoresis, 7, 430*, **1993.**
49. X. Huang, K.T. Pang, M.J. Gordon, R.N. Zare, *Anal. Chem., 59, 2747,* **1987.**
50. X. Huang, R.N. Zare, S. Sloss, A.G. Ewing, *Anal. Chem., 63, 189*, **1991.**
51. X. Huang, R.N. Zare, *Anal. Chem., 63, 2193,* **1991.**
52. C. Haber, W.R. Jones, J. Soglia, M.A. Surve, M. Mcglynn, J.R. Reineck, C. Krstanovic, *J. Capillary Electrophoresis, 3, 1,* **1996.**
53. B. Gaš, M. Demjanenko, J. Vacik, *J. Chromatogr., 192, 253–257,* **1980.**
54. A.J. Zemann, E. Schnell, D. Volgger, G.K. Bonn, "Contactless conductivity detection for capillary electrophoresis", *Anal. Chem., 70, 563–567,* **1998.**
55. Alexandre Zatkovskis Carvalho, José A. F. da Silva, Claudimir L. do Lago, "Determination of mono- and disaccharides by capillary electrophoresis with contactless conductivity detection", *Electrophoresis, 24, 2138–2143,* **2003.**
56. Pavel Coufal, Jirí Zuska, Tom van de Goor, Vonda Smith, Bohuslav Gas, "Separation of twenty underivatized essential amino acids by capillary electrophoresis with contactless conductivity detection", *Electrophoresis, 24, 671–677*, **2003.**
57. V. Lopez-Avila, Tom van de Goor, Bohuslav Ga, Pavel Coufal, "Separation of haloacetic acids in water by capillary zone electrophoresis with direct UV detection and contactless conductivity detection", *J. Chromatogr. A, 993, 143–152,* **2003.**
58. J. Tanyayiwa, P.C. Hauser, "High-Voltage contactless conductivity detection of metal ions in capillary electrophoresis", *Electrophoresis, 23, 3781–3786,* **2002.**
59. A. Cifuentes, X. Xu, W.Th. Kok, H. Poppe, "Optimum conditions for preparative operation of capillary zone electrophoresis", *J. Chromatogr. A, 716, 141*, **1995.**
60. X. Xu, W.Th. Kok, H. Poppe, "Change of pH in electrophoretic zones as a cause of peak deformation", *J. Chromatogr. A, 742, 211*, **1996.**
61. G. Ross, *LCGC Europe, January* **2001.**

62. Special Issue: *Capillary Electrophoresis-Mass Spectrometry, Electrophoresis, 29(10), 1955–2239,* **2008.**

63. Special Issue: *Capillary Electrophoresis-Mass Spectrometry, Electrophoresis, 28(9), 1303–1473,* **2007.**

64. Special Issue: *Capillary Electrophoresis-Mass Spectrometry, Electrophoresis, 27(11), 2025–2259,* **2006.**

65. W. Kolch, C. Neusüß, M. Pelzing, H. Mischak, "Capillary electrophoresis-mass spectrometry as a powerful tool in clinical diagnosis and biomarker discovery", *Mass Spectrom. Rev., 24, 959,* **2005.**

66. Cech N.B.; Enke C.G., "Practical implications of some recent studies in electrospray ionization fundamentals", *Mass Spectrom. Rev., 20, 362,* **2001.**

67. A.P. Bruins, "Mechanistic aspects of electrospray ionization", *J. Chromatography A, 794, 345,* **1998.**

68. Smith, R. D., Olivares, J. A., Nguyen, N. T., Udseth, H. R., "Capillary zone electrophoresis-mass spectrometry using an electrospray ionization interface", *Anal. Chem., 60, 436–441,* **1998.**

69. E. J. Maxwell and D.D.Y. Chen, "Twenty years of interface development for capillary electrophoresis–electrospray ionization–mass spectrometry", *Anal. Chim. Acta, 627, 25–44,* **2008.**

70. Mehdi Moini, "Simplifying CE-MS Operation. Interfacing Low-Flow Separation Techniques to Mass Spectrometry Using a Porous Tip", *Anal. Chem., 79, 4241–4246,* **2007.**

71. E. Jane Maxwell, David D.Y. Chen, "Twenty years of interface development for capillary electrophoresis–electrospray ionization–mass spectrometry", *Analytica Chimica Acta, 627, 25–33,* **2008**

CHAPTER 4:
Practical operation and method development

72. S.A. Swedberg, "Characterization of protein behavior in high performance capillary electrophoresis using a novel capillary system", *Anal. Biochem., 185, 51–56,* **1990.**

73. C.A. Lucy, N.E. Baryla, K.K.C. Yeung, "Capillary Electrophoresis of Proteins and Peptides", *M.A.L. Strege (Ed.), Humana Press, p. 1*, **2004.**

74. C.A. Lucy, A.M. MacDonald, M.D. Gulcev, "Non-covalent capillary coatings for protein separations in capillary electrophoresis", *J. Chromatogr. A, 1184, 81–105*, **2008.**

75. N.E. Baryla, J.E. Melanson, M.T. McDermott, C.A. Lucy, "Characterization of Surfactant Coatings in Capillary Electrophoresis by Atomic Force Microscopy", *Anal. Chem., 73, 4558,* **2001.**

76. H. Katayama, Y. Yshihama, N. Asakawa, "Stable Capillary Coating with Successive Multiple Ionic Polymer Layers", *Anal. Chem., 70, 2254,* **1998.**

77. T.W. Graul J.B. Schlenoff, "Capillaries Modified by Polyelectrolyte Multilayers for Electrophoretic Separations", *Anal. Chem., 71, 4007,* **1999.**

78. S. Kaupp, R. Steffen, H. Wätzig, "Characterization of inner surface and adsorption phenomena in fused-silica capillaries in capillary electrophoresis", *J. Chromatogr. A, 744, 93–101,* **1996.**

79. S. Kaupp, H. Bubert, L. Bauer, G. Nelson, H. Wätzig, "Unexpected surface chemistry in capillaries for electrophoresis", *J. Chromatogr. A, 894, 73–77,* **2000.**

80. C.E. Sänger-van de Griend, "Capillary electrophoresis methods for pharmaceutical analysis; Vol. 9 of separation science and technology series", *S. Ahuja, M.I. Jimidar (Eds), Academic Press, Chapter 6,* **2008.**

81. H. Wätzig, C. Dette, "Capillary electrophoresis (CE): a review. Strategies for method development and applications related to pharmaceutical and biological sciences", *Pharmazie, 49, 83–96,* **1994.**
82. M.I. Jimidar, P. van Nyen, W. van Ael, M. Desmet in "Capillary electrophoresis methods for pharmaceutical analysis; Vol. 9 of separation science and technology series", *S. Ahuja, M.I. Jimidar (Eds), Academic Press, in Chapter 4,* **2008.**
83. B. Skoog, A. Wichman, "Calculation of the isoelectric points of polypeptides from the amino acid composition", *Trends in Anal.Chem., 5, 82–83,* **1986.**
84. P.D. Grossman, K.J. Wilson, G. Petrie, H.H. Lauer, "Effect of buffer pH and peptide composition on the selectivity of peptide separations by capillary zone electrophoresis", *Anal. Biochem., 173, 265–270,* **1988.**
85. B. Gas, M. Jaros, V. Hruska, I. Zuskova, M. Stedry, "PeakMaster: a freeware simulator of capillary zone electrophoresis", *LC-GC Europe, 18, 282-288 http://www.natur.cuni.cz/gas,* **2005.**
86. R. Kuhn, F. Stoecklin, F. Erni, "Chiral separations by host-guest complexation with cyclodectrin and crown ether in capillary zone electrophoresis", *Chromatographia, 33, 32–36,* **1992.**
87. A. Westall, T. Malmström, P. Petersson, "An observation of unusual temperature effects for enantioselective CZE employing highly sulphated-ß-cyclodextrin", *Electrophoresis, 27, 859–864*, **2006.**
88. M.M. Dittmann, G.P. Rozing, "Capillary electrochromatography — a high-efficiency micro-separation technique", *J. Chromatogr. A, 744, 63,* **1996.**
89. M.M. Dittmann, G.P. Rozing, "Capillary electrochromatography: Investigation of the influence of mobile phase and stationary phase properties on electroosmotic velocity, retention, and selectivity", *J. Microcolumn. Separations, 5, 399–408,* **1997.**
90. M.R. Taylor, P. Teale, S.A. Westwood, D. Perrett, "Analysis of Corticosteroids in Biofluids by Capillary Electrochromatography with Gradient Elution", *Anal. Chem., 69, 2554,* **1997.**
91. M.R. Euerby, C.M. Johnson, S.C.P. Roulin, P. Myers, K.D. Bartle, "Capillary electrochromatography in the pharmaceutical industry. Practical reality or fantasy?", *Anal. Commun., 33, 403,* **1996.**
92. A. Guo, G. Camblin, M. Han, C. Meert, S. Park, "Capillary electrophoresis methods for pharmaceutical analysis; Vol. 9 of separation science and technology series", *S. Ahuja, M.I. Jimidar (Eds), Academic Press, chapter 14*, **2008.**

Index

S

T

U

V

W

X, Y, Z

This information is subject
to change without notice.

Printed in Germany, November 1, 2018
Publication Number 5990-3777EN

www.agilent.com/chem/CE

Agilent Technologies